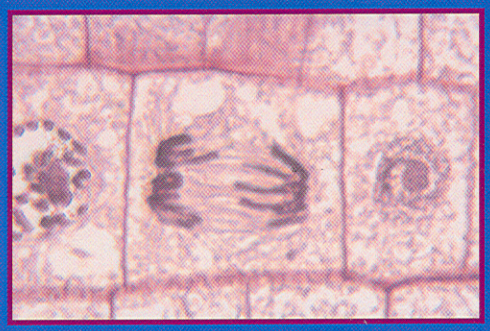

The Integrated Approach to Chemistry Laboratory

Selected Experiments

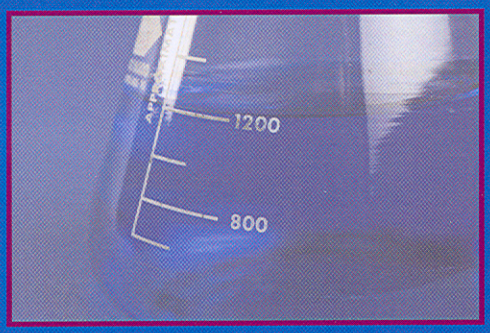

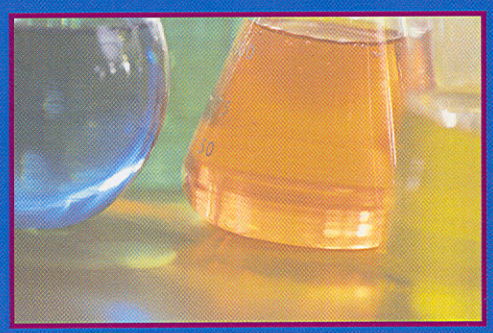

EDITED BY

PARTHA BASU

MITCHELL JOHNSON

www.ebook3000.com

The Integrated Approach
to Chemistry Laboratory

HOW TO ORDER THIS BOOK

BY PHONE: 866-401-4337 or 717-290-1660, 9AM–5PM Eastern Time

BY FAX: 717-509-6100

BY MAIL: Order Department
DEStech Publications, Inc.
439 North Duke Street
Lancaster, PA 17602, U.S.A.

BY CREDIT CARD: American Express, VISA, MasterCard, Discover

BY WWW SITE: http://www.destechpub.com

www.ebook3000.com

The Integrated Approach to Chemistry Laboratory

Selected Experiments

Edited by
Partha Basu, Ph.D. and
Mitchell E. Johnson, Ph.D.
Duquesne University

DES*tech* Publications, Inc.

The Integrated Approach to Chemistry Laboratory

DEStech Publications, Inc.
439 North Duke Street
Lancaster, Pennsylvania 17602 U.S.A.

Copyright © 2009 by DEStech Publications, Inc.
All rights reserved

No part of this publication may be reproduced, stored in a
retrieval system, or transmitted, in any form or by any means,
electronic, mechanical, photocopying, recording, or otherwise,
without the prior written permission of the publisher.

Printed in the United States of America
10 9 8 7 6 5 4 3 2 1

Main entry under title:
The Integrated Approach to Chemistry Laboratory: Selected Experiments

A DEStech Publications book
Bibliography: p.
Includes index p. 107

ISBN: 978-1-932078-88-6

www.ebook3000.com

Table of Contents

www.ebook3000.com

www.ebook3000.com

Acknowledgments

OVER the years, it has been a pleasure to teach IL to our undergraduate students, who routinely put in significant effort to excel in this demanding course. We have been very fortunate to work with numerous dedicated teaching assistants, without whom this exercise would not have been successful. We also are thankful to those of our colleagues who have helped develop and teach the integrated lab. Finally, we are thankful to Duquesne University for providing an atmosphere where undergraduate teaching is valued. Out sincere thanks to Dr. Joseph Eckenrode who have been very instrumental in shaping this book and his endless patience. We hope this book will serve the next generation of chemists in shaping their ideas about the breadth and multidisciplinary possibilities of experimental chemistry.

PARTHA BASU AND MITCH JOHNSON
Pittsburgh, PA

www.ebook3000.com

Introduction

TEACHING undergraduate laboratory classes in an integrated fashion, that is, the representation of multiple disciplines in a single curricular event, is not rare, but it is not a common practice. By contrast, a more widely used (traditional) approach in chemistry laboratory instruction is to include a laboratory section with each lecture class. Although the difficulty levels in these latter laboratory experiments range from simple to very complex, they have the common feature of being strongly predicated on the associated class lectures series. The integrated chemistry laboratory, on the other hand, deliberately introduces multiple disciplines into a single course or laboratory experiment. For example, a synthetic component can be incorporated into an experiment wherein students construct and test an electrochemical sensor. There are advantages to both methods. This book focuses on the integrated laboratory (IL) by describing and explaining a variety of experiments that follow the IL concept.

In recent years, the number of publications describing integrated laboratory experiments has increased considerably, and many chemistry programs are adopting some form of the integrated laboratory. This book is a direct result of the adoption or in practice of the IL, is intended to promote the practice of the integrated laboratory, and is designed to give IL instructors access to workable experiments that embody the integrated concept. They range from relatively simple labs for less-experienced students to complex experiments for advanced students. The book is also designed to illustrate the concept of "integrated laboratory" with the anticipation that laboratory instructors in higher education give some consideration can use the ideas to develop to an effective, alternative strategy for teaching students to be laboratory scientists.

Research in the sciences often occurs at the interface between disciplines, or requires the tools of multiple disciplines to succeed. Given chemistry as the central science, integration of concepts and practices from different disciplines as part of instructional practice in chemistry is of paramount importance. In the last several decades, chemistry has seen significant changes at its interface with other disciplines, from material science to chemical biology. Thus, there is a clear need for future scientists to be trained in a multi-faceted manner. Just as research is also often carried out within the confines of a particular discipline (synthesis of a class of molecules, for example, or the development of sensors for the measurement of heavy metal contaminants of groundwater), there is also justification for a year spent learning the nuances of organic synthesis or instrumental analysis. Many curricula that contain some form of integrated laboratory also include traditional laboratory classes in a complimentary way.

There are several different styles for approaching the integrated laboratory (IL) concept. For example, a curriculum may have organic, physical, and inorganic chemistry laboratory courses, each of which is integrated with other disciplines, for a comprehensive approach to IL. Alternatively, two or three chemistry disciplines, such as analytical and physical chemistry, or organic and inorganic, may be combined. In our own department, two semesters of IL are taught in place of traditional, upper-class instrumental, inorganic, and physical chemistry laboratories. In addition, we include biochemistry as a sub-discipline. Some departments use the integrated laboratory series through several years of the curriculum; whereas some use a semester of IL as a capstone laboratory course, or one leading into undergraduate thesis research. Other pro-

grams, however, teach laboratory classes across departmental lines, combining experiments in biology, chemistry, and physics.

The breadth of difficulty of the experiments also diverges widely among programs, with experiments that range from carefully tested procedures meant to have readily achieved and reproducible results to open-ended explorations in experimental chemistry (or biochemistry, or physics, etc.). Many of the experiments presented in this volume have standard, fully tested protocols that are meant to be followed closely. These experiments also have junctures where there is opportunity for further study or experimentation, and most can be modified by the instructor so that the topic can be expanded. The book also contains advanced experiments that are designed to work in a manner similar to that of a graduate level research project, in that the goals are well defined but the outcome of the experiment is left open, and likely to beget further experiments or alternative approaches. In IL experiments of this type, the experience for the students begins to approach that of a real research project, complete with teamwork and communication issues.

The way an IL course is structured in terms of the level of student involvement in the decision-making process, that is, whether the laboratory is mainly experiments based on protocols or mainly project/problem-based experiments, depends on how the integrated laboratory experience fits within the curriculum. If the students have a significant amount of experience leading into the IL, then the IL experiments can be primarily problem-based, and the IL course can serve as a capstone or research transitional laboratory. "Experience" is a relative term, and perusal of the experiments herein will show just how much effort and insight any particular experiment will demand. Generally, we have found that, in order to be effective, the IL ought to be preceded by at least one laboratory course that involves basic laboratory manipulations and data analysis. One such laboratory course is the traditional "quant lab". Although many of the traditional techniques (titrations, for example) are not generally touted as being useful or relevant, there is still a need for teaching students the basic techniques-volumetric manipulations, proper weighing techniques, quantitative transfers, absorption spectrophotometry, the laboratory notebook, regression analysis, basic statistics, etc. in such a way that they are familiar and can be assumed to have been mastered by students before they take IL. The IL approach certainly does not preclude taking multiple semesters to teach basic techniques and advanced techniques. Another advantage to the IL approach is that students are more engaged in the learning process.

One viable approach for the IL is to make the labs progressively more difficult, by starting with simple experiments that require a limited skill set, and follow them with experiments that demand an increasing amount of student decision-making and involve more complicated measurements. Although it is not a necessary part of the IL, the concept of IL lends itself to experiments that are open-ended in the outcome, or are similar to actual research projects. This approach fosters critical thinking and problem solving. For example, inorganic synthesis, in a research regime, is not generally an end into itself; the outcome of the synthesis is a compound that can be used in catalysis in a synthetic method, or mimics electron transfer in an enzyme, or constitutes a ligand for a metal sensor, etc. Where a traditional experiment might stop with successfully synthesizing and characterizing an organometallic complex, a more realistic experiment is to measure the bond angles and lengths of the compound, perform electronic spectroscopy, use computational methods to analyze the spectroscopy, and compare it to the properties of the catalytic center of an enzyme.

There are a number of ways to develop such experiments, but a very good approach is to base the experiment, even if it is relatively simple, on active research areas in the department. A common approach is to assign multiple faculty members to the IL course, so that each can bring their research experience to the development of the experiments. Experiments can be based on methods developed in faculty research laboratories that have been tested and vetted over time, or they can be new directions in research based on literature methods that require translation to the local venue, or they can be completely novel experiments that call for extensive method development. A caution on the latter is that, although faculty members still see the value of the learning experience in such cases, students are apt to be frustrated without at least some measurable outcomes. These restrictions are primarily what prevent the IL course from being an actual research venue. We have found it helpful to spend some time explaining to students exactly what to expect from the more advanced experiments.

www.ebook3000.com

As with many types of laboratory courses, IL benefits, when appropriate, from using a group structure where each group is assigned a specific task towards a common goal. The simplest experiments tend not to have enough content to split among groups, but more complicated experiments lend themselves to this approach. Using groups for different tasks has several benefits. It compresses the time element by allowing more tasks to be carried out simultaneously. If the work assignments are developed carefully, groups will be required to share data or methods with other groups, thereby encouraging teamwork and the development of professional standards of conduct. Students are also held accountable by their peers. On a more practical level, students will also be forced to learn things like standardization of data formats and methods for the meaningful transfer of data. These considerations are not unique to IL, but the format does work well within the overall framework of an integrated approach to laboratory instruction.

The chapters in this book are arranged in two segments. The first eight chapters are introductory laboratory experiments that have been used repeatedly, so that likely pitfalls and problems have been ironed out. The later chapters contain more complicated experiments, suitable for more advanced students. Each chapter has a set of Learning Objectives, meant to help the instructor and the student understand the purposes of each experiment. The Learning Objectives are also good shorthand for identifying experiments that might fit together in the IL course, depending on where it fits in the curriculum. They are followed by the description of the experiment and typical results. References follow, then Suggested Reading. The Instructor's Resource is meant to help the instructor customize the experiment, or avoid common pitfalls. Safety considerations are listed in cases where they may not be met by employing usual and customary common laboratory safe practice, and we have assumed that students receive regular safety instruction prior to the laboratory.

www.ebook3000.com

Preparation and Photocatalysis of Zinc Oxide Nanocrystals

D. SCOTT BOHLE and CARLA JEANN SPINA
Department of Chemistry Otto Maass Chemistry Building 801 Sherbrooke Street West, McGill University Montréal, Québec, Canada H3A 2K6

LEARNING OBJECTIVES: In this experiment, zinc oxide nanocrystals are synthesized in a transparent colloidal suspension. The nanocrystals are then utilized in the photocatalytic degradation of methyl red azo dye.

Preparation of Nano-sized Semiconductor Material

Many procedures exist for the synthesis of ZnO semiconductor nanomaterials including: sol-gel, electrochemical, air oxidation, thermal decomposition, ultrasonic, and various wet-chemical processes.[1–6] Each method has benefits and drawbacks to consider, including the composition, size, dispersity, morphology, and spectral characteristics of the nanocrystals, and ease of synthesis. In this experiment, zinc oxide (ZnO) nanocrystals (NC) are prepared via the addition of a base to an alcoholic solution of zinc salts resulting in a transparent colloidal suspension of semiconductor nanocrystals.

Analysis of ZnO Nanocrystal Reactivity in Solution

The unique characteristics of nanomaterials create unique applications including optoelectronic systems such as light emitting diodes and photovoltaic cells, or as components of nanoelectronic devices.[7–9] In this experiment, the photocatalytic properties of ZnO NCs towards the degradation of dyes in solution are utilized.

Understanding of ZnO Nanocrystal Photochemical Processes

The role of ZnO NC in the photocatalytic degradation of azo dyes is also investigated.

INTRODUCTION

History of Nano-materials

THE basis of nano-research hinges on the fact that properties of bulk materials will change when the same materials are reduced down to the quantum scale. When the particle size of an inorganic crystalline solid is on the order of nanometers it is well known that interesting optical and electronic characteristics will result. Semiconductors, defined as having a bandgap from ~0.5 to ~3.5eV, of nano-dimension may be referred to as quantum dots, semiconductor nanocrystals, or nanoparticles. In this size range, quantum mechanical effects may be observed in the promotion of an electron from the valence band to the conduction band. General synthesis of nanomaterials stems from either a chemical approach, where synthesis based on smaller precursors is utilized, or an engineering approach, where smaller materials are either lithographically or electrochemically obtained from a bulk source. Applications as light sources, photonics, photovoltaics, photocatalysts, and as dyes or sensors have created a demand on the field to produce new and interesting nanomaterials.

ZnO Nanocrystals and Azo Dyes

Bulk zinc oxide material has been used historically in a variety of technical applications, including as an

additive in porcelain enamels and heat resistant glass, as an activator in vulcanization, as an additive for rubber and plastics, pigments in paints (with UV-protective and fungistatic properties), as spacecraft protective coatings, as a constituent of cigarette filters and healing ointments, as semiconductor devices, as a catalyst, in optical waveguides, in piezoelectric materials, and many more.[10] Since the 1960s, investigations into the properties of ZnO nanomaterials have caught the interest of many scientists.[11] With the reduction in ZnO size, novel electrical, mechanical, chemical and optical properties were introduced, believed to be the result of surface and quantum confinement effects, to be discussed later.[12] Investigation into the nanomaterials of ZnO has led to a field of chemistry devoted to the study, characterization, and understanding of nanomaterials of ZnO and their potential applications. One particular application, which will be investigated in this experiment, is the photocatalytic potential of ZnO NCs. Semiconductor nanomaterials have long attracted attention as effective photocatalysts for the degradation of organic pollutants.[13–16] Given that photochemical reactions occur on the surface of the catalyst, utilization of nanoscale materials is ideal due to their higher surface-to-volume ratio.

The discovery of azo dyes, Figure 1.1, was made in 1863 by Martius, and now encompasses a large class of organic dyes that contain the nitrogen as the azo group [–N=N–] as part of their molecular structures. The ability to alter the substituents on the azo functionality permits the broad usage of azo dyes, including water soluble dyes, metal chelation, and acid-base sensitive pH indicators. In industry dyes and pigments are a cause of major concern due to their environmental effects. During synthesis and processing, it is estimated that 15% of the dyes produced worldwide are leached into wastewater.[17] Concern for the toxicity of the dyes in water has lead to the development of various methods of treatment. Physical, non- destructive, methods such as flocculation, reverse osmosis, filtration, and adsorption, in effect, act to simply transfer the pollutant.[18,19] Chemical methods are costly and bio-treatment has been linked to generation of carcinogenic byproducts.[20,21] The development of heterogeneous catalysts, as an advanced oxidation process, has proven to be an economic, effective, and safe method of degradation for various dyes.[22]

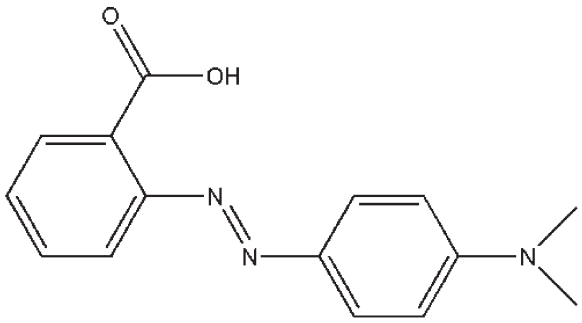

Figure 1.1. Azo dye 4-Dimethylaminoazobenzene-2′-carboxylic acid (methyl red).

Photochemistry

The possibility of harnessing the energy of light is an intriguing idea for most chemists. Nature, as usual, has beaten us to the punch by a long shot! For more than 3.4 billion years, bacteria have been using solar energy through photosynthesis:[22]

$$2\ H_2O + 2\ NADP^+ + 2\ ADP + 2\ P_i + \text{light} \rightarrow$$
$$2\ NADPH + 2\ H^+ + 2\ ATP + O_2$$

It is with this inspiration that science has been making great strides to exploit the energy of light to try and solve many problems faced today. Photochemistry, and more specifically in this laboratory, photocatalysis, does just that. During the 1970s and 1980s, there has been much investigation into the photochemical production of fuel using semiconductors, or sensitizers. The most common system investigated was that of the cleavage of water using solar energy:[23]

$$2H_2O + h\upsilon \rightarrow 2H_2 + O_2$$

For an effective catalytic system, critical considerations must include turnover, efficiency, phase, and recoverability of the catalyst involved. In photocatalysis it is also important to consider the wavelength of the excitation source, the absorption range of the catalyst, and any scattering or absorption of the other reagents or solvents in the system.

www.ebook3000.com

THEORETICAL ASPECTS

Nanocrystals

Zinc oxide is a unique semiconductor material, reflective of the many synthetic routes for the preparation of ZnO. It is one of the richest family of nanomaterials, in structure and properties.[24] Many of the electrical and thermodynamic properties of quantum sized semiconductors show strong size dependence, and their properties can therefore be controlled through careful manufacturing processes. In the quantum size regime, where the radius of the particle is smaller than the Bohr exciton radius, calculation of the spatial separation of the electron and its hole, collectively known as an *exciton*, may be resolved using a Bohr model:[25]

$$r = \varepsilon h^2 / \pi m_r e$$

where r is the radius of the three-dimensional sphere containing the exciton, ε is the dielectric constant of the semiconductor, m_r is the reduced mass of the electron-hole pair, h is Planck's constant, and e is the charge on the electron. In this size range, when the nanocrystal is excited, the electron-hole pair is confined within the physical dimensions of the particle, similar to the particle-in-a-box analogy. In principle, quantum effects such as quantization of energy levels may be observed, Figure 1.2.

As the growth of semiconductor nanocrystals proceeds, the HOMO and LUMO orbitals hybridize to create a quasi-homogeneous conduction band and valence band, simultaneously the E_g decreases, until the particles reach a microcrystalline size, where the quantum effects on the band gap are no longer observed. By

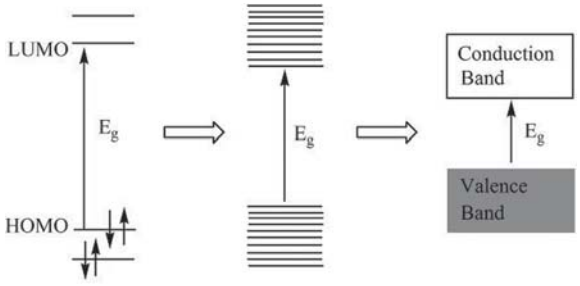

Figure 1.2. Energy level diagram progressing from (left to right): molecular to nanocrystal to bulk semiconductor. The vertical arrow in each denotes the relative energy of the band gap (E_g).

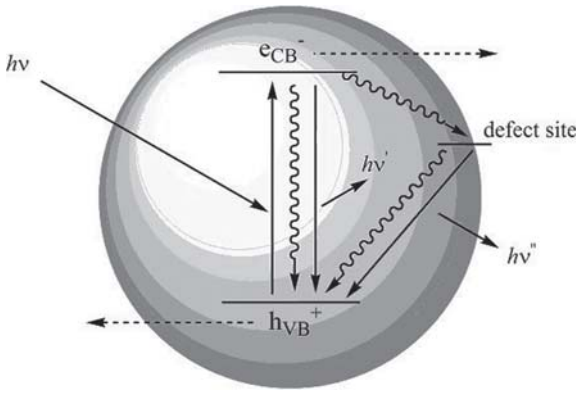

Figure 1.3. Excitation and relaxation pathways of a ZnO nanocrystal. Photon excitation ($h\nu$) results in the creation of an e_{CB}^-/h_{VB}^+ (exciton) pair. The relaxation pathway of the e_{CB}^- may proceed either through direct recombination with the h_{VB}^+ or transfer to a surface defect site where recombination with the h_{VB}^+ may then proceed, these processes may occur either radiatively or non-radiatively. Alternate pathways (dashed arrows) for the e_{CB}/h_{VB}^+ may progress through interaction with surrounding species.

tracing the growth of this band edge, one may follow the growth of the nanoparticles, and determine their size.[25, 26]

Zinc oxide is a wide band gap (3.37eV) semiconductor, wurtzite crystal lattice, with a high exciton binding energy of 60 meV at room temperature. The bulk semiconductor exhibits a strong light absorption at energies higher than the bandgap (E_g), where quantum sized nanomaterials exhibit substantially different photophysical properties.[26] Excitation of the ZnO nanocrystals, with a photon of energy greater than that of the band gap, results in the production of an exciton:

$$ZnO + h\nu \rightarrow e_{CB}^- + h_{VB}^+$$

This excited state may relax through a variety of pathways, Figure 1.3. Many applications rely on the emission characteristics of the nanocrsytals; however, the non-radiative relaxation pathways are also utilized in other applications of the nanocrystals. It is through these pathways that photochemistry may proceed.

Azo Dyes

Azo dyes account for a great portion of all commercial dyes. These chromophores contain one azo functionality [–N=N–] linked to sp^2 hybridized carbons;

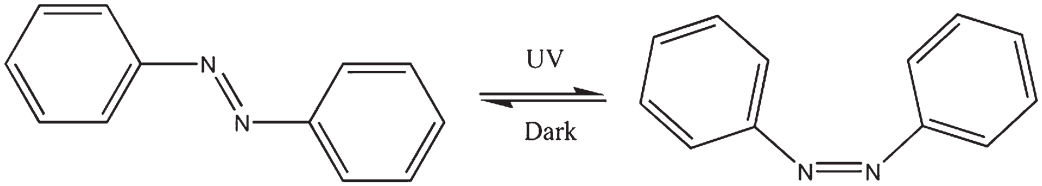

Figure 1.4. Photoisomerization of azobenzene from the *trans*-isomer (left) to the *cis*-isomer (right).

although *di* and *triazo* compounds are known, the azo groups are often conjugated with aromatic substituents, though this is not always the case.[27] Azo dyes are brightly colored, much more so than the next common class of dyes, anthraquinones. Even though carbonyl and phthalocyanine dyes have greater light-fastness, the simple synthetic procedures, great structural diversity, and good extinction coefficients of azo dyes make them highly sought after.[28] It was not until the 1930s that examination into the photochemistry of azo dyes began with Krollpfeiffer and Hartley, investigating the photodegradation products and photoisomerization.[27] At room temperature the trans isomer is prevalent, as it is more thermodynamically stable. Upon excitation from a UV source, the dye may undergo photoisomerization, Figure 1.4.[29] Photodegradation of azo dyes is a known method of treatment for dye-contaminated systems.[30–32] Pathways for degradation involve advanced oxidation processes, and result in the decoloration, detoxification, and/or mineralization of the dye.

Photochemistry

Photochemistry is the interaction between atoms or small molecules and light; more specifically, it may be defined as a reaction that proceeds by the absorption of light or a photon by a chemical system. In a photochemical reaction, upon photon absorption, the system becomes excited to a higher energy state, and it is from those excited states that various chemical pathways may proceed. The key to a successful photocatalytic system is the separation of photoinduced charge. In the situation that there is rapid recombination of the separated charges in a photochemical system, the excited state is no longer available to carry out photocatalytic pathways.[23] Subsequently, this excited system can react either with itself or another substance in the system. As observed above in Figure 1.3, there are many relaxation pathways of an excited ZnO nanocrystal. In the processes of photodegradation of organic dyes, alternate pathways (dashed arrows) of the exciton are as follows:[31]

$$ZnO + h.\upsilon \rightarrow e_{CB}^{-} + h_{VB}^{+}$$

$$(O_2)_{ads} + e_{CB}^{-} \rightarrow O_2^{-\bullet}$$

$$Dye + h_{VB}^{+} \rightarrow Dye^{+\bullet}. \text{ Degradation Products}$$

DESCRIPTION OF THE EXPERIMENT

Chemicals and solvents were of reagent grade and were used without further purification. All glassware used in the preparation of ZnO NC was dried in a 110°C oven prior to use. Absorption spectra of samples were obtained with an HP 845× UV-Visible system. Photocatalytic experiments were carried out using a Driel Instruments Hg-lamp (λ_{254nm}) Model 66033 as the excitation source.

Preparation of Colloidal ZnO NC in a 2-Propanol Solution

This procedure was adapted from that of Bahnemann *et al.*[22] A 100mL round bottom flask was charged with $Zn(OAc)_2 \cdot 2H_2O$ (5×10^{-5} mol), ^{i}PrOH (4.5 mL), and stirbar. The solution was heated, while stirring, to 50°C until the dissolution of the zinc salt was complete. Dissolution may be aided with the use of a sonicator. The zinc acetate solution and a NaOH (0.020 M in ^{i}PrOH, dissolved by heating or sonication) were chilled to 0°C in an ice/salt bath. The 0°C NaOH solution (9×10^{-5} mol) was then added dropwise, over approximately 2 min, to the rapidly stirring $Zn(OAc)_2$ solution. Once the addition is complete, the flask is transferred to a 65°C bath, and left to stir for 3h. The reaction was then removed from the heat and left to stir at room temperature overnight. Progress of the reaction was monitored on a UV-Vis spectrophotometer by the onset of the band edge in the absorption spectrum.

www.ebook3000.com

Photocatalytic Degradation of Methyl Red

The prepared ZnO NC solution (2.5 mmol) was added to a quartz 1 cm cuvette. Using ^{i}PrOH as a blank, the UV-visible spectrum was observed. This solution may now be used as a blank for the remainder of the reaction. To the ZnO NC solution, methyl red (1.7×10^{-7} mol, 10 mM solution in MeOH) was added, and spectrum was observed. The solution was then exposed to UV light, Hg lamp ($\lambda_{max} = 254$ mm), in 1 minute intervals, monitoring the UV-vis spectrum after each exposure until no change was observed. For comparison this procedure was then repeated in the absence of ZnO NC, using ^{i}PrOH as the solvent.

PROBLEMS

What is an alternative synthetic procedure for ZnO nanoparticles?

What advantages/disadvantages do these syntheses have over that used here?

Why are azo dyes so strongly colored?

What are some effects of functionalizing of the core azo benzene unit?

What solvents are inappropriate for this photochemical reaction?

How could one determine the size of the nanoparticles from the UV-Vis spectrum?

What is the effect of the ZnO NC on the dye during UV exposure?

How does it compare to the sample without ZnO NCs?

SUGGESTED READINGS

Meulenkamp, E.A.. *J. Phys. Chem. B,* **1998**, 102, 5566.

Kaneko, M.; Okura, I. *Photocatalysis: Science and Technology,* Japan, Kodansha and Springer, **2002**.

Bahnemann, D.W.; Kormann, C.; Hoffmann, M.R.; *J. Phys. Chem.*, **1987**, 91, 3789.

Zollinger, H. *Color Chemistry: Synthesis, Properties, and Applications of Organic Dyes and Pigments 3rd Ed.,* Weinheim, Wiley-VCH, **2003**.

REFERENCES

1. Cozzoli, P.D.; Curri, M.L.; Agostiano, A..; Leo, G.; Lomascolo, M. *J. Phys. Chem. B,* **2003**, 107, 4756.
2. Poul, L.; Ammar, S.; Jouini, N.; Fiévet, F. *J. Sol-Gel Sci. Tech. 2003*, 26, 261.
3. Hosono, E.; Fujihara, S.; Kimura, T.; Imai, H.. *J. Sol-Gel Sci. Tech.* **2004**, 29, 71.
4. Meulenkamp, E.A.. *J. Phys. Chem. B,* **1998**, 102, 5566.
5. Dong, L.; Liu, Y.C.; Tong, Y.H.; Xiao, Z.Y.. *J. Colloid Interf. Sci.,* **2005**, 283, 380.
6. Kumar, R.J.; Diamant, Y.; Gedanken, *A.. Chem. Mater.* **2000**, 12, 2301.
7. Colvin, V. L.; Schlamp, M. C.; Alivisatos, A. P.. *Nature,* **1994**, 370, 354.
8. Dabbousi, B. O.; Bawendi, M. G.; Onitsuka, O.; Rubner, M. F.. *Appl. Phys. Lett.* **1995**, 66, 1316.
9. O'Regan, B.; Graetzel, M.. *Nature,* **1991**, 353, 737.
10. Hirschwald, W.H.. *Acc. Chem. Res.* **1985**, 18, 228.
11. Wang, Z.L.. *J. Phys. Chem. B: Condens. Matter.* **2004**, 16, R829.
12. Alivisatos, A.P.. *J. Phys. Chem.* **1996**, 100, 13226.
13. Hoffmann, M. R.; Martin, S. T.; Choi, W.; Bahnemann, D. W. *Chem. Rev.* **1995**, 95, 69.
14. Lewis, L. N. *Chem. Rev.* **1993**, 93, 2693.
15. Nedeljkovic, J. M.; Nenadovic, M. T.; Micic, O. I.; Nozic, A. J. *J. Phys. Chem.* **1986**, 90, 12.
16. Jing. L.; Xu, Z.; Sun, X.; Shang, J.; Cai, W.; *Appl. Surface Sci.* **2001**, 180, 308
17. Sahoo, C.; Gupta, A.K.; Pal, A.. *Desalination,* **2005**, 181, 91.
18. Georgiou, D.; Aivazidis, A.; Hatiras, J.; Gimouhopoules, K.. *Water Research,* **2003**, 37, 2248.
19. Baban, A.; Yediler, A.; Lienert, D.; Kemerdere, N.; Kettrup, A.. *Dyes and Pigments,* **2003**, 58, 93.
20. Ge, J.; Qu, J.. *Applied Catalysis B: Environmental,* **2004**, 47, 133.
21. Wong, P.K.; Yuen, P.Y.. *Water Research,* **1996,** 30, 1736.
22. Raven, P.H.; Evert, R.F.; Eichhorn, S.E.. Biology of Plants, 7th Edition. 2005, New York: W.H. Freeman and Company Publishers, 124-127.
23. Kaneko, M.; Okura, I.. *Photocatalysis: Science and Technology,* Japan, Kodansha and Springer, **2002**.
24. Wang, Z.L.. *Materials Today,* **2004**, 7, 26.
25. Murphy, C.J.; Coffer, J.L.; *Appl. Spectroscopy,* **2002**, 56, 16A.
26. Bahnemann, D.W.; Kormann, C.; Hoffmann, M.R.; *J. Phys. Chem.,* **1987**, 91, 3789.
27. Griffiths, *J.; Chemical Society Reviews,* **1972**, 1, 481.
28. Zollinger, H. *Color Chemistry: Synthesis, Properties, and Applications of Organic Dyes and Pigments 3rd Ed.*, Weinheim, Wiley-VCH, **2003**.
29. Mateev, V.; Markovsky, P.; Nikolova, L.; Todorov, T.. *J. Phys. Chem.* **1992**, 96, 3055.
30. Comparelli, R.; Fanizza, E.; Curri, M.L.; Cozzoli, P.D.; Mascolo, G.; Agostiano, A.. *Appl. Cat. B : Environmental*, **2005**, 60, 1
31. Sahoo, C.; Gupta, A.K.; Pal, A; *Desalination,* **2005**, 181, 91
32. Suarez-Parra, R.; Hernandez-Perez, I.; Rincon, M.E.; Lopez-Ayala, S.; Roldan-Ahumanda, M.C. *Solar Energy Materials and Solar Cells,* **2003**, 76, 189

Pedagogy and Teaching Notes

Preparation of ZnO nanoparticles was interpreted from the procedure developed by Bahnemann et al. through the hydrolysis and condensation in an iPrOH solution as seen in Reaction 1:[26]

$$Zn(OAc)_2 + 2OH^- \rightarrow ZnO + H_2O + 2OAc^- \quad (1)$$

As described by Bahnemann, and repeated in our experiments, ZnO nanocrystal growth can be monitored via the band gap absorption feature in the UV-visible spectra, Figure 1.5. The band shape narrowing and shifting to lower energy may be interpreted as size distribution focusing, arising from size-dependent growth kinetics and later in the growth—Ostwald ripening. Nucleation of the ZnO nanoparticles and later, a strong absorbance feature at about 30,000 cm^{-1}, becomes readily apparent and is associated with the 1st excitonic transition of ZnO. It is this band edge that can be monitored to follow the growth of the ZnO nanoparticles in solution. With time, the intensity of the band edge indicates additional nucleation of ZnO, and the slight shift in energy indicates the growth of the average nanoparticles.

Common pitfalls or problems associated with the experiment may include the determination of the exact concentration of the NaOH solution, due to the hygroscopic nature of the reagent. The temperature, stirring speed, and rate of NaOH addition in the nanoparticles preparation may also cause concern. The addition of the sodium hydroxide solution to the zinc acetate solution must be carried out dropwise at 0°C with rapid stirring or there may be inhomogeneous nanocrystals, or at worst—formation of micro- crystalline particles. This may be observed in the UV-Visible spectrum through lack of shifting in the band edge during growth.

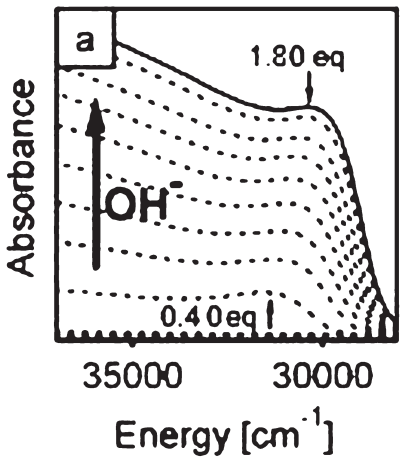

Figure 1.5. Growth of ZnO nanoparticles following the band edge of the absorption spectra.

www.ebook3000.com

Synthesis and Evaluation of Inhibitors for Mushroom Tyrosinase

TIMOTHY A. SHERWOOD and PETER M. SMITH
Westminster College, Department of Chemistry, New Wilmington, PA 16172

LEARNING OBJECTIVES: The student will learn how the sub-disciplines of organic chemistry and biochemistry can be integrated.

- The student will perform multi-step organic syntheses including product workup and characterization.
- The student will use kinetic analysis of an enzymatic reaction to determine the V_{Max} and K_M for the reaction.
- The student will use kinetic analysis to determine the mode of inhibition for potential inhibitors of an enzymatic reaction.

INTRODUCTION

TYROSINASE enzymes are present in plant and animal cells and are responsible for the browning of plant and animal materials as they age. Examples of this would be the browning of a sliced apple or a mushroom. The reaction responsible for this browning is shown in Figure 2.1.

This reaction is easily monitored, as dopachrome has a significant absorption of visible light (λ_{max} = 475 nm) while the reactants do not. Inhibition of the tyrosinase reaction is important as it helps food look and remain fresh longer.

The tasks within this project are to synthesize and evaluate potential inhibitors of tyrosinase. The three potential inhibitors are shown in Figure 2.2. Each inhibitor mimics a portion of the tyrosine structure but omits other parts. Research teams will synthesize and investigate each potential inhibitor, and therefore the binding relationship between tyrosine and tyrosinase.

Kinetic Analysis

The kinetic analysis of tyrosinase is a straightforward Michaelis-Menten evaluation of this enzyme that can be accomplished with a visible spectrometer and a stopwatch (or kinetic instrument control software). Michaelis-Menten kinetics evaluates the hyperbolic dependence of the initial rate of reaction, V_0, on the concentration of substrate, [S] for a constant concentration of enzyme. The V_0s must first be determined in a series of assays where the [S] is varied. The value of each V_0 arises from the initial linear portion of the plot of amount of product vs. time, as shown in Figure 2.3.

When the V_0, from each assay, is plotted versus [S], the hyperbolic Michaelis-Menten relationship is revealed providing kinetic information on the enzyme.

$$V_0 = \frac{V_{Max}[S]}{K_M + [S]}$$

This relationship follows the Michaelis-Menten equation, where V_{Max} in the maximum velocity or reaction rate and K_M is the Michaelis constant. V_{Max} is the rate of catalysis that occurs at infinite concentration of substrate, and is used to evaluate the speed of catalysis. K_M is the concentration of enzyme that yields one-half the maximum velocity and is used to rate the tightness of binding between the enzyme and

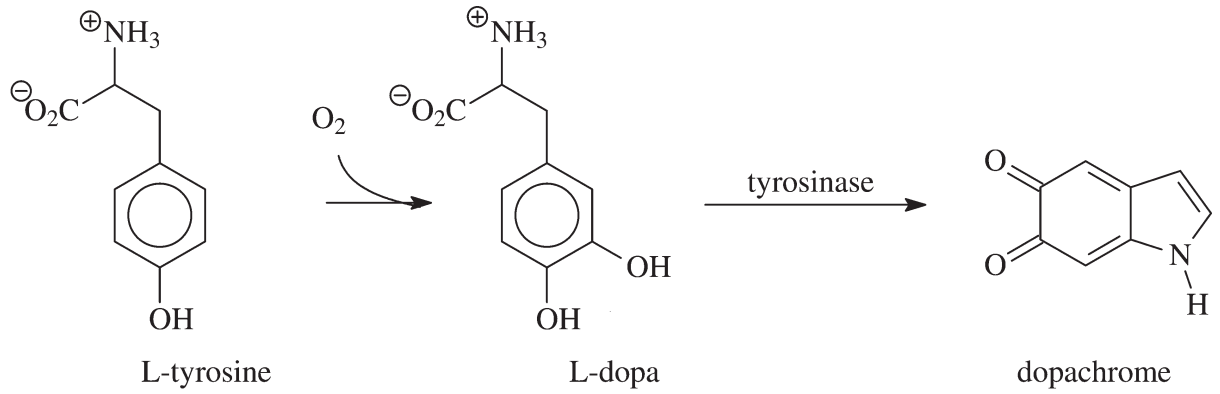

Figure 2.1.

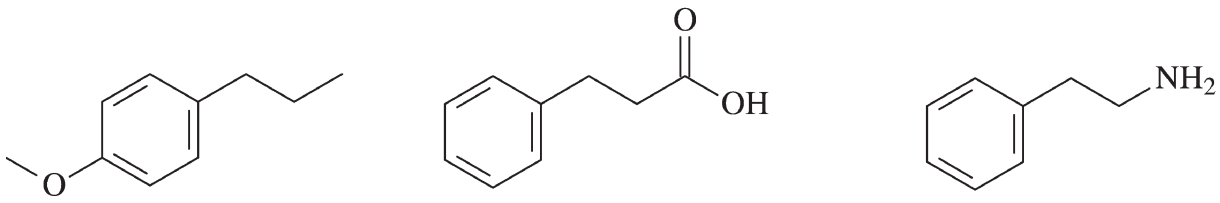

Figure 2.2.

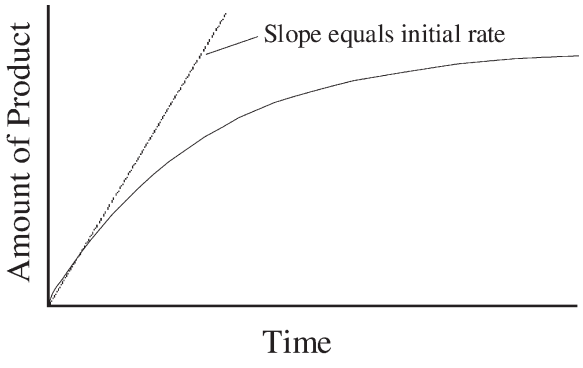

Figure 2.3.

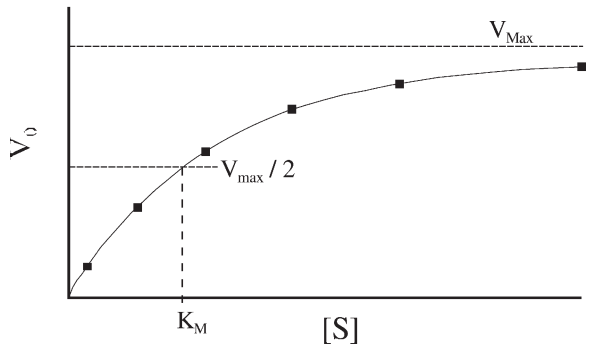

Figure 2.4.

www.ebook3000.com

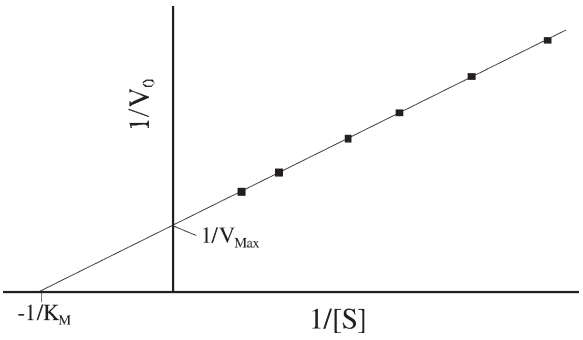

Figure 2.5.

the substrate. These two values can be determined much more accurately when the Michaelis-Menten equation is rearranged into the linear form known as the Lineweaver-Burk equation:

$$\frac{1}{V_0} = \frac{K_M}{V_{Max}}\left(\frac{1}{[S]}\right) + \frac{1}{V_{Max}}$$

In the Lineweaver-Burk equation, $1/V_0$ is the y-axis and 1/[S] is the x-axis. Use of this equation or plot yields $1/V_{Max}$ as the y-intercept and $-1/K_M$ as the x-intercept.

Inhibitors slow the catalysis of enzymes by affecting the binding of the substrate, affecting the conversion of the substrate to product, or affecting binding and conversion. This yields three different types of enzyme inhibitors, competitive, uncompetitive, and mixed, which can be distinguished by the changes in V_{Max} and K_M when the inhibitor is present.

Competitive inhibitors bind to the same site on the enzyme as does the substrate and can be overcome with large amounts of substrate. Therefore, they affect K_M but not V_{Max}. Uncompetitive inhibitors bind only to the complex of the substrate bound to the enzyme, actually increasing the tightness of binding, and decrease both V_{Max} and K_M. Mixed inhibitors bind to the enzyme at a site other than the substrate binding site, decreasing V_{Max} and increasing K_M.

Table 2.1.

Aspect	V_{Max}	K_M
Competitive	unchanged	increases
Uncompetitive	decreases	decreases
Mixed	decreases	increases

MATERIALS AND EQUIPMENT

Inhibitor Synthesis

2-Phenylethanol
48% Hydrobromic acid, HBr(aq)
Sodium azide (NaN_3)
Sodium borohydride ($NaBH_4$)
Magnesium ribbon, Mg(s)
Dry ice, CO_2(s)
Concentrated hydrochloric acid, HCl(aq)
Sodium hydroxide (NaOH)
Anisole
Propionic anhydride
85% Phosphoric acid, H_3PO_4(aq)
Granular zinc, Zn(s)
Sodium chloride (NaCl)
Anhydrous magnesium sulfate ($MgSO_4$)
Diethyl ether
Hexanes
Ethyl acetate
95% Ethanol
Standard organic lab glassware
Magnetic stir bars
Stirring hotplates
Thin-layer chromatography (TLC) plates and elution chambers
Glass fritted funnel
Silica gel for flash chromatography
Glassware drying oven

Inhibitor Evaluation

Sodium phosphate buffer, NaH_2PO_4, 100 mM pH 7.0
L-dopa, 15 mM in buffer (wrap in Al foil to shield from light)
Mushroom Tyrosinase, 100 units/mL in buffer (store on ice during experiment)
Inhibitor, 5 mM in buffer
Spectrometer
Cuvettes
Stopwatch or (computer controlled spectrometer with kinetic software) automatic pipettors

PROCEDURES FOR INHIBITOR SYNTHESES

Conversion of 2-phenylethanol to (2-bromoethyl)benzene

Working in a fume hood, pour 20 g of

2-phenylethanol and 30 mL of 48% aqueous hydrobromic acid, HBr(aq), into a 250-mL round-bottom flask containing a magnetic stir bar. Attach a water-cooled condenser to the flask and reflux the mixture, with constant stirring, for 2–3 hours. Two phases should appear in the flask after ~30 minutes. Monitor the progress of the reaction by thin-layer chromatography (TLC) of the upper, organic phase using a eluting solvent solution of 9:1 hexanes:ethyl acetate. When the conversion of 2-phenylethanol to (2-bromoethyl)benzene is complete, remove reaction flask from the heat and allow it to cool to room temperature. Pour the entire contents of the round-bottom flask, except the stir bar, into a separatory funnel. Extract the (2-bromoethyl) benzene into 25 mL of diethyl ether. Separate the two layers, saving both. Extract any remaining product from the aqueous phase twice more using 25-mL aliquots of diethyl ether. Combine the ether extracts and dry over anhydrous magnesium sulfate. Filter the solution from the drying agent and remove the solvent under reduced pressure (i.e. rotary evaporation). The residue contains (2-bromoethyl)benzene and unreacted 2-phenylethanol. Separate the (2-bromoethyl)benzene from the 2-phenylethanol using flash chromatography on silica gel with the same eluting solvent solution as the TLC. Verify that your product is (2-bromoethyl)benzene using ^{1}H-NMR and IR.

Synthesis of 2-phenylethylamine

Conversion of (2-bromoethyl)benzene to (2-azidoethyl)benzene

Dissolve half of the (2-bromoethyl)benzene, synthesized in V-A, in 25 mL of 95% ethanol and pour into a 250-mL round bottom flask containing a magnetic stir bar. Dissolve 2 molar equivalents of sodium azide (NaN_3) in 25 mL of distilled, deionized water and add this solution to the (2-bromoethyl)-benzene solution in the flask. Add solid NaN_3 to the reaction solution in small amounts until the solution is saturated (no more NaN_3 will dissolve). Attach a water-cooled condenser to the flask and reflux the mixture, with constant stirring, for 2–3 hours. When the reaction is complete, remove the reaction flask from the heat and allow the solution to cool to room temperature. Pour the entire solution into an equal volume of distilled, deionized water. A pale yellow oil should form. Extract this oil with three 25-mL aliquots of diethyl ether. Combine the ether extracts and pour into a 250-mL round-bottom flask.

Hydrogenation of (2-azidoethyl)benzene

To the ether solution of (2-azidoethyl)benzene add 1.25 molar equivalents of sodium borohydride ($NaBH_4$). While constantly stirring the mixture, add just enough distilled, deionized water to start the hydrogenation reaction (small bubbles of gas will evolve from the solution). When the reaction is complete (no more gas evolution), separate the ether solution from the water using a separatory funnel. Dry the ether solution over anhydrous magnesium sulfate. Filter the solution from the drying agent and remove the ether under reduced pressure (i.e. rotary evaporation). Verify that your product is 2-phenylethylamine using ^{1}H-NMR and IR.

Synthesis of Hydrocinnamic Acid via Grignard Reaction

Place a 250-mL round-bottom flask, a compatible claisen adapter, water-cooled condenser and addition funnel in a glassware drying oven until rigorously dry, preferably overnight. Working quickly to minimize exposure to moisture, weigh out 1.1 molar equivalent of magnesium metal (compared to half of the (2-bromoethyl)benzene). Polish the metal if necessary, cut into small pieces and add the pieces to the dry round bottom flask containing a magnetic stir bar. Add 25 mL of dry diethyl ether and a small crystal of I_2(s) to the flask. Connect the claisen adapter, condenser, and addition funnel (stopcock closed) to the flask. Turn on the condensing water and stir the magnesium and iodine to activate the surface of the magnesium. While the magnesium is stirring, dissolve half of the (2-bromoethyl)benzene synthesized in **V-A** in 25 mL of dry diethyl ether and pour into the addition funnel (stopcock closed). Add the ether solution of (2-bromoethyl)benzene dropwise to the magnesium. Carefully watch for signs of reaction. The formation of the Grignard reagent should be exothermic enough for the solution to reflux without adding additional heat. After the reaction is complete, disassemble the apparatus and pour the contents of the flask onto ~10 g

www.ebook3000.com

of crushed dry ice, CO_2(s). Cover the vessel with a watch glass and allow this mixture to sit until all of the dry ice has sublimed. Quench any remaining Grignard reagent by pouring the reaction solution over ~40 g of crushed ice containing 5 mL of concentrated HCl. When all of the ice has melted, pour the ether and water into a separatory funnel and discard the aqueous phase. Wash the ether solution with two portions of distilled, deionized water. Extract the hydrocinnamic acid from the ether by shaking the ether solution with an ~20 mL of 5% NaOH(aq) twice. Combine the basic aqueous extracts and neutralize by adding small portions of concentrated HCl. Hydrocinnamic acid should precipitate from the neutral aqueous solution. Collect the hydrocinnamic acid by vacuum filtration and wash with distilled, deionized water. Verify that your product is hydrocinnamic acid using ^{1}H-NMR and IR.

Synthesis of 1-methoxy-4-propylbenzene

Friedel-Crafts acylation of anisole

Working in a fume hood, pour 1 g of anisole into a 100-mL round-bottom flask containing a magnetic stir bar. Add 20 mL of propionic anhydride and 4 mL of 85% aqueous phosphoric acid to the anisole. Attach a water-cooled condenser to the flask and reflux, with constant stirring, the solution for 2–3 hours. After the reaction is complete, pour the contents of the flask, except the stir bar, over ~60 g of crushed ice. Stir the mixture to dissolve the ice and then make the solution basic by adding freshly powdered sodium hydroxide, NaOH(s). Using a separatory funnel extract the 4′-methoxypropiophenone with two 25-mL aliquots of diethyl ether. Combine the ether extracts and dry over anhydrous magnesium sulfate. Filter the solution from the drying agent and remove the solvent under reduced pressure (i.e. rotary evaporation). Verify that your product is 4′-methoxypropiophenone using ^{1}H-NMR and IR.

Modified Clemmensen reduction of 4′-methoxypropiophenone

Working in a fume hood, add 3 molar equivalents of granular or powdered zinc metal to the 4′-methoxypropiophenone in a 250-mL round-bottom flask containing a magnetic stir bar. Add 50 mL of distilled, deionized water and 50 mL of concentrated hydrochloric acid to the reaction mixture. Attach a water-cooled condenser to the flask and reflux the mixture for 2–5 hours. Monitor the progress of the reaction by TLC using an eluting solvent solution of 5:1 hexanes:ethyl acetate. When the reaction is complete, remove the flask from the heat and allow the solution to cool to room temperature. Saturate the solution with sodium chloride (add NaCl(s) until no more will dissolve) and extract the 1-methoxy-4-propylbenzene with three 25-mL aliquots of diethyl ether. Combine the ether extracts and dry by adding anhydrous magnesium sulfate. Filter the solution from the drying agent and remove the solvent under reduced pressure (i.e. rotary evaporation). Verify that your product is 1-methoxy-4-propylbenzene using ^{1}H-NMR and IR.

PROCEDURES FOR INHIBITOR EVALUATION

Determination of an Appropriate Tyrosinase Concentration

For the evaluation of enzyme kinetics, there needs to be a sufficient rate of reaction to see changes in rate. Since the amount of enzyme present in a reaction mixture affects the rate, a series of reactions (assays) must be performed to yield a reasonable reaction rate. Kinetics are also influenced by temperature, so all solutions, except the enzyme solution, should be kept in a constant temperature bath set at 25°C to yield the more consistent results. The most consistent results are

Table 2.2. Determination of an Appropriate Tyrosinase Concentration.

	Assays				
Reagent	Tube 1	Tube 2	Tube 3	Tube 4	Tube 5
Buffer	1.35 mL	1.30 mL	1.20 mL	1.10 mL	1.00 mL
L-dopa	0.60 mL	0.60 mL	0.60 mL	0.60 mL	0.60 mL
tyrosinase	0.05 mL	0.10 mL	0.20 mL	0.30 mL	0.40 mL

Table 2.3. Determination V_{Max} and K_M for Tyrosinase.

	Assays				
Reagent	Tube 1	Tube 2	Tube 3	Tube 4	Tube 5
Buffer	1.75 mL	1.45 mL	1.25 mL	1.05 mL	0.85 mL
L-dopa	0.10 mL	0.40 mL	0.60 mL	0.80 mL	1.00 mL
tyrosinase	0.15 mL	0.15 mL	0.15 mL	0.15 mL	0.15 mL

obtained by using a UV-VIS spectrometer that has a constant temperature cell holder.

In this series of assays, the amount of L-dopa will be held constant and the amounts of tyrosinase and buffer will vary. The total volume of the reaction mixture is held constant at 2.0 mL as this is slightly greater than the volume of low volume cuvettes. The spectrometer should be set at 475 nm and allowed to warm up for ten minutes. Zero the spectrometer with a cuvette filled with buffer. This wavelength and zeroing should be used for all assays. A suggested mixing protocol is provided.

In the mixing of the solutions, a clean test tube should be used for each assay. The buffer and the L-dopa may be added to each separate test tube ahead of time and then stored in the constant temperature bath. The tyrosinase should be added immediately prior to the transfer to the cuvette and the spectrometer. Once the cuvette is in the spectrometer observe the reaction for two minutes, recording the absorbance every 10 seconds. Use this data (or the kinetics software on the spectrometer) to determine the initial rate. The target rate is between 0.2 and 0.3 absorbance units per minute. Use the volume of tyrosinase that yields this rate for all subsequent assays.

Determination V_{Max} and K_M for Tyrosinase

In this series of assays the amount of tyrosinase is constant and the amount of L-dopa will vary. The volume of buffer used in each assay will also change to give each reaction mixture a volume of 2.0 mL. A sample protocol is provided, but this should be adjusted to use the appropriate amount of enzyme determined in the previous section.

Use a clean test tube for each assay. Add the tyrosinase to the test tube last, immediately prior to the transfer to the cuvette and the spectrometer. Once the cuvette is in the spectrometer observe the reaction for two minutes, recording the absorbance every 10 seconds. Use this data (or the kinetics software on the spectrometer) to determine the initial rate. The initial rates are then used in a Lineweaver-Burk analysis to determine V_{Max} and K_M.

Determination of an Appropriate Inhibitor Concentration

This series of assays will determine the amount of synthesized inhibitor necessary for sufficient inhibition of the enzyme. In this experiment the amounts of enzyme and L-dopa will be constant for each assay and the amounts of inhibitor and buffer will vary. A sample protocol is provided. Adapt this protocol to use your predetermined amount of enzyme.

Using the amount of tyrosinase determined earlier, determine the amount of inhibitor that will yield 50% of the reaction rate of the uninhibited reaction.

As before, use a clean test tube for each assay, and add the tyrosinase to the test tube immediately prior to the transfer to the cuvette and the spectrometer. Once the cuvette is in the spectrometer observe the reaction for two minutes, recording the absorbance every 10 seconds. Use this data (or the kinetics software on the

Table 2.4. Determination of an Appropriate Inhibitor Concentration.

	Assays				
Reagent	Tube 1	Tube 2	Tube 3	Tube 4	Tube 5
Buffer	1.15 mL	0.85 mL	0.65 mL	0.45 mL	0.25 mL
L-dopa	0.60 mL	0.60 mL	0.60 mL	0.60 mL	0.60 mL
Inhibitor	0.10 mL	0.40 mL	0.60 mL	0.80 mL	1.00 mL
tyrosinase	0.15 mL	0.15 mL	0.15 mL	0.15 mL	0.15 mL

www.ebook3000.com

Table 2.5. Determination of the Type of Inhibitor.

	Assays				
Reagent	Tube 1	Tube 2	Tube 3	Tube 4	Tube 5
Buffer	1.50 mL	1.20 mL	1.00 mL	0.80 mL	0.60 mL
L-dopa	0.10 mL	0.40 mL	0.60 mL	0.80 mL	1.00 mL
Inhibitor	0.25 mL	0.25 mL	0.25 mL	0.25 mL	0.25 mL
tyrosinase	0.15 mL	0.15 mL	0.15 mL	0.15 mL	0.15 mL

spectrometer) to determine the initial rate and the amount of inhibitor to use in subsequent assays.

Determination of the Type of Inhibitor

In this series of assays, the amounts of inhibitor and the tyrosinase will be constant and the amounts of the L-dopa and the buffer will vary in order to determine the effect of the inhibitor on V_{Max} and K_M. A sample protocol is provided. Adapt this protocol to use your predetermined amount of enzyme and amount of inhibitor.

As before, use a clean test tube for each assay, and add the tyrosinase to the test tube immediately prior to the transfer to the cuvette and the spectrometer. Once the cuvette is in the spectrometer observe the reaction for two minutes, recording the absorbance every 10 seconds. Use this data (or the kinetics software on the spectrometer) to determine the initial rate and the amount of inhibitor to use in subsequent assays. The initial rates are then used in a Lineweaver-Burk analysis to determine the new V_{Max} and the new K_M. The manner in which V_{Max} and K_M are affected will indicate the manner in which the inhibitor interacts with the enzyme.

PROBLEMS

1. The three potential inhibitors synthesized in this lab are substrate structural mimics. Which type of inhibitor are structural mimics most likely to be? Why?
2. One of the potential tyrosinase inhibitors is based on anisole. However, tyrosine contains a phenol group and not a methoxy group. Why did you use anisole instead of phenol in the Friedel-Crafts acylation reaction?
3. To synthesize 1-methoxy-4-propylbenzene you first performed a Friedel-Crafts acylation on anisole and then reduced the acyl group to an alkyl group. The addition of an alkyl group to anisole could potentially have been accomplished via Friedel-Crafts *alkylation*. Using a mechanistic explanation, describe why you did not perform the alkylation reaction.
4. Methoxy groups are ortho/para directing during electrophilic aromatic substitution. Why is the amount of 2′-methoxypropiophenone formed?
5. Typically, V_{Max} and K_M of an enzyme-catalyzed reaction are determined by interpolation from a graph of the kinetics data ($1/V_0$ versus $1/[S]$). However, V_{Max} and K_M can be determined mathematically from the Lineweaver-Burk equation. Describe how you would perform these calculations.
6. Do each of the three potential inhibitors of tyrosinase show inhibition activity? Using your kinetics data, determine which type of inhibitor each compound is. Explain.
7. What data would be necessary in order to determine the K_I values for the inhibitors? How would you collect this data? What equation would you use to calculate the K_I values?

BIBLIOGRAPHY AND FURTHER READING

Ashley, J.N.; Barber, H.J.; Ewins, A.J.; Newberry, G.; Self, A.D.H. *J. Chem. Soc.* **1942**, 103–116.

Boyer, R.F. *Modern Experimental Biochemistry,* 3rd ed.; Prentice Hall: Upper Saddle River, New Jersey, 2001.

Bulavka, V.N. Reduction of alkylarylketones to alkylbenzenes with zinc dust and hydrochloric acid: comparison with zinc amalgam reduction. *8th International Electronic Conference on Synthetic Organic Chemistry*. November 1–30, 2004.

Farrell, S. O.; Taylor, L. E. *Experiments in Biochemistry: A Hands-On Approach,* 2nd ed.; Thomson Brooks/Cole: Belmont, California, 2006.

Nelson, D. L.; Cox, M. M. Lehninger: *Principles of Biochemistry,* 4th ed.; W. H. Freeman and Company: New York, 2005.

Smith, P.A.S.; Brown, B.B. *J. Am. Chem. Soc.* **1951**, 73, 2435–2437.

www.ebook3000.com

Determination of the Heat of Combustion of Biodiesel Using Bomb Calorimetry: A Multidisciplinary Undergraduate Chemistry Experiment

KEITH B. RIDER, STEPHEN M. AKERS, JEREMY L. CONKLE and STEPHANIE N. THOMAS
Department of Chemistry and Physics, Longwood University

LEARNING OBJECTIVES:

- Learning about biodiesel synthesis
- Learning about fuel testing and standards
- Planning for an extended series of experiments

INTRODUCTION

DURING the oil shortage of the 1970s, there was an effort to find ways to relieve America's fossil fuel dependence and find ways of producing a sustainable supply of fuel for cars and trucks. Some suggested using vegetable oil in diesel engines, which does work (Rudolf Diesel's first engines ran on peanut oil), but vegetable oil turns rancid and clogs engines with sooty deposits called coke. Currently, concern about the greenhouse effect, as well as instability in our oil supply, has renewed interest in plant-derived diesel fuel substitutes like ethanol and biodiesel.

Biodiesel is a diesel fuel substitute made from used fry-vat oil that eliminates or minimizes the problems with using vegetable oil as a motor fuel, but maintains many of the environmental benefits. Biodiesel will not turn rancid due to bacterial action when it is in storage, but when it is spilled in soil, the combination of soil microbes and moisture cause it to biodegrade rapidly. Unlike vegetable oil, which clogs the engine with coke, biodiesel burns completely, which reduces the hydrocarbon emissions of the engine.[1,2] As you will find in this experiment, the heat of combustion of biodiesel is less than that of petroleum diesel. One would expect to see a corresponding decrease in the power output of an engine burning biodiesel, but the oxygen content of biodiesel makes it burn more completely, which partially mitigates the power loss. Sulfur dioxide is a major cause of acid rain, so petroleum diesel has to be processed to reduce sulfur to 0.05% or less. Vegetable oil contains no sulfur, so biodiesel-fueled engines produce very little sulfur dioxide.[3] Finally, burning biodiesel releases less carbon dioxide into the atmosphere than burning petroleum diesel. Both fuels produce carbon dioxide as the byproduct of combustion, but the process of growing plants to produce vegetable oil removes carbon dioxide from the air. The end result is that producing and using biodiesel releases about 50% to 78% less carbon dioxide than producing and using petroleum diesel.

Of course, there are some significant drawbacks to using biodiesel. The most serious problem preventing widespread use of biodiesel is our limited capacity for producing vegetable oil. If we grew enough oil-producing crops to satisfy all of our fuel needs, there would not be enough arable land left for food production. Biodiesel burning engines also produce 10% to 20% more nitrogen oxides than similar engines burning petroleum diesel. Nitrogen oxides are a source of acid rain and a major contributor to urban smog. Most engines do not need any modification to run on biodiesel, but some types of rubber degrade when they

are exposed to it. Low temperature performance is another problem; biodiesel becomes thick and begins to solidify at a much higher temperature than petroleum diesel. The current solution to these problems is to blend 20% biodiesel with 80% petroleum diesel. This mixture, called B20, is available at 600 service stations in the United States and is being used in hundreds of unmodified fleet vehicles.

DESCRIPTION OF THE EXPERIMENT

In this experiment you will be synthesizing biodiesel from used cooking oil. This synthesis involves a transesterification reaction. In this type of reaction the alkoxy group of one ester is exchanged with that of an alcohol to form the desired ester product. The reaction you will be performing is expressed in the equation in Scheme 3.1.

The R- groups in the vegetable oil and the fatty acid ester represent hydrocarbon chains containing 15 to 20 carbons and may have one or more double bonds.

Once you have obtained your biodiesel product, you will be performing several tests to determine the viability of biodiesel as a fuel source by comparing it to petroleum diesel. The first test will be finding the heat of combustion through bomb calorimetry. The heat of combustion is a measure of the amount of energy released when a substance is burned in an oxygen-rich environment.

Another element in determining the viability of an alternative fuel source is the cloud point. When diesel or biodiesel is cooled, wax crystals begin to form.[4] The temperature at which this occurs is known as the cloud point. In order to determine cloud point, you will find the transmittance as a function of temperature using UV-Visible spectroscopy. To calculate cloud point values, you will create a plot of the transmittance (λ = 540 nm) as a function of the sample temperature. The cloud point occurs in the temperature range where the transmittance rapidly decreases toward zero[5]. The value of the cloud point can be defined as the inflection point of a curve that represents the gathered data. You will fit the data generated from each cloud point trial with a polynomial function. You will find the inflection point of this polynomial in the range where the transmittance decreases rapidly toward zero. Set the second derivative equal to zero, and determine the root of the function. This will correspond to your cloud point.

You will also find the density for each sample by accurately pipetting known volumes of fuel into a beaker and weighing them on an analytical balance.

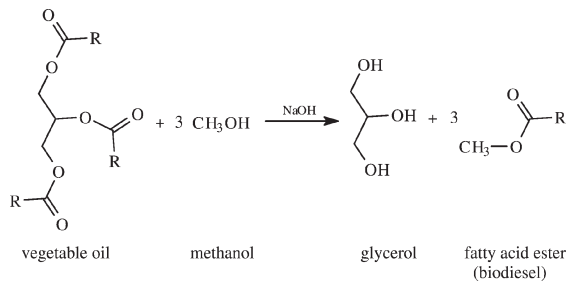

Scheme 3.1. Transesterification of vegetable oil.

HAZARDS AND SAFETY PROCEDURES

Wear safety goggles at all times when you are working in the lab. Hot vegetable oil and methanol are flammable; do not handle them near open flame. Sodium hydroxide is caustic; wear gloves when handling it. The bomb calorimeter uses high-pressure oxygen, which is a very strong oxidizer. Let your instructor show you how to use the gas regulator.

PROCEDURE AND TIMELINE

Week 1—Synthesis of Biodiesel

(Note: Be sure to record all data, calculations, and results in a lab notebook.)

Assemble the following apparatus, lightly greasing all of the ground glass joints: A 500 mL three-necked round-bottomed flask equipped with a condenser, ground glass stopper, a thermometer assembly, and hot plate/magnetic stirrer. See Figure 3.1 for a typical experimental apparatus. Connect tubing to the inlet and outlet of the condenser and begin water flow. Immerse the flask into a hot water bath (65°C), which is heated with a hot plate. To the round-bottomed flask, add 300 mL of filtered cooking oil,[1] methanol (methanol/oil 8 mol : 1 mol,[6] and NaOH (1% wt. of

[1]Vegetable oil does not have a uniform molecular weight because it is a natural product. Reference [6] has a table of fatty acids found in many common vegetable oils that can be used to calculate an average molecular weight.

www.ebook3000.com

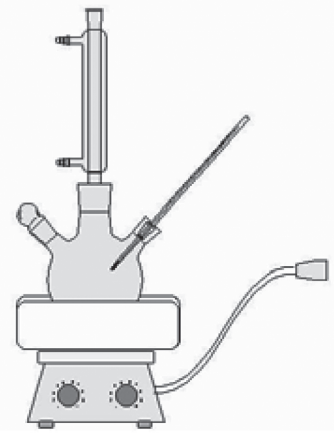

Figure 3.1. Experimental apparatus for biodiesel synthesis.

oil). The NaOH should be dried for at least 24 hours at 100°C to remove water then ground with a mortar and pestle. Allow the mixture to react while stirring for one hour. Carefully remove the bottom glycerol layer by pipetting and then allow the mixture to react for an additional 30 minutes. Transfer the mixture to two separatory funnels (500 mL) and allow them to rest for at least 24 hours. Remove any remaining glycerol from the biodiesel product. Add water dropwise to the mixture and drain the aqueous layer into a clean beaker. Test the pH of the wash water and repeat until a neutral pH is achieved. (*Note:* Do not shake the separatory funnel as an emulsion will result.) Once a neutral pH is attained, drain off any excess water.

Week 2—Determination of Heat of Combustion and Density

The instructions for using the bomb calorimeter are found in the manual. Read them and familiarize yourself with the calorimeter, then ask your instructor to help you load and fire the bomb. Following the instructions for your bomb calorimeter, calibrate the instrument to determine its heat capacity. Weigh out several 0.5000 ± 0.0001 g samples of your biodiesel and petroleum diesel. While samples are running in the calorimeter, determine the density of your biodiesel and the petroleum diesel. Carefully pipette a 10.00 mL sample into a beaker and record the sample's weight to ± 0.1 mg. Calculate the density and repeat at least five times for each sample. Using the information collected from the bomb calorimeter, calculate the heats of combustion for each sample.

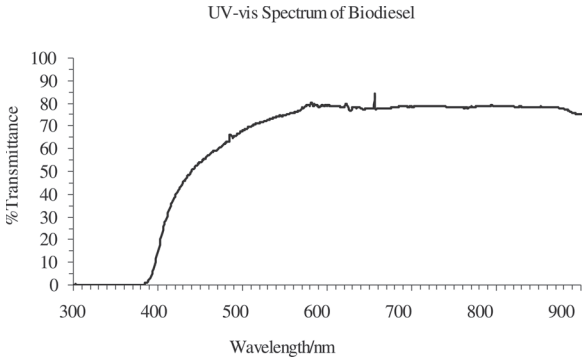

Figure 3.2. The UV-vis spectrum of biodiesel at room temperature.

Week 3—Determination of Cloud Point

Place an aliquot of biodiesel into a plastic or quartz cuvette and place it in the sample holder. (*Note:* Plastic cuvettes are degraded by biodiesel over time, so dispose of them when you are done.) Obtain the UV-Vis spectrum of the sample (300–900 nm) at room temperature. Compare your spectrum with the example data in Figure 3.2. Adjust the temperature controller to 15°C and obtain the spectrum. Repeat step 3 using the following temperatures: 10°C, 5°C, 4°C, 3°C, 2°C, 1°C, and 0°C. Using the data collected, determine the cloud point of biodiesel. Plot the transmittance as a function of temperature and fit the data with a polynomial. Take a derivative of the polynomial and find the temperature that corresponds to the maximum of the derivative; this is the cloud point temperature. The cloud point of the example data in Figure 3.3 is approximately 2.5°C.

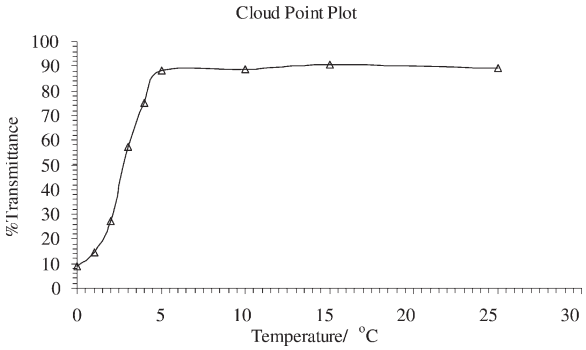

Figure 3.3. Transmittance (λ = 540 nm) of biodiesel as a function of temperature.

WRITTEN ASSIGNMENT OR ORAL PRESENTATION

You will prepare either a written lab report or an oral presentation. Format your written lab report as if it is a manuscript for submission to the *Journal of Physical Chemistry.* Follow the advice and guidelines in *The ACS Style Guide* (found on the Web at www.acs.org) and the Instructions for Authors (found in *J. Phys. Chem.*). Your oral presentation should be approximately 15–20 slides and 20 minutes long.

SUGGESTED READING

Encinar, J. M.; Gonzalez, J. F.; Sabio, E.; Ramiro, M. *J. Ind. Eng. Chem. Res.* **1999**, 38, 2927–2931.

Encinar, J. M.; Gonzalez, J. F.; Rodriguez, J. J.; Tejedor, *A. Energy & Fuels* **2002**, 16, 443–450.

REFERENCES

1. Pacific Biodiesel. www.biodiesel.com (accessed May 2007).
2. National Biodiesel Board. www.biodiesel.org (accessed May 2007).
3. Pouton, M. L. *Alternative Fuels for Road Vehicles;* Computational Mechanics Publications: Boston, 1994.
4. Chevron U. S. A. www.chevron.com (accessed May 2007).
5. Yin, X.; Stover, H. D. H. *Macromolecules* **2003**, 36, 9817–9822.
6. Cyberlipid Center. www.cyberlipid.org (accessed May 2007).

www.ebook3000.com

Aquifer in a Bottle: Detecting Geologic Origin from Bottled Water Chemistry

DOROTHY J. VESPER
G37 Brooks Hall, Dept of Geology & Geography, West Virginia University, Morgantown, WV 26506-6300

LEARNING OBJECTIVES: In this laboratory students will analyze major ion chemistry of several commercial bottled waters and interpret the source of the water from the data. In particular, students will learn about the geochemistry of karst waters.

Analysis of Chemical Parameters in Bottled Water Samples

Water sources can often be identified through the measurement of just a few chemical parameters. In this experiment the students will learn how to measure screening-level parameters such as pH and specific conductance (SC), alkalinity, and calcium and magnesium concentrations.

Calculations of Derived Parameters

The calculation of additional parameters from the chemical data can also be helpful in recognizing water sources. These are to be calculated based on chemical reactions for rock weathering.

Understanding of the Links Between Water Sources and the Geologic Setting

Using the laboratory and calculated values, one will identify likely sources for a selection of bottled waters.

INTRODUCTION

Water and Rock Weathering

THE chemistry of ground water and surface water is controlled primarily by mineral weathering. As rain water interacts with minerals and solids on the land surface or subsurface, chemical reactions occur that change both the solid and what is contained in the water (Figure 4.1). The final water chemistry reflects the solids through which the water flowed.

The chemistry of the final water depends on what minerals are present and what chemical reactions occur. Some reactions which are common in nature:

- Congruent dissolution occurs when a mineral dissolves completely with no solid products:

$$NaCl\ (halite) \rightarrow Na^+ + Cl^- \qquad (1)$$

Halite is table salt and readily soluble in liquids (e.g., in one's kitchen).

- Incongruent dissolution occurs when at least one of the reaction products is a solid:

$$Al_2Si_2O_5(OH)_4\ (kaolinite) + 5H_2O \rightarrow 2Al(OH)_3\ (gibbsite) + 2H_4SiO_4 \qquad (2)$$

The breakdown of clay minerals, such as kaolinite, into hydroxide solids, such as gibbsite, is important to the formation of soils.

- Precipitation occurs when the dissolved constituents in water form a new mineral:

$$Ca^{2+} + CO_3^{2-} \rightarrow CaCO_3\ (calcite) \qquad (3)$$

The formation of stalactites and stalagmites

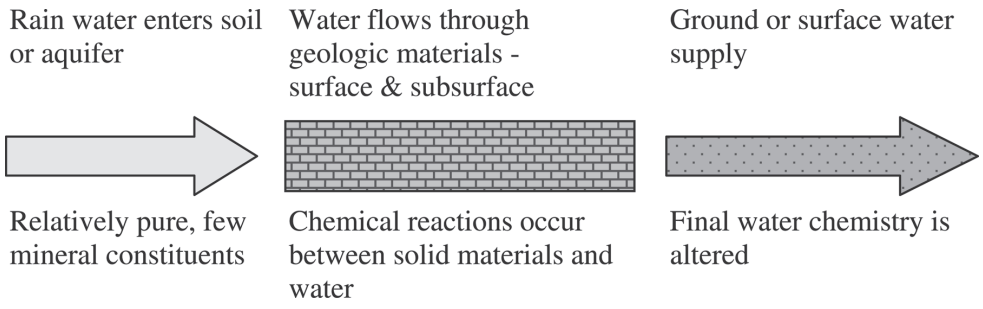

Figure 4.1. Changes in water chemistry due to chemical weathering of geologic materials.

inside caves occurs via the precipitation of calcite. Note that this same reaction, if it progresses from right to left, is the congruent dissolution of calcite which is how caves are formed.

Karst Waters

Karst refers to geologic settings in which the underlying rock is soluble; the rock dissolution results in characteristic surface and subsurface features such as sinkholes, springs, sinking creeks, and caves. Karst topography forms most commonly in areas underlain by carbonate rocks such as limestone and dolomite. Karst water, particularly from springs, is an important source of drinking water worldwide. It has been estimated that more than 20% of the world consumes karst water.[1]

Bottled Waters

Many consumers presume that bottled waters come from natural springs and are healthier than public water supplies. However, neither assumption is always true. Some bottled water sources are springs; however, wells, surface waters, and treated public water supplies are also used. Furthermore, many companies purify, treat or somehow change the water chemistry in the bottling process so that the final product is a poor reflection of the original source water.

The discrepancy between public presumption and fact can lead to confusion and may tarnish corporate images. For example, in 2007, in response to public pressure, Pepsi agreed to label its bottled water (Aquafina®) to indicate that the sources were public water supplies and not natural springs.[2]

THEORETICAL ASPECTS

Screening Parameters pH, Alkalinity and Conductivity

Screening parameters are those things we can be measured using meters or field kits and are readily completed in the field. These tend to be of lower data quality than measurements made with laboratory instrumentation, but they provide a useful means of initial assessment and can be helpful in identifying water sources.

The pH of a solution is a measure of the activity of the hydrogen ion:

$$pH = -\log [H^+] \quad (4)$$

Where $[H^+]$ is the concentration of hydrogen in mol/L. pH values range from 0 to 14. pH 7 defines the neutral point; solutions with pH less than 7 are acidic and those greater than 7 are basic (Figure 4.2). Natural waters can span a wide range depending upon the reactions that occurred (Figure 4.2).

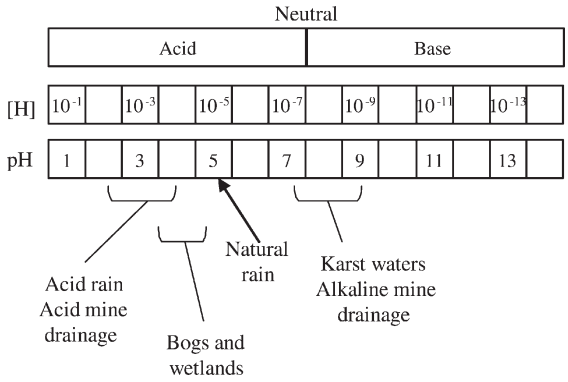

Figure 4.2. pH ranges for waters from different sources. Modified from Andrews et al.,[3] Woof and Jackson.[4]

www.ebook3000.com

If the pH is known, the $[H^+]$ can be calculated by rearranging Equation 1:

$$[H^+] = 10^{-pH} \quad (5)$$

Alkalinity is a measure of the pH buffering capacity in water. A pH buffer is a solution which is resistant to change in pH when either an acid or base is added. Alkalinity is measured by titrating a known volume of solution with a known concentration of acid and monitoring the resultant change in pH.

Conductivity

The electrical conductivity of water is an approximation of its total dissolved solids (TDS) and is measured in units of Siemens (S). Waters can range from fresh (low TDS) to brackish or saline (high TDS). Specific conductance (SC) is measured using a meter and reported in units of µS/cm to account for the geometry of the meter. In karst waters, the SC is directly proportional to the sum of the calcium and magnesium concentrations because they dominate the ion concentration.

Carbonate Rock Dissolution

The two most common carbonate rocks are limestone (mineral calcite), and dolomite (mineral dolomite). Both calcite and dolomite dissolve congruently releasing calcium, magnesium and carbonate into the water:

$$CaCO_3 \text{ (calcite)} \rightarrow Ca^{2+} + CO_3^{2-} \quad (6)$$

$$CaMg(CO_3)_2 \text{ (dolomite)} \rightarrow Ca^{2+} + Mg^{2+} + 2CO_3^{2-} \quad (7)$$

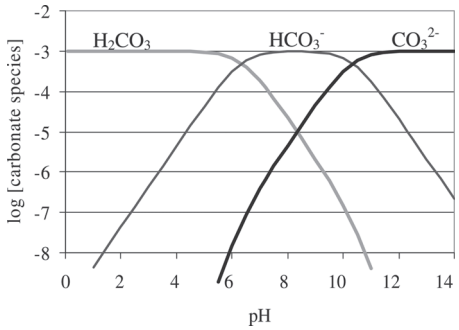

Figure 4.3. Distribution of carbonate species with pH (calculated from data in Drever).[5]

Calcium and magnesium are primarily present in water as the cations Ca^{2+} and Mg^{2+}. However, the carbonate ion (CO_3^{2-}) changes species depending on the pH (Figure 4.3).

Three carbonate species can be present depending on the pH (Figure 4.3). At low pH values, fully-protonated, neutral carbonic acid (H_2CO_3) is the dominant species. At high pH values, the fully-deprotonated carbonate ion (CO_3^{2-}) dominates. In the pH region between those two, the bicarbonate ion (HCO_3^-) dominates.

The carbonate chemistry is further complicated by the addition of inorganic carbon via carbon dioxide (CO_2) gas. The two most common sources of CO_2 are the atmosphere and the microbial breakdown of organic carbon in the soil zone. The later reaction can be simplified as follows using CH_2O as a proxy for organic carbon:

$$CH_2O + O_2(gas) \rightarrow CO_2(gas) + H_2O + \text{energy} \quad (8)$$

The relationship between the inorganic carbonate species is defined by the following reactions and mass action equations in Table 4.1:

Table 4.1. Summary of carbonate reactions.

Reaction Type	Chemical Reaction	Equilibrium Constant at 25°C[5]	Mass Action Equation for Reaction*
Formation of carbonic acid [Rxn 9]	$CO_2 + H_2O \rightarrow H_2CO_3$	$KCO_2 = 10^{-1.47}$	$K_{CO_2} = \frac{[H_2CO_3]}{P_{CO_2}}$
First acid dissociation [Rxn 10]	$H_2CO_3 \rightarrow HCO_3^- + H^+$	$K_1 = 10^{-6.35}$	$K_1 = \frac{[H^+][HCO_3^-]}{[H_2CO_3]}$
Second acid dissociation [Rxn 11]	$HCO_3^- \rightarrow CO_3^{2-} + H^+$	$K_2 = 10^{-10.33}$	$K_2 = \frac{[H^+][HCO_3^{2-}]}{[HCO_3^-]}$

*Brackets designate concentrations of given species in units of mol/L; P_{CO2} is the partial pressure of CO_2 in atmospheres; the concentration of H_2O is 1 and has been canceled from the equation.

In most karst waters, the pH is slightly basic (Figure 4.2) and so the dominant carbonate species is the bicarbonate ion (Figure 4.3). The capacity of the solution to change carbonate species creates a pH buffer. The buffering capacity, or alkalinity, is essentially equal to the bicarbonate concentration in karst waters.

In summary, karst waters can be recognized by the high concentrations Ca^{2+}, Mg^{2+} and HCO_3^-.

Partial Pressure of CO_2 in Water (P_{CO2})

Henry's Law states that the concentration of a gas in solution is directly proportional to the partial pressure of the overlying gas in equilibrium with the solution. The reaction that defines that relationship is:

$$CO_2\ (gas) \leftrightarrow CO_2\ (dissolved) \qquad (12)$$

The dissolved CO_2 rapidly forms carbonic acid which then dissociates (Table 4.1). The P_{CO2} can be estimated by combining the definition of pH with the mass action equations for reactions 10 and 11 above, and rearranging the equation to solve for P_{CO2}:

$$P_{CO2} = \frac{10^{-pH}[HCO_3^-]}{K_1 K_{CO2}} \qquad (13)$$

Where $[HCO_3^-]$ is the alkalinity in mol/L and P_{CO2} is calculated in atmospheres (atm). The excess P_{CO2} (eP_{CO2}) can then be calculated as the ratio of the estimated sample values to the pressure of CO_2 in the atmosphere:

$$excess P_{CO2} = \frac{P_{CO2}(sample)}{P_{CO2}(atmosphere)} \qquad (14)$$

Natural water samples with high P_{CO2} values are generally interpreted as having had a significant interaction with the soil zone. In bottled waters it is possible to have a high P_{CO2} because CO_2 was added in the bottling process (the process of carbonation).

Charge Balance Error

Water has a net neutral charge and therefore the positive charge contributed by the cations must equal the negative charge contributed by the anions:

$$\underset{\text{all cations}}{\Sigma[cation]Z_c} = \underset{\text{all anions}}{\Sigma[anion]Z_a} \qquad (15)$$

Where the brackets are the concentrations in mol/L and z is the absolute value of the charge on the ion. The charge balance error can be calculated as:

$$\text{Charge balance error (in percent)} = \frac{\Sigma[cation]z_c - \Sigma[anion]z_a}{\Sigma[cation]z_c + \Sigma[anion]z_a} \times 100 \qquad (16)$$

If the error is greater than 10%, it is likely that either the data are of poor quality or that the concentration of an important ion was missed in the analysis.

DESCRIPTION OF THE EXPERIMENT

Bottled Water

Four commercially-available bottled water samples were used for the experiment. They were provided to the students in bottles labeled A through D without any other identifying information. On a separate handout, the students were provided with the commercial labels for those samples.

Measurement of pH, Temperature, SC and Alkalinity

Temperature and pH were measured using a Hanna Instrument HI-9025 pH-temperature meter with automatic temperature compensation. The meter was equipped with a HI-1230 gel-filled pH electrode. Prior to use, the pH meter was calibrated with pH buffers at pH 4 and 7. SC was measured using a Hanna Instruments HI-9033 conductivity meter. The meter was calibrated using a 0.01 N KCl solution (1408 µS/cm) prior to use. Alkalinity was measured using a two-endpoint method.[6,7] A Hach Company digital titrator was used to titrate 50 mL of sample with 1.6 N acid to pH endpoints at 4.2 and 3.9. The alkalinity was calculated as follows:

$$\text{Alkalinity (as mg/L } HCO_3^-) = \left(\frac{2B - C}{800}\right)\left(\frac{61{,}000N}{V}\right) \qquad (17)$$

where B is the titrator digits to reach a pH of 4.2, C is the titrator digits to reach a pH of 3.9, N is the normality of the acid (typically 1.6, listed on tube), V is the volume of sample used in mL (typically 50), 800

www.ebook3000.com

converts the titrator reading into mLs (there's 800 clicks/mL), 61,000 is a conversion factor between equivalents of acid and mg/L as HCO_3^-.

Analyzing the Water for Ca^{2+}, Mg^{2+}

Ca^{2+} and Mg^{2+} were measured using a Hach DR/890 pocket colorimeter and Hach method 8030.8 The method uses calmagite, an indicator dye for both Ca^{2+} and Mg^{2+}. The total hardness (Ca^{2+} and Mg^{2+}) is measured by use of the indicator. The Mg^{2+} is measured by re-running the same test but with the Ca^{2+} chelated by EGTA, Ca^{2+} is determined by the difference.

Calculating the Derived Paramters

The P_{CO2} and excess P_{CO2} of each sample were calculated using Equations 13 and 14. The charge balance error was calculated using Equation 16. All parameters were tabulated for comparison.

Identifying Water Sources

The following indicators were used to link water sources to water chemistry.

- The water with the lowest concentrations of Ca^{2+}, Mg^{2+} and alkalinity has been de-ionized (purified) in the bottling process. Its source cannot be determined.
- The water with the highest P_{CO2} is either naturally carbonated or has had CO_2 added in the bottling process. The estimated P_{CO2} decreased over the course of the experiment as degassing occurred.
- The water with a good charge balance and the highest concentrations of Ca^{2+}, Mg^{2+} and alkalinity is the karst water.

Optional: Blind Taste Test

A blind taste test was conducted in conjunction with the laboratory experiment. Students had strong preferences that were not consistent.

PROBLEMS

Acid samples can contain measurable alkalinity. Over what pH range is this possible?

Derive the equation for estimating P_{CO2}.

How could one identify a karst water from a dolomite source versus one from a limestone source?

Why should the charge balance be good for a carbonate water source?

If one samples a glacial water source, what would be expected to find with regards to Ca, Mg and P_{CO2}?

SUGGESTED READINGS

Drever, J.I. *The Geochemistry of Natural Waters, Surface and Groundwater Environments, Third Edition,* Upper Saddle River, NJ, Prentice Hall, **1997**.

Hem, J.D. *Study and Interpretation of the Chemical Characteristics of Natural Water, 3rd Edition,* Alexandria, VA, United States Government Printing Office, **1986**.

LaMoreaux, P.E.; Tanner, J.T. *Springs and Bottled Waters of the World. Ancient History, Source, Occurrence, Quality and Use,* Berlin, Springer, **2001**.

White, W.B. *Geomorphology and Hydrology of Karst Terrains,* New York, Oxford University Press, **1988**.

REFERENCES

1. Ford, D.; Williams, P. *Karst Hydrogeology and Geomorphology, 2nd Ed.,* West Sussex, England, John Wiley & Sons Ltd., **2007**.
2. CBS News, *Aquafina Labels To Show Source: Tap Water, Corporate Accountability Group Pushes Company To Change Labels To Show Water Is From Public Sources.* New York, **2007**.
3. Andrews, J.E.; Brimblecombe, P.; Jickells, T.D.; Liss, P.S.; Reid, B.J. *An Introduction to Environmental Chemistry, 2nd Edition,* Malden, MA, Blackwell Publishing, **2004**.
4. Woof, C.; *Jackson, E. Field Studies* FSTUBX **1988,** 7(1), 159.
5. Drever, J.I. *The Geochemistry of Natural Waters, Surface and Groundwater Environments, Third Edition,* Upper Saddle River, NJ, Prentice Hall, **1997.**
6. American Public Health Association, 2320 Alkalinity. In *Standard Methods for the Examination of Water and Wastewater, Seventeenth Edition,* American Public Health Association: Washington, **2000**; 35.
7. Thomas, J.F.J.; Lynch, J.J. *JAWWA* **1960**, 52(2), 259.
8. Hach Company. *DR/890 Colorimeter Procedures Manual,* Loveland, CO, **2004**.

INSTRUCTOR'S RESOURCE

Pedagogy and Teaching Notes

Potential Bottled Waters

- Perrier® or San Pellegrino®—both of these have a high P_{CO2}; San Pellegrino has a higher SC of the two.
- Aquafina® or Dasani® for de-ionized water. These are identified by low values for all parameters.
- Nova Blue® for karst water (from Roaring Spring, PA). Charge balance should be good using these parameters.

$$[Ca^{2+}] + [Mg^{2+}] = 2[HCO_3^-]$$

- Fiji Water® is a Si-HCO_3 water, however it unlikely that it can be distinguished from the karst water in this experiment.

Some useful information can be found about bottled waters at:

http://www.finewaters.com/Bottled_Water/Index.asp
http://www.bottledwaterstore.com/products.htm

Some additional waters that could be included for comparison:

- The local drinking water
- Local rainwater
- A bottled water from a glacial source

Alternative Methods

Alkalinity can be measured using various techniques; ones that use pH meters (rather than color indicators) are preferred. The titration endpoint can be a single value (4.5), double values (4.2 and 3.9), or based on the inflection point of the titration curve. The National Field Manual for the U.S. Geological Survey has a helpful chapter on alkalinity:

http://water.usgs.gov/owq/FieldManual/Chapter6/section6.6/

Calcium and magnesium concentrations can be measured using field kits such as those produced by Hach Company, colorimetric or spectrophotometric methods (some of which are used with test kits), ion specific electrodes, or more complex laboratory instrumentation such as inductively-coupled plasma atomic emission spectroscopy (ICP-AES). The accuracy of the students' answers will depend on the selected instrumentation.

Potential Problems

The high-P_{CO2} samples may degas over the laboratory period changing the answers obtained by the students. If the students track the time at which they analyzed the samples, the degassing could be graphed to explain what happened.

www.ebook3000.com

Green Chemistry: The Marriage of Wood and Wine

BRUCE BEAVER, PAUL KOLESAR, BRIAN ZLOBECKI, SCOTT SAJDAK and MITCHEL FEDAK
Department of Chemistry & Biochemistry, Duquesne University, Pittsburgh, PA 15282

LEARNING OBJECTIVES: In this experiment, students learn (or re-learn) a number of technical skills: pipette use; liquid-solid extraction; and distillation. They learn how to use gas chromatography with mass spectrometric detection (GC/MS): how to set up and use the instrument independently, how to acquire data and interpret both chromatograms and mass spectra, how to integrate peaks, how to calibrate the instrument, and in short, how to run quantitative GC/MS. They also are exposed to "extra-chemical" concepts, including worst-first forestry, the concept of vocation, and the social and environmental impact of chemistry.

INTRODUCTION

In Wendell Berry's 1996 essay, *Charlie Fisher*,[1] Berry discusses the importance of horse logging to the field of restorative forestry. Correcting a forest's past mismanagement is the goal of restorative forestry. Much of the forest in the United States has been significantly abused through past management practices.[2] Restorative forestry, also known as *worst first forestry*, involves the partial removal (~20%) of the lowest quality trees from a forest every decade or so. This practice tends to promote the health and vigor of the remaining forest. In addition, this approach provides the best genetic seed stock for forest regeneration. The best example of the positive effects on forest health after 150 years of practicing this type of forestry is the Menominee tribal forest in Wisconsin.[3]

People in the restorative forestry profession have chosen to follow their personal vocation and leave more lucrative and comfortable jobs as conventional loggers; instead they typically work with horses to log in a manner that restores and promotes forest health. The primary reason why horses are generally used, rather than a mechanical skidder, is economics. Since *worst first forestry* is practiced, not much money is generated from the initial timber sales. Consequently, the advantage of using horses, as opposed to a skidder, is that horses are cheaper to buy and maintain. However, horses require more skill to train and use in skidding logs and are not as productive (as mechanical skidders) in terms of log volume. On balance, the fact that horse loggers have less money invested in their logging 'equipment' means that they are better able to sustain a reduced profit from a particular logging job. Nonetheless, loggers engaged in restorative forestry tend to earn less money and work harder than conventional loggers; in addition, forest owners who hire horse loggers also make significantly less money on their initial timber sale. Restorative forestry on private land in the US is primarily done because of the personal satisfaction gained in improving the quality of the forest. Although only a tiny fraction of private forest owners and loggers are engaged in restorative forestry, they have chosen to promote forest health regardless of the cost.

In this experiment we will explore how chemistry could in principle be used to support the restorative forestry movement. To be useful, the chemistry must inform us about ways to enhance the value of logs generated while restoring a forest with *worst first forestry.*

Value Added Timber

As previously noted, one of the hurdles of *worst first*

forestry is the low economic value of the low quality timber initially harvested. The economic value of timber is determined by both tree quality and species. The most valuable timber is that which yields the greatest amount of unblemished lumber from a commercially popular species. Currently, Pennsylvania black cherry and red oak are desired world wide for quality furniture, flooring and paneling. Various species of hickory, white oak and maples are less desired and therefore lower value economically. For instance, comparing logs of similar volume and quality, black cherry is currently about nine times more valuable than white oak. Since restorative forestry is economically supported by a portion of the revenue generated by the sale of the logs removed from a particular forest, it is easier to finance the effort if the species removed have more economic value.[4]

Good Wood Good Wine

Wine barrels (cooperage) used for making quality wines are made from white oak. The process starts by cutting unblemished staves from logs. These staves are then allowed to season for 2–3 years outdoors to dry the wood and to allow some important, but not well understood, physical-chemical changes to occur. From the seasoned staves, the barrel is 'raised' by heating over an oak fire with the final step being toasting the barrel's interior. By timing the extent of heating over the oak fire, barrels with differing degrees of toasting can be obtained. A new wine is added to the finished barrel and allowed to age for months to years. After an appropriate degree of barrel aging, the wine is bottled. Gerald Asher, the wine critic for *Gourmet* magazine, explains how oak aging can affect wine quality:

> Oak barrels are not used to introduce the flavor of oak. They are used for an effect that becomes fully apparent only when the wine has been aged for a while in bottle. Though our knowledge of precisely what happens and why is scant, a wine, held in a barrel, changes in ways that are both subtle and complex. . . . Wine aged in wood is less angular (it tastes "rounder"); its components are better integrated (the acidity, tannin, alcohol, and so on are bound more harmoniously); both aroma and flavor are richer and deeper (they seem to be released from within the wine rather than from the surface). Most important of all, however, the time that wine spends aging in bottle is a major factor in the development of those aromas and flavors we call bouquet. [5]

The previous quote identifies the importance of molecules derived from oak in affecting the bouquet of a wine. Four important molecules responsible for contributing to the wood derived portion of wine aroma are shown below.

It is believed that the concentration of *cis*- oak (or whiskey) lactone is extremely important in providing wines with the most pleasing bouquet.[6] An important aspect of the winemaker's skill is reflected in the ability to craft an appealing bouquet by the appropriate marriage of the wood- and grape-derived aromas.

One of the goals of this experiment is to determine

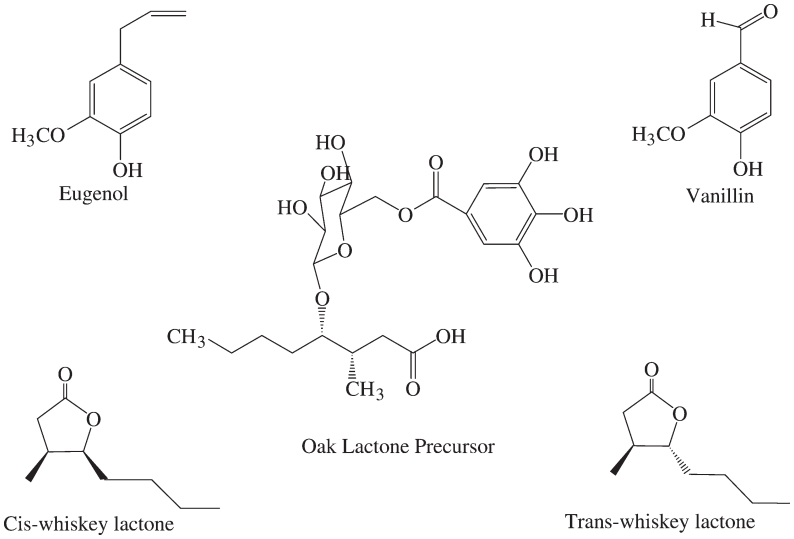

Scheme 5.1. Important molecules in the flavoring of wine from oak barrels.

www.ebook3000.com

whether there are regional populations of white oak that differ in the way they potentially affect wine bouquet. Toasted white oak stave wood from three different regions in the world is examined to estimate its oak-derived bouquet potential. We define a wood's bouquet potential as a quantitative estimate of the capacity of a particular wood to flavor wine with some of the known aroma nuances, namely, the compounds shown above. Wood derived from France, Hungry and the United States are analyzed to determine the concentration of the four compounds shown above.

Wine barrels made from French oak are generally considered by wine makers to be superior and consequently are sold at about twice the price as barrels from other parts of the world. We have previously found the bouquet potential for medium toast French oak to be ~18, 9, 40, and 95 μg/gm wood for *cis*- and *trans*-oak lactone, eugenol and vanillin, respectively. The goal of this experiment is to compare with French oak the potential of Hungarian and American derived oak in terms of their oak derived bouquet potential.

EXPERIMENTAL

Needed Materials

White Oak powder can be purchased at www.midwestsupplies.com. Alternatively, White Oak chips are available at: www.brew-winemaking.com and www.ldcarlson.com. Methanol was spectrophotometric grade and was purchased from Fisher Scientific (Fairlawn, NJ), as were acetone, pentane, dichloromethane, and concentrated 12 M sulfuric acid. 0.01 M KOH was prepared in methanol. Whiskey (oak) lactone, eugenol, vanillin, δ-decanolactone, 2-nonanol were purchased from Sigma-Aldrich (Milwaukee, WI) and were used as received.

GC-MS Conditions

Samples were injected into a Varian 3400 GC-MS. A volume of 0.5 μL of the sample was injected with a Varian 8100 auto-sampler, set with an injector temperature of 200°C. The GC program began with a 60°C hold for 1 minute followed by a column temperature increase of 7°C per minute to the final temperature of 200°C. The column was a Phenomenex, Zebron ZB-5, with a length of 30 m, a 0.25 μm id and a 0.25 μm film thickness. After the 7 minute filament delay, the samples were then scanned for the rest of the 21 minute program by the Saturn II mass spectrometer. The masses were scanned from 50-200 m/z with 3 μscans = 0.5 seconds. The peak threshold was set to one count and samples were ionized at 72 eV in the electron ionization mode. There was no ion preparation and the ion control was set on auto.

Volatile Oak Analysis Options

Toasted white oak chunks can be analyzed in two different ways. The chunks must first be cut into smaller pieces. Then the smaller pieces (chips) can be analyzed as either a powder or as small chips. Previous research[7] has indicated that the most efficient method of oak volatiles analysis involves grinding the chips into a fine powder with a particle size less than 0.5 mm. We use a commercial Wiley Mill with a 40 mesh filter to insure small particle size. However, if a commercial grinder is not available, the larger sized manually produced chips can still be analyzed. An absolute number for the oak volatiles will not be obtained, but similar trends should be seen. If chips are used, instead of using one gram of powder, use 2 grams of chips; this may allow for enough of the desired compounds to elute into the solution. Another alternative is to use commercial toasted oak powder.

Finally, in oak wood there are two different sources of oak lactones: so called *free oak lactones* are simply those dispersed throughout the wood; so called *total oak lactones* are the sum of the free lactones plus any oak lactone precursors which are believed to be the hydrolyzed (i.e. open ring) form of oak lactone ultimately derived from the oak lactone precursor shown earlier.

Time Management Overview

This experiment can be done in two laboratory periods of three hours if very careful time management is practiced. The laboratory instructor will have to run the GC/MS for the standard solutions and provide the students with the experimental data to analyze during the second laboratory period. Students should work in pairs with each group analyzing an oak sample from a specific region. At the end of the experiment the

groups will share their data and the class average concentration for *cis*- and *trans*-oak lactone, eugenol and vanillin from the three different regions will be determined. Our experience has been that the class average values, when composed of at least four separate analyses, has been close to the value obtained by an experienced analyst. This experiment has several hours of dead time while the oak samples are stirring. This time should be used to complete three different activities.

First, each student should learn how to use a micropipette accurately (see procedure below). Once students are proficient at using the micropipette, each group is to prepare standard solutions for a calibration curve. When the different samples for the standard curve are prepared the GC/MS analysis should immediately begin. Finally, all additional 'dead' time should be used to answer the questions at the end of the laboratory.

Step 1: Oak Volatiles Extraction-1[7]

The *free* lactone analysis begins by placing one gram of oak wood powder in a vial with 12 mL of methanol. In addition, prepare another sample for total oak lactone analysis by taking one gram of oak powder in a vial and adding 2 mL of 0.01 M KOH in methanol and 10 mL of methanol. Both solutions are stirred for forty five minutes with a magnetic stir bar on a stir plate at room temperature. Given that the concentrations we are analyzing are in the ppm quantity, great care should be given to pipetting. To insure proper pipetting procedure, it is advised that during the forty-five minute stir, the following pipetting procedure should be completed.

Step 2: Mastering the Pipette (Optional Depending on Experience Level)

Obtain 1000 µL and 100 µL automated pipettes and appropriate pipette tips. An automated pipette is operated by pushing the button on the top of the pipette down to the first stop, placing the pipette in the liquid and slowly releasing the button to aspirate. The liquid is then released by pushing the button down again to the first stop. Expel the final bit of liquid by pressing down to the second stop. Practice drawing deionized water into the pipette and releasing the water back into the solution so that you get a feel for the stops. Once you are comfortable with using the pipette the accuracy and precision of the automated pipettes will be measured. Fill a beaker with at least 50 mL of deionized water. Tare a clean small beaker on the balance. Pipette 1000 µL of deionized water into the beaker, and measure the mass. Repeat this process nine times for a total of ten measurements. You can determine each individual measurement by taring the beaker each time. Record the weights on the data sheet that is provided with this experiment. Do the same measurement with the 100 µl pipette. Calculate the average mass for each and the standard deviation. The instructor should check each students' results in order to determine whether further practice is needed.

Step 3: Oak Volatiles Extraction-2

After the initial 45 min stir is complete, 12 mL of water are added to the free lactone vial and 12 mL of 12 M sulfuric acid are added to the total lactone vial. These solutions are allowed to stir for 1 additional hour. During this hour, a calibration curve can be completed.

Step 4: Calibration Curve for Oak Volatiles

Analysis of the oak derived volatiles will require a calibration curve. This curve should cover the anticipated concentration range of *cis*- and *trans*-oak lactone, eugenol and vanillin.

The calibration curve is prepared by serial dilution of a stock solution. It is suggested that the high-end values of the calibration curve should all be around 2 µg/mL in 100 mL. The stock solution is prepared by adding 4.20 µL of oak lactone, 1.88 µL eugenol and 2.0 mg of vanillin to a 100 mL volumetric flask. Commercial oak lactone is a 50:50 mixture of the *cis*- and *trans*-isomers which means that the amount of total lactone added is equivalent to adding 400 µg of oak lactone; however, being that it is a mixture, it is roughly 200 µg of each the *cis*- and *trans*- isomers. The 100 mL volumetric flask is then filled with spectrophotometric grade acetone. The final stock solution is then diluted into 10 mL samples of various concentrations. The first dilution will be 1 mL of the stock solution, 0.05 µL of γ-decalactone and 0.05 µL of 2-nonanol, the two internal standards, with the rest of the 10 mL volume being filled with spectrophotometric grade acetone. This yields a

www.ebook3000.com

Table 5.1. Concentrations of Dilutions for Calibration Curve.

Volume of Stock Solution (mL)	Concentration of *cis*-whiskey lactone (μg/gram of wood)	Concentration of *trans*-whiskey lactone (μg/gram of wood)	Concentration Of eugenol (μg/gram of wood)	Concentration of Vanillin (μg/gram of wood)
1	20	20	20	20
2	40	40	40	40
4	80	80	80	80
6	120	120	120	120
8	160	160	160	160
10	200	200	200	200

solution with 20 μg per gram wood of each compound of interest. The second dilution will be of 2 mL of the stock solution into a 10 mL volumetric flask. The two internal standards, 0.05 μL of γ-decalactone and 0.05 μL of 2-nonanol are then added with the rest of the volume being filled with spectrophotometric grade pentane. This yields a solution of 40 μg per gram wood of each compound of interest. These dilutions will be repeated for 4 mL, 6 mL, 8 mL and 10 mL of stock solution. A table of concentrations can be seen in Table 5.1.

The standard solutions are immediately set up and run on a GC/MS equipped with an auto-sampler. This data should be provided to the students for the next laboratory period. More experienced students should perform the GC/MS analyses themselves.

Step 5: Adding Internal Standard #1 and Filtering

After the additional hour of stirring has expired, 0.05 μL of internal standard #1, γ-decalactone is added to both the free and total solutions. The wood powder and solvent mixture is then filtered by gravity filtration and the wood is disposed. Each solution is then extracted three times with 10 mL of a solution of 2:1 pentane: dichloromethane and carefully stored until the next laboratory period.

Week 2

Step 6: Simple Distillation

For each sample, the organic layer (pentane/dichloromethane) is dried over anhydrous magnesium sulfate and concentrated to ~8 mL by simple distillation with a Vigreaux column. The second internal standard, 0.05 μL of 2-nonanol is then added. These samples are then analyzed by GC/MS and quantified with the calibration curve constructed in the next step.

Step 7: The Calibration Curve

GC/MS analysis of the standard solutions (from the last lab) yields a calibration curve for each of the four desired compounds, *cis*- and *trans*- oak lactone, eugenol and vanillin. Each chromatogram has 6 different peaks: the 4 compounds and the two internal standards. With GC/MS either GC peak area or intensity of the MS base peak can be used to quantify a compound. Examining Figure 5.1, a sample chromatogram, the peaks from left to right are 2-nonanol, *trans*-whiskey lactone, *cis*-whiskey lactone, eugenol, vanillin, and γ-decalactone. If analysis is performed by MS base peak analysis, the ions chosen for quantification are: *m/z* 69 for 2-nonanol, *m/z* 99 for *trans*- and *cis*-whiskey lactone,

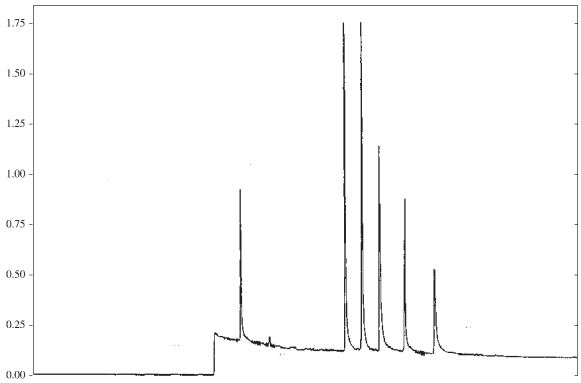

Figure 5.1. Sample GCMS chromatogram for the calibration curve for analysis of *cis*-whiskey lactone, *trans*-whiskey lactone, eugenol and vanillin.

m/z 164 for eugenol, *m/z* 151 for vanillin, and *m/z* 85 for γ-decalactone.

The first step in setting up the calibration curves is to find the data points from each individual injection. It is suggested that the data for the *cis*- and *trans*-oak (whiskey) lactone concentrations are set up as in Table 5.2. Each individual injection (i.e. chromatogram) will yield 2 data points; one point for the ratio of the base peak of *cis*-oak lactone divided by the base peak for internal standard #1 and a similar ratio with internal standard #2. These ratios will be determined for all 6 concentrations of *cis*- oak lactone of the standard curve solutions. Calculations can be determined by following the data in Table 5.2 and can be repeated for the other compounds: *trans*-oak lactone, eugenol and vanillin, as each individual spectrum is interpreted and the ratios of their base peaks versus the intensity of the base peaks of both internal standards are calculated. The ratios of *cis*-oak lactone versus standards 1 and 2 (Columns I and J from Table 5.2) will be plotted versus the concentrations listed in Column H of Table 5.2. Once the points are plotted, a trend line can be added and a slope line can be calculated for internal standard #2, which will be used for the calibration curve. When the calibration curve is plotted for vanillin and eugenol, the standard values of 20, 40, 80, 120, 160 and 200 μg are plotted versus the ratios of the vanillin peak verses internal standard #1 and also versus internal standard #2.

The ratio of internal standard #1 to internal standard #2 from the calibration curve must also be calculated. When an oak wood sample is analyzed, the ratio of its internal standard #1 to internal standard #2 is calculated. This value is then normalized to the average ratio of standard #1/standard #2 values from the calibration curve. An example oak wood sample analysis is shown in Table 5.3.

The correction factor (Column O) is multiplied by the base peak intensity (Column P) for each of the four compounds of a sample. This correction accounts for any loss of the compounds that may occur during filtration and extraction. This usually scales up the values of the desired compounds. This new value is the corrected intensity value (Column Q), which will be divided by the base peak intensity of its internal standard #2 (Column M) to obtain a ratio (Column R). This ratio will then be applied to the equation from the calibration curve and the sample's concentration can be calculated.

Table 5.2. Calibration Curve Data Template.

Column A	Column B	Column C	Column D	Column E	Column F	Column G	Column H	Column I	Column J
Amount (μg) total lactone added	GC-MS Base Peak Intensity Internal Standard #1	GC-MS Base Peak Intensity Internal Standard #2	Col B/Col C Std #1/ Std #2	GC-MS Base Peak Intensity Trans	GC-MS Base Peak Intensity Cis	Col F / (Col E + Col F) % Cis	Col G x Col A Actual Cis	Col F/ Col B Cis/Std #1	Col F/ Col C Cis/Std #2
40	47109	30755	1.5318	6226	5632	0.4750	18.9981	0.1196	0.1831
40	40127	28070	1.4295	5536	5305	0.4893	19.5738	0.1322	0.1890
40	42087	25047	1.6803	4919	4896	0.4988	19.9531	0.1163	0.1955
80	59106	37227	1.5877	17604	15692	0.4713	37.7030	0.2655	0.4215
80	38377	30710	1.2497	14074	12688	0.4741	37.9284	0.3306	0.4132
80	40403	35939	1.1242	15628	12916	0.4525	36.1996	0.3197	0.3594
160	48766	37795	1.2903	64870	47912	0.4248	67.9711	0.9825	1.2677
160	47422	34421	1.3777	58678	46923	0.4443	71.0948	0.9895	1.3632
160	38629	32769	1.1788	58342	43825	0.4290	68.6327	1.1345	1.3374
240	48587	38008	1.2783	100272	75574	0.4298	103.1457	1.5554	1.9884
240	33537	29938	1.1202	85316	60785	0.4160	99.8515	1.8125	2.0304
240	46790	33637	1.3910	95952	72640	0.4309	103.4070	1.5525	2.1595
320	57038	33038	1.7264	155087	110022	0.4150	132.8021	1.9289	3.3302
320	36921	21547	1.7135	111279	80142	0.4187	133.9740	2.1706	3.7194
320	35349	22695	1.5576	116123	84654	0.4216	134.9222	2.3948	3.7301
400	50105	34865	1.4371	172541	132964	0.4352	174.0908	2.6537	3.8137
400	54050	40971	1.3192	185451	133719	0.4190	167.5834	2.4740	3.2637
400	67305	34421	1.9553	191017	141735	0.4259	170.3791	2.1059	4.1177

Average ratio std 1/std#2 *Correction Value* (Column D) = 1.4416

www.ebook3000.com

Table 5.2. Example Calculation of Oak Wood Samples Using the Correction Factor.

Column K	Column L	Column M	Column N	Column O	Column P	Column Q	Column R	Column S
	GC-MS Value	GC-MS Value	Col L / Col M	Correction Value/ Column N	GC-MS Value	Column O*/ Column P	Column Q/ Column M	Value obtained from slope of Cis/Std #2 on Calibration curve
Sample	Std#1	Std #2	Std#1/#2	Correction Value =1.44/ (Std#1/#2)	Cis	Corrected = Cis* Correction Factor	Corr/std2	
AF	3429	7787	0.44	3.27	4694	15367.04	1.97	92.39
AT	2393	7456	0.32	4.49	4188	18811.11	2.52	113.53
HF	11258	15850	0.71	2.03	150	304.44	0.02	17.23
HT	3227	9137	0.35	4.08	46	187.76	0.02	17.28
FF	4314	8230	0.52	2.75	633	1740.88	0.21	24.63
FT	2838	7182	0.40	3.65	577	2105.01	0.29	27.77

Analysis of the free lactone number will give values for the free cis-oak lactone, the free *trans*-oak lactone, eugenol and vanillin. The analysis of the total lactone sample will yield the data needed for determining the concentration of the *cis*- and *trans*-oak lactone precursor. The eugenol and vanillin values are taken from the free analysis because of the acid used in the total method may alter the actual concentration of the eugenol and vanillin found in the sample. Because the total method will hydrolyze the precursors into their respective lactones, the values of the *cis* and *trans* whiskey lactones will be higher than the values obtained by the free analysis. The free number can then be subtracted from the total number to yield a concentration for the oak lactone precursor.

QUESTIONS

1. Based on the class results how could regional white oak derived from both the U.S. and Hungry be used to make a barrel affecting wine bouquet similarly to French oak?
2. How might this information positively affect the restorative forestry effort in these regions?
3. Compare your results with those of the class average and comment on any differences.
4. Explain why two different internal standards are used in this experiment.
5. When sodium hydroxide is added to a methanolic solution of oak chips, the oak lactone precursor undergoes sponification. What is the expected product of this reaction? Write a mechanism for this conversion.
6. When the product formed in question five is subject to hydrolysis, with concentrated acid, oak lactone is formed. Write a mechanism for this reaction.

Additional Research

What are the possibilities of supporting the local restorative forestry movement in your region? Could the value of the white oak timber from your region be enhanced by cooperage use? To explore this possibility seek the assistance of your local forestry officials to obtain local oak wood samples.

REFERENCES

1. Wendell Berry, *Charlie Fisher, The Way of Ignorance,* Shoemaker & Hoard, 2005. For additional reading see, Wendell Berry, *Conserving Forest Communities,* http://www.tipiglen.dircon.co.uk/berryfc.html.
2. www.na.fs.fed.us/spfo/pubs/misc/diam_limit_cut/diameter%20limit%20cutting%20screen.pdf.
3. http://www.menominee.edu/sdi/SchabelAndPecore.html.
4. Typically the money derived from the sale of timber to a saw mill is split between the land owner and the logger.
5. Gerald Asher, *Vine Yard Tales,* Chronicle Books, p. 111–112, 1996.
6. Spillman, P. J.; Sefton, M. A.; Gawel, R., *The Contribution of Volatile Compounds Derived During Oak Barrel Maturation to the Aroma of a Chardonnay and Cabernet Sauvignon Wine,* Australian Journal of Grape & Wine Research, **2004**, 10, 227–35.
7. Adapted from, Masson, E.; R. Baumes and J.L. Puech, *Comparison of Direct and Indirect Methods of Measuring Precursors of* β*-methyl-*γ*-octalactone and their application to the analysis of Sessile Oak Wood[Quercus petraea].* Journal of Chromatography A, **2001**, 905, 183–191

www.ebook3000.com

Protein Unfolding Kinetics

MITCHELL E. JOHNSON, SEAN PAWLOWSKI, LAUREN E. MARBELLA, KRISTIN A. DORNON and MEGAN A. HART

Duquesne University, Department of Chemistry and Biochemistry, 600 Forbes Ave., Pittsburgh, PA 15282

LEARNING OBJECTIVES: This experiment, which is based on the protein unfolding experiment by Jones[1], is meant to be an introductory or first-semester experiment for integrated laboratory. It brings together elements of kinetics, the three-dimensional structure of proteins, absorbance and fluorescence spectroscopy, molecular visualization methods, nonlinear curvefitting, statistics, and perhaps most importantly, the art of data collection and analysis. Essentially, the experiment consists of denaturing a protein using a chemical denaturant and following the process of unfolding by spectroscopy. The process itself is relatively simple, as the protein, horse heart metMyoglobin, unfolds following a simple, first order kinetic process. This description applies to the experiment described by Jones; it has been modified to include temperature-dependent kinetics, a more thorough theoretical description of the absorbance and fluorescence traces, statistical assessment of the kinetics of the unfolding, and the application of protein structural visualization tools to help understand the spectroscopy. Consequently, it makes a good experiment for an advanced laboratory that emphasizes cross-disciplinary science.

INTRODUCTION

In proteins, the correctly folded 3-dimensional structure is necessary for proper function; the spongiform encephalopathies (Jacob-Creutzfeld disease, scrappie, mad cow disease, etc.) are examples of diseases that occur when proteins do not fold correctly. Protein folding/unfolding is an area of intense current interest, and there are many spectroscopic techniques for studying the process of protein unfolding[2]: X-ray diffraction[3], NMR[4], fluorescence[3,5], Raman, infrared[6], mass spectrometry[7], and others. Additionally, this is an area of wide focus in computational chemistry[8]. The *Protein Folding Handbook*, in the suggested reading section, is a comprehensive, recent treatise on the field.

This experiment is a very simple, but effective introduction to the subject. Horse heart metMyoglobin (metMb) is forced to denature by acidic guanidine (GuHCl). Because the absorbance spectrum of the heme shifts as the protein is exposed to solvent, a process known as solvatochromism, monitoring the absorbance spectrum is an effective way of observing the gross unfolding process. MetMyoglobin is also fluorescent. It is weakly fluorescent in the native state because the phenylalanine residues are only weakly fluorescent, the tyrosine residues are quenched by the tryptophan residues, and tryptophan residues are either quenched by the heme group or are self-quenched. When the protein unfolds, the residues become too far apart to be quenched, and their fluorescence emission wavelength red-shifts by about 15 nm. Therefore, there is a significant increase in fluorescence intensity upon unfolding, providing a second measurement of the same process as the absorbance measurement. See the Lakowicz book for a discussion of quenching, and the Jones paper for a basic discussion of fluorescence and protein structure.

This experiment involves preparing the solutions, including GuHCl, which must have its concentration calculated from the refractive index of the solution; recording absorbance, fluorescence excitation, and fluorescence emission spectra of the native protein; recording multiple traces of absorbance and

fluorescence kinetic traces at room temperature, until consistent data are obtained; recording spectra of the unfolded protein; recording absorbance or fluorescence kinetic traces at a series of lower temperatures; fitting the data and obtaining kinetic and absorptivity data (see below); and comparing absorbance values with fluorescence values and experimental with theoretical or literature values.

THEORY

Assuming that the system can be described as having only two species, native and unfolded protein, and that the unfolding occurs in a single step, a very simple kinetic analysis results, using *N* for the native or folded species, and *U* for the unfolded or denatured species:

$$N \rightarrow U \tag{1}$$

$$\frac{-dN}{dt} = \frac{dU}{dt} = k[N] \tag{2}$$

Using the common derivation leads to the well-known result:

$$[N] = [N]_i e^{-kt} \tag{3}$$

$$[U] = [N]_i - [N] = [N]_i(1 - e^{-kt}) \tag{4}$$

In the case of the absorbance measurement, both the native and unfolded species absorb at the measurement wavelength of 409.5 nm. While the absorbance of the unfolded species is small relative to the native species, it is non-negligible, so we write:

$$A^{409.5} = A_N^{409.5} + A_U^{409.5} \tag{5}$$

$$A^{409.5} = \varepsilon_N^{409.5} b[N] + \varepsilon_U^{409.5} b[U] \tag{6}$$

and substituting the time-dependent concentrations (and dropping the wavelength superscripts) yields:

$$A(t) = \varepsilon_N b[N]_i e^{-kt} + \varepsilon_U b[N]_i (1 - e^{-kt}) \tag{7}$$

So the general equation for the time-dependent absorbance is:

$$A(t) = \varepsilon_U b[N]_i + (\varepsilon_N b[N]_i - \varepsilon_U b[N]_i)\, e^{-kt} \tag{8}$$

and two simple results emerge:

$$A(0) = \varepsilon_N b[N]_i \tag{9}$$

$$A(\infty) = \varepsilon_U b[N]_i \tag{10}$$

Time dependent kinetic traces are fit to the following equation:

$$y = a_0 + a_1 * \exp(-a_2 * x) \tag{11}$$

Comparison with Equation 8 allows the calculation of "experimental" molar absorptivities. The molar absorptivity of horse heart metMb has been reported to be 188,000 L · $mol^{-1}cm^{-1}$ at 409.5 nm and pH 6.4[1]. This value is used to calculate $[N]_i$, so values of ε_N that differ from the accepted value are evaluated with a view to establishing the quality of the kinetic data. Values of ε_U can be taken to be correctly determined.

EXPERIMENTAL

Chemical denaturant, GuHCl, approximately 7 M in 0.10 M, pH 7 phosphate buffer, was prepared by dissolving sequanal grade GuHCl (Pierce, Rockford, IL), monobasic phosphate, and dibasic phosphate in ultrapure water. The final concentration was determined by measuring its refractive index, calibrated against pure water, at 25°C, and applying the formula[1]:

$$[GuHCl](M) = 60.836 * RI - 81.106 \tag{12}$$

Final concentrations were between 6.5 and 6.9 M for all groups.

1 M monobasic and dibasic phosphate stocks were prepared from their respective potassium salts and ultrapure water, then mixed 2:3 and diluted in ultrapure water to form a 0.10 M phosphate buffer. The pH was determined, and was about 7.0 for most groups. This phosphate buffer was used for all protein solutions.

Protein stock solution was prepared by dissolving 10 mg of metMyoglobin in minimal phosphate buffer. This solution was diluted 30× and an absorption spectrum was obtained (see Results and Discussion). The concentration of protein in the stock solution was determined by assuming that the molar absorptivity at the peak wavelength of 409.5 nm was 188,000 L · $mol^{-1}cm^{-1}$. This protein stock concentration was typically about 150 μM. With the protein and GuHCl concentration known, volume parameters for the

www.ebook3000.com

construction of solutions for the kinetic runs could be calculated. The kinetic runs required a concentration of protein of 5.00 μM and GuHCl of 2.00 M; the remainder of the solution in the cuvette was the 0.1 M phosphate buffer.

To make kinetic runs, the calculated amount of phosphate buffer and GuHCl were mixed in the cuvette by repipetting (absorbance) or stirring and repipetting (fluorescence). For temperature-controlled experiments, the cuvette was equilibrated at the set temperature for a considerable time while repipetting and/or stirring. The calculated volume of protein stock solution was added, the solution was rapidly mixed by repipetting and/or stirring, and the instrumental acquisition was started. Every attempt was made to achieve temporal consistency in starting the kinetics run. Initial runs were made at room temperature, or 25°C. For the temperature dependent experiments, the temperature range spanned 30°C to 5°C in 5°C increments. At least three kinetic traces were acquired for each set of conditions.

Absorbance spectra and kinetic data were obtained on a Cary 3 or Cary 1E double-beam spectrophotometer (Varian, Palo Alto, CA) with thermoelectric temperature control. Buffer was used as the reference solution, and the instrument was zeroed on buffer prior to measurements. For the kinetic runs, the spectral bandpass was 0.5 nm, wavelength was 409.5 nm, and the data collection rate for room temperature was 10 points per second. Fluorescence spectra were collected on a Photon Technology (PTI) QM-1 spectrophotometer with a thermostatted sample cell. For kinetic runs, the excitation wavelength was 280 nm, emission wavelength was 345 nm, and data points were collected once per second with an integration time of 1 s.

Nonlinear curvefitting and statistical analysis of data was carried out using Igor Pro software (Wavemetrics, Eugene, OR). Molecular visualization experiments were carried out in MOE, the Molecular Operating Environment (Chemical Computing Group, Montreal, Quebec, Canada).

RESULTS AND DISCUSSION

Visualization of Fluorophores Embedded in Protein

The purpose of this part of the experiment was to demonstrate the exact spatial relationship between the relevant groups involved in fluorescence and quenching. The X-ray crystallographic parameters for horse heart metMyoglobin (metMb) were downloaded from the protein databank and imported into MOE. The protein was displayed, typically in ribbon form, and the heme, phenylalanines, tyrosines, and tryptophans were highlighted. Important distances were between heme and tryptophans and between the two tryptophans, as these were the most important species in terms of fluorescence[1]. Distances were measured to demonstrate the fact that they were close enough to undergo Förster energy transfer. Figure 6.1

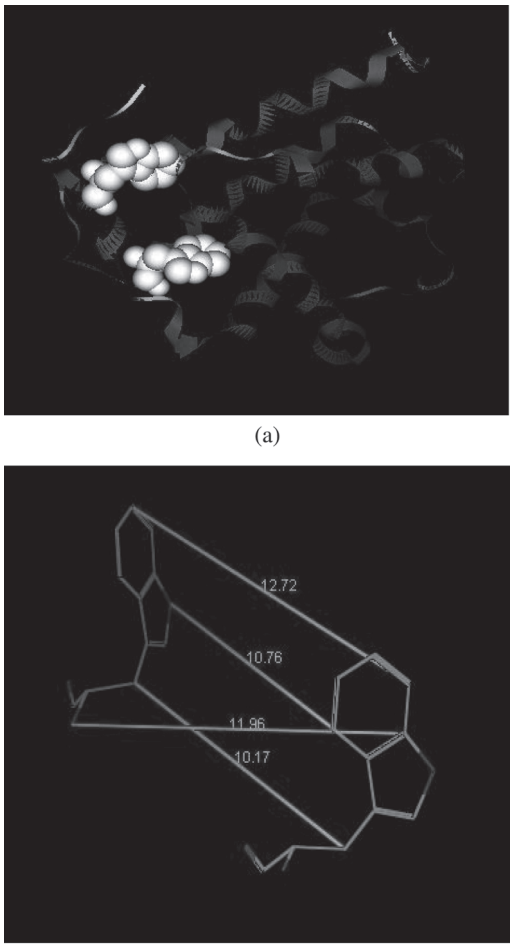

(a)

(b)

Figure 6.1. Representations of horse heart metMyoglobin, rendered in MOE. (a) ribbon diagram of the full protein, with space-filled representation of the two tryptophans (white). (b) line drawings of the tryptophans showing selected distances between atoms in the two tryptophans. Distances in Å.

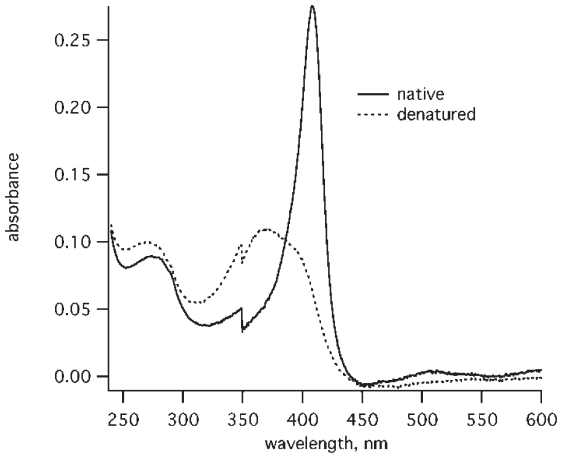

Figure 6.2. Absorbance spectra of native (solid line) and unfolded (dashed line) absorbance spectra of horse heart metMb at an approximate concentration of 3 μM.

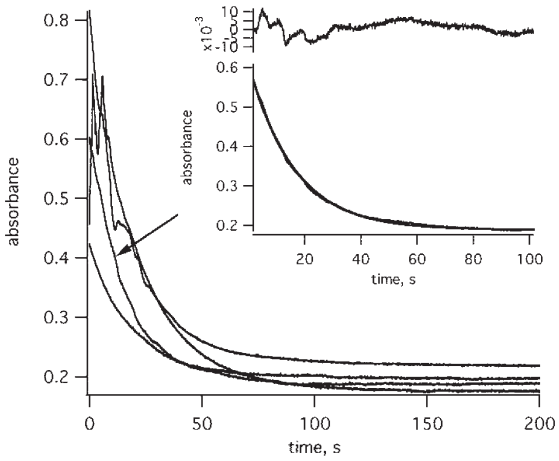

Figure 6.3. Representative kinetic traces (Group 3 data, summarized in Table 6.2) obtained with absorbance spectroscopy. The inset shows a closeup of one particular trace, indicated by the arrow, with the exponential fit and fit residuals.

shows an example of the measurement of the distance between the two tryptophans in metMb. The species involved in fluorescence are only a few nanometers apart, easily within the 50 nm rule of thumb range for Förster energy transfer.

Absorbance Measurements

Figure 6.2 shows example spectra of native and unfolded protein. Peaks can be seen for the protein backbone in the UV at 280 nm and for the heme Soret band just into the visible at 375 nm (unfolded) and 409.5 nm (native). The absorbance of the heme in the folded state was sharper, more intense, and red-shifted, as it was shielded from solvent and held in a more rigid environment. The interaction with solvent molecules-water and GuHCl-upon unfolding broadened the spectrum and increased the energy of the transition. Clearly, the shift in the spectrum and the decrease in intensity were sufficient to enable the observation of the unfolding event. It was also apparent that there was still quite significant absorbance at the wavelength of the kinetic measurement, as discussed above.

Figure 6.3 shows a typical set of absorbance kinetic measurements at room temperature. Note that there was some level of irreproducibility inherent in the measurements, most probably due to mixing issues in the cuvette. All groups had to practice a significant number of times before being able to achieve a reasonable (see below) level of precision. One means of determining whether the data is internally consistent is to assess the quality of the measured absorbance parameters. The theory is outlined above.

Table 6.1 shows a set of absorbance data from recent experiments from two representative groups. The table contains effective molar absorptivities from the native protein, as calculated from the fits to kinetic traces (see the Theory section). The way the sample was prepared (see above), it did not matter what the actual molar absorptivity was; 188,000 L/mol · cm was the value that should have been calculated from the absorbance data when 5 μM was used as the starting concentration.

Table 6.1. Effective molar absorptivities for native metMb (column 1) derived from the absorbance kinetic data for two representative groups, taken at 409.5 nm. See text for details of the calculations. Values represent average absorptivities, and uncertainties are given as standard deviations ($n = 4$). The 4th column is the effective molar absorptivity expressed as a percentage of the theoretical value, 188,000 L/mol•cm. The fifth column is the molar absorptivity of the unfolded protein. %RSD is relative standard deviation.

Group	ε_N (L/mol•cm)	%RSD(ε_N)	%theor	ε_U (L/mol•cm)	%RSD (ε_U)
1	141200±7600	5.4	0.75	50200±2000	4.0
3	125300±31000	25.0	0.67	39000±3800	9.7

www.ebook3000.com

Discrepancies were due to experimental bias. Two basic facts emerged from this data. The absorbance at the beginning of the run was not as great as it should have been based on concentration and molar absorptivity. Therefore, this measurement was taken to indicate that protein had already begun to denature by the time the absorbance measurement was begun. Run to run reproducibility was also something of an issue. Some groups were much better at obtaining highly reproducible results, while others required significant practice before achieving reasonable precision. This points out the value in doing this analysis. This conclusion was reinforced by the finding that the effective molar absorptivity increased with decreasing temperature (though not to 100%, data not shown), as the "pre-measurement" unfolding decreased.

The second to last column in the table represents the measured molar absorptivity of the unfolded protein at 409.5 nm. As all of the protein was clearly unfolded at this point, the only assumptions that needed to be made were that there were no side reactions (unlikely) and that the concentration of the original protein, 5 μM, was accurate. The latter number was based, of course, on using the assumed value of 188,000 L/mol•cm for the molar absorptivity when the stock solution concentration was calculated, so that could be a source of error. It is possible to make more carefully prepared solutions, were a more definitive number desired. For this experiment, the average molar absorptivity of the unfolded protein was an excellent measure of reproducibility of sample preparation between groups. For the cases shown in Table I, a t-test showed that the two average values were significantly different between the two groups. The precision of the absorptivity measurement for the unfolded protein was an excellent measure of the inherent irreproducibility of the process. Note that the precision (%RSD) of the initial absorbance measurement was higher, generally, because it incorporated the imprecision of the mixing as well.

Fluorescence Measurements

Figure 6.4 shows fluorescence spectra of the native and unfolded protein. The native protein was only weakly fluorescent, as discussed above and in Jones[1], because the tryptophan emission was quenched by the heme. The unfolded protein showed intense fluorescence and a red-shifted spectrum. Elimination

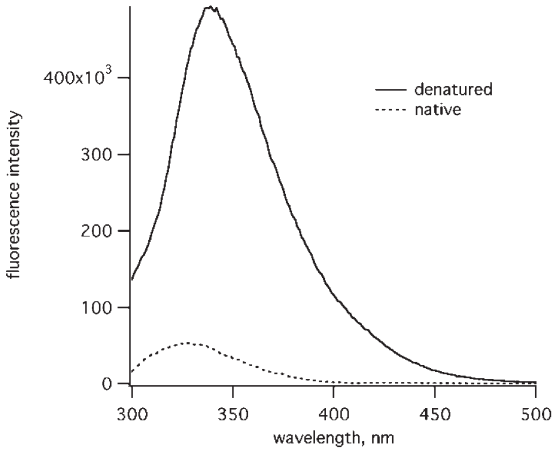

Figure 6.4. Absorbance spectra of native (dashed line) and unfolded (solid line) fluorescence spectra of horse heart metMb at an approximate concentration of 3 μM.

of quenching and exposure to a polar solvent caused the red shift. Monitoring emission at 345 nm certainly allowed the measurement of the rate of unfolding.

Kinetic traces for a set of representative fluorescence kinetic traces are shown in Figure 6.5. Reproducibility of the runs was similar to that found by absorbance, as can be seen by comparing traces at long times, where all the protein has denatured. Initial fluorescence at "zero" time also showed similar irreproducibility to the initial absorbance. While fluorescence could be calibrated to reveal derived

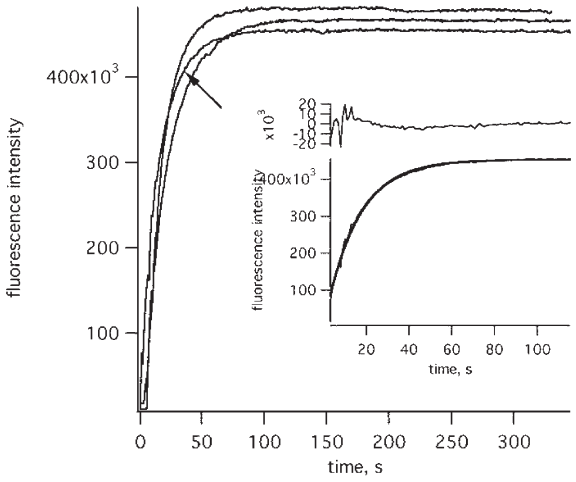

Figure 6.5. Representative kinetic traces (Group 3 data, summarized in Table 6.2) obtained with fluorescence spectroscopy. The inset shows a closeup of one particular trace, indicated by the arrow, with the exponential fit and fit residuals.

Table 6.2. Representative kinetic rate constants (k) for the unfolding of metMb following exposure to 2 M GuHCl. Average rate constants are given with standard deviations ($n = 4$ for absorbance, $n = 3$ for fluorescence). The final column indicates whether the two determined values were significantly different at the 95% confidence level based on a t-test. See text for experimental details.

Group	k (absorbance) (s^{-1})	k (fluorescence) (s^{-1})	Different at 95%?
1	0.0533±0.0093	0.0916±0.0069	Y
2	0.0522±0.0055	0.0558±0.0078	N
3	0.0513±0.0090	0.0587±0.0093	N

values similar to those discussed above for absorbance, such a procedure was not attempted. Figure 6.6 shows a combined plot of fluorescence and absorbance kinetic traces, which demonstrates the fact that, when technique is good, either experiment gives reliable, consistent data.

Kinetics of Protein Unfolding

Table 6.2 shows a summary of recent kinetic data obtained from three groups. Inter-group repeatability was remarkably good, given the demonstrated problems discussed above respecting mixing and the precision of the experiment. The precision of the three absorbance measurements averaged 15% RSD, and t-tests showed no difference among the three groups in terms of the rate constants. Also, except for one group, fluorescence and absorbance yielded rate constants that were statistically indistinguishable. Because careful analysis of the absorbance and fluorescence traces, as discussed above, allowed reasonable assessment of whether technique was good, groups were able to practice until good technique was attained. Consistent results were the consequences.

The data were generally fit quite well with a single exponential, as shown in Figures 6.3 and 6.5. By itself, this observation meant nothing with respect to the order of the reaction. Further data would need to be obtained as a function of protein concentration, but it appeared that the assumption of first order in the theoretical analysis was adequate for obtaining parameters from the data.

Most kinetic processes are temperature dependent. In solution, nearly every parameter that affects the rate of the reaction (solution dielectric constant, viscosity, etc.) is temperature dependent, in a solution-specific manner. Therefore, analyzing temperature dependent solution phase kinetics can be a difficult enterprise. Figure 6.7 shows rate constants from two temperature experiments. Overall, the rates decreased with temperature, though the data were not very reproducible between groups. Simple gas-phase kinetic theory predicts an exponential decay with temperature, with the rate of decay yielding the activation energy. The figure shows exponential fits to the data. The fits are reasonable, but given the imprecision of the data, one would be hard-pressed to defend such a choice. The best that can be said is that the system is well-behaved with respect to

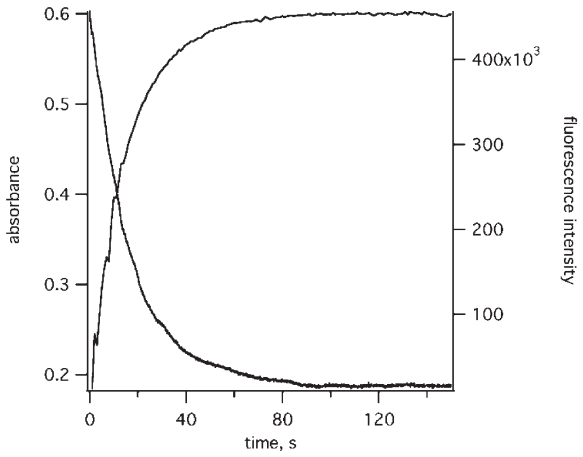

Figure 6.6. The traces from the insets in Figures 6.3 and 6.5, on the same time axis, showing concordance of kinetic data from absorbance and fluorescence spectroscopy.

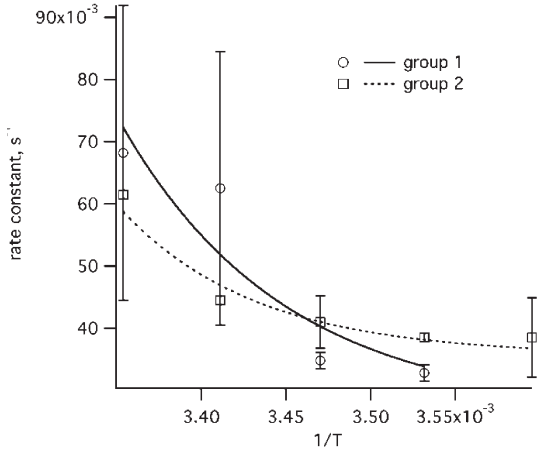

Figure 6.7. Two examples of the decrease in rate constant with temperature.

www.ebook3000.com

temperature. One difficulty with lower temperatures was that the solution viscosity, already high from the GuHCl, increased significantly, and the mixing issue, although mediated by the fact that the reaction rate was lower, was still problematic.

REFERENCES

1. Jones, C. M., Protein Unfolding of metMyoglobin Monitored by Spectroscopic Techniques. *The Chemical Educator* **1999**, 4, 94–101.
2. Kliger, D. S.; Chen, E.; Goldbeck, R. A., Kinetic and spectroscopic analysis of early events in protein folding. *Methods in Enzymology* **2004**, 380, (Energetics of Biological Macromolecules, Part E), 308–327.
3. D'Auria, S.; Staiano, M.; Kuznetsova, I. M.; Turoverov, K. K., The combined use of fluorescence spectroscopy and X-ray crystallography greatly contributes to elucidating structure and dynamics of proteins. *Reviews in Fluorescence* **2005**, 2, 25–61.
4. Korzhnev, D. M.; Kay, L. E., Probing Invisible, Low-Populated States of Protein Molecules by Relaxation Dispersion NMR Spectroscopy: An Application to Protein Folding. *Accounts of Chemical Research* **2008**, 41, (3), 442–451.
5. Michalet, X.; Weiss, S.; Jaeger, M., Single-molecule fluorescence studies of protein folding and conformational dynamics. *Chemical Reviews (Washington, DC)* **2006**, 106, (5), 1785–1813.
6. Arrondo, J. L. R.; Iloro, I.; Garcia-Pacios, M.; Goni, F. M., Two-dimensional infrared correlation spectroscopy. *Springer Series in Biophysics* **2006**, 10, (Advanced Techniques in Biophysics), 73–88.
7. Kheterpal, I.; Wetzel, R., Hydrogen/Deuterium Exchange Mass Spectrometry-A Window into Amyloid Structure. *Accounts of Chemical Research* **2006**, 39, (9), 584–593.
8. Joshi, R. R., A decade of computing to traverse the labyrinth of protein domains. *Current Bioinformatics* **2007**, 2, (2), 113–131.

SUGGESTED READING

Lakowicz, J. R. *Principles of Fluorescence Spectroscopy, 3rd Ed.*, Springer: NY; 2007.

Skoog, D. A.; Holler, F. J.; Crouch, S. R. *Principles of Instrumental Analysis, 6th Ed.*, Thomson Brooks/Cole: Belmont, CA; 2007

Wright, M. R. *An Introduction to Chemical Kinetics*, John Wiley & Sons: Chichester, England; 2004.

Buchner, J. and Kiefhaber, T., Eds. *Protein Folding Handbook (5 volumes)*, Wiley-VCH: Weinheim, Germany; 2005.

INSTRUCTOR'S RESOURCES

Visualization of the overall protein structure, and the relative positioning of the heme group, tryptophans, tyrosines, and phenylalanines with the MOE program is included in the experiment for several reasons. It is a good exercise to get students using MOE to display proteins from the protein data bank (pdb), if they have not already. Having them quantify the distance between amino acids makes them use a set of tools that are easy enough to use, but to which they may not have been exposed. There is a subtle point as well: what is meant by "distance" between tryptophans, for example. Students invariably ask, which allows the instructor to initiate a discussion of why distance is important, and gives them the opportunity to choose their own reason for the interatomic distances they actually report (most of them report an average distance, or several individual distances, between atoms on the aromatic rings). More complex experiments can be devised from this jumping off point. For example, molecular dynamics simulations are currently in use for helping to understand spectroscopic observations of the protein unfolding/folding process (see the *Handbook*), and experiments could be devised to take off on that point. Quantum dynamics could also be relatively reliably performed to demonstrate quenching efficiency among the different groups involved in fluorescence and quenching.

The spectra obtained from folded and unfolded protein are wonderfully illustrative of a number of spectroscopic principles. Solvatochromism is one example, as is the sharpening of a spectrum in a rigid, nonpolar environment. Quenching, excited state dynamics, and quantum yield in fluorescence are others. These topics may or may not find their way into undergraduate instrumental analysis or analytical chemistry courses, or in any case, probably need reinforcement. Are the observed transitions at about 400 nm $\pi - \pi^*$ or $n - \pi^*$? How can one tell? Is the interior of the protein more hydrophobic or less than the buffer the protein is dissolved in? What are the consequences for observing kinetics of unfolding?

One way this experiment can be modified is to use a photodiode array to observe the absorbance spectra. A relatively modern photodiode array, with a sub-s readout time, would be needed, but recording of the

full spectrum allows a number of more sophisticated data treatments to be used for the determination of kinetic parameters. Spectra can be decomposed and kinetic parameters can be determined by multivariate analysis, singular value decomposition, etc.

The other rather obvious way to alter the experiment is to use some kind of stopped-flow accessory for the spectrometer, or have the students construct a stopped-flow apparatus. A very good experiment is to have one or two groups use a stopped-flow accessory and one or two groups do the mixing by hand, and demonstrate more forcibly the issues regarding reproducibility.

SAFETY CONSIDERATIONS

The chemicals used in this experiment pose no unusual hazard. Ordinary safety apparel and good lab practice should ensure student safety.

ACKNOWLEDGEMENTS

Data reported in this chapter were collected by the authors and by undergraduate students Tharina Alexander, Brian Bloom, Austin Bowen, William Minsterman, Meghann Moreau, Michael Nypaver, Zachary Otaibi, Hao Vu, and Amanda Watson.

www.ebook3000.com

Syntheses and Properties of Thiomolybdates and Thiotungstates

PARTHA BASU, ERANDA PERERA, RAGHVENDRA S. SENGAR, MEDHAVI BOLE, JENNA DAGGETT, LAUREN MATOSZIUK and SCOTT SAJDAK
Department of Chemistry and Biochemistry, Duquesne University, Pittsburgh, PA 15282

LEARNING OBJECTIVES: An intensive training of senior undergraduate students in the experimental inorganic chemistry laboratory using inexpensive chemicals and the careful data analysis are the main objectives of this project. This project will expose students to general chemical laboratory techniques used by inorganic and organometallic chemists. They will perform chemical reactions by carefully following procedures using toxic chemicals and compressed gases. Purification techniques like precipitation and recrystallization will also be a major part of the learning process in this project. Hands-on practice on the laboratory instruments like infrared and UV-visible spectrophotometers, and X-ray powder diffractometer will be very useful in building the student's confidence as a chemist.

Preparation of thiomolybdates and thiotungstates. The most common method for synthesizing thiomolybdate and thiotungsate complexes is to react a metal oxide or acid with a sulfurizing agent, e.g., H_2S. Students will learn how different compounds can be synthesized using the same reagents altering reaction conditions. Some of these compounds are kinetically controlled products while others are thermodynamically stable products.

Data collection and analysis of physical measurements of the synthesized compounds. Students will learn how to characterize metal complexes using spectroscopic techniques as well as learn how changes in the anion or cation can affect the physical properties (e.g., infrared spectra, powder diffraction pattern) of the material in the solid state.

INTRODUCTION

SYNTHESIS of new molecules is an essential cornerstone of chemistry. It allows for inquiring into fundamentals of biology and chemistry and opens doors for new applications. Not surprisingly, undergraduate chemistry curricula value new experiments that can be adopted in a laboratory setting. A successful experiment is one that can be easily repeated, cost effective and most importantly that can be used in teaching students.

The chemistry of the transition metal-sulfur complex has been widely utilized in biology.[1] Many metal-sulfur complexes, including those of molybdenum and tungsten, are mononuclear, and can catalyze chemical reactions and/or electron transfer. Prominent examples include the pterin-dithiolene linked to molybdenum centers in sulfite oxidase, and nitrate reductase.[2,3,4] Involvements of tungsten-sulfur complexes in biology, while less common, are known. In some cases the sulfur unit is linked as a terminal sulfido ligand.

Metal sulfides are well known in industrial and commercial contexts. Molybdenum sulfides are used in lubrication, battery technology, and photovoltaic systems. Solid molybdenum disulfide is a naturally occurring lubricant that has properties similar to graphite. Many molybdenum complexes also catalyze important reactions such as hydrodesulfurization. Thus, these materials are significant in biological as well as industrial contexts.

PREPARATION OF STUDENTS

Students must be introduced to the possible hazards

of H_2S gas and the chemicals being used before they perform experiments and must be instructed about proper waste disposal. Proper labeling and storage of synthesized compounds with the appropriate name (or formula) of chemical should be part of general laboratory practice. All the reactions must be performed inside a properly ventilated reaction hood. The required apparatus include Erlenmeyer flasks, measuring cylinders, filtration flasks, beakers, Büchner funnel, volumetric flasks and glass pipettes. Due to the bad smell of sulfur compounds, glassware should be put in a bleach bath (made by adding 1 liter of bleach in 3 liter of water) overnight after use. Training on the UV-visible and IR spectrophotometer, and powder diffractometer, may be helpful for students who are expected to operate them independently. This module works well as a group project where individual students perform specific tasks and share the information, which also increases collaboration.

CHEMICAL AND EXPERIMENTAL HAZARDS

All alkyl halides, molybdenum, and tungsten salts are toxic powders. Hydrogen sulfide (H_2S) is a toxic gas, which can cause permanent injury. Isopropanol (i-PrOH), ethanol (EtOH), and diethyl ether (Et_2O) are flammable liquids. Ammonium hydroxide (NH_4OH) is a toxic liquid. Due to the toxic nature of chemicals used in the reactions, rubber gloves, suitable goggles for eye protection, and laboratory coats must be worn during the experiments.

EXPERIMENTAL PROCEDURE

Synthesis of $[NH_4]_2[MoS_4]$

A mixture of concentrate NH_4OH (60 mL) and H_2O (20 mL) in a 250 mL Erlenmeyer flask is prepared and sodium molybdate $[Na_2MoO_4{\cdot}2H_2O]$ (10 g) is dissolved into this mixture. The solution is filtered using a Büchner funnel and filtration flask and H_2S gas is bubbled rapidly into the reaction mixture for 25–30 minutes. The temperature of the reaction mixture is raised to 60°C (monitored by a thermometer) by placing the flask in the water bath while maintaining a slow stream of H_2S. After 30 minutes of heating, the reaction mixture is cooled in an ice bath for 30 minutes. The red-brown precipitate is isolated by filtration and washed with i-PrOH and Et_2O. The sample is air dried on a petri dish, and stored in a vial. The compound is isolated in ~87% yield.

Synthesis of $[Me_4N]_2[MoS_4]$

A solution of tetramethylammonium chloride $[Me_4N]Cl$ (2.1 g) and NaOH (0.75 g) in H_2O (15 mL) is prepared in a 100 mL Erlenmeyer flask. In another 100 mL Erlenmeyer flask an aqueous solution of $[NH_4]_2[MoS_4]$ (2.5 g in 20 mL) is prepared. The ammonium chloride solution is added to the solution of $[NH_4]_2[MoS_4]$ using a pipette, causing a rapid precipitation of red crystals. The solution is stirred using a glass rod and left on an ice bath for 15 minutes. The precipitate is isolated by filtration and washed with i-PrOH and Et_2O, dried in air and stored in a vial. The target compound is isolated in 60% yield.

Synthesis of $[Et_4N]_2[MoS_4]$

This compound is prepared following the same procedure described for $[Me_4N]_2[MoS_4]$. A solution of tetraethylammonium bromide $[Et_4N]Br$ (4.0 g), and NaOH (0.75 g) in H_2O (20 mL) is reacted with $[NH_4]_2[MoS_4]$ (2.5 g) into H_2O (15 mL) resulting in a rapid precipitation of red crystals. The resulting solution is kept on ice for 15 minutes. In most cases, crystals can be isolated, but in some cases overnight refrigeration is required. The target compound is isolated by filtration and washed with i-PrOH and Et_2O, dried in air and stored in a vial. The target compound is isolated in 82% yield.

Synthesis of $[n\text{-}Bu_4N]_2[MoS_4]$

This compound is prepared as above. A solution of tetra(n-butyl)ammonium bromide $[n\text{-}Bu_4N]$ Br (6 g), and NaOH (0.8 g) in H_2O (35 mL) is reacted with a solution of $[NH_4]_2[MoS_4]$ (2.5 g) in H_2O (40 mL) resulting in a brown gel. To this solution ~100 ml of i-PrOH is added to precipitate a red solid. The solution is cooled for 10 minutes on ice, the red precipitate is isolated by filtration and washed with i-PrOH and Et_2O. The solid is air dried, and stored in a vial. This compound is isolated in 94% yield.

Synthesis of $[Ph_4P]_2[MoS_4]$

This complex is isolated in a similar manner. A

www.ebook3000.com

solution of tetraphenylphosphonium bromide, Ph_4PBr (8 g) in ethanol (25 mL) in a 50 mL beaker is prepared. A solution of NaOH (0.8 g) in H_2O (10 mL) in a 25 mL beaker is prepared and added to the Ph_4PBr solution to prepare a homogeneous mixture. A solution of $[NH_4]_2[MoS_4]$ (2.5 g) in H_2O (35 mL) is prepared in a 100 mL Erlenmeyer flask. The $[Ph_4P]Br$ solution is added to the solution of $[NH_4]_2[MoS_4]$, resulting in a rapid precipitation of an orange solid. The solution is stirred for 20 minutes on the ice bath. The precipitate is isolated by filtration and washed with i-PrOH and Et_2O, dried in air, and stored in a vial. The compound is isolated in 76% yield.

Synthesis of $[NH_4]_2[MoO_2S_2]$

To a solution containing 50 mL of concentrated NH_4OH and 30 mL of H_2O in a 200 mL Erlenmeyer flask, 10 gm of $[NH_4]_6[Mo_7O_{24}]*6H_2O$ is dissolved. The solution is cooled for 15 minutes on an ice bath. H_2S gas is passed slowly over the surface of the reaction mixture resulting in a precipitation of the product. It is important to monitor the flow of the gas in the reaction mixture. Once completed, the reaction flask is covered and kept on ice for 5 min. The target compound is isolated by filtration and washed with EtOH and Et_2O, dried in air, and stored in a vial. The compound is isolated in 81% yield.

Synthesis of $[Et_4N]_2[MoO_2S_2]$

From the stock, 30 mL of 10% solution of $[Et_4N]OH$ solution is prepared. To this solution, 2.0 g of $[NH_4]_2[MoO_2S_2]$ is dissolved. The reaction mixture is then placed under nitrogen for 1 hour to remove NH_3 gas. To this solution, 80 mL i-PrOH and 160 mL of Et_2O is added. This results in a separation of phases. The phases are separated using a separatory funnel, and the oily layer is dissolved in 200 mL i-PrOH. 200mL of Et_2O is then slowly added to this solution leading to the precipitation of crystals. The crystals are filtered, washed with Et_2O, and allowed to dry.

Synthesis of $[NH_4]_2[WS_4]$

20 grams of tungstic acid (H_2WO_4) is dissolved in 160 mL of concentrated NH_4OH in a 200 mL Erlenmeyer flask. At room temperature, H_2S gas is bubbled through this solution until saturation. The temperature of the reaction is raised to 60°C while maintaining a slow stream of H_2S for 8 hours. The reaction mixture is cooled to 10–15°C on ice-water bath while maintaining the H_2S flow. The target compound is isolated by filtration and washed with i-PrOH and Et_2O. The target compound is dried in air overnight and stored in a vial. The compound is isolated in 63% yield.

Synthesis of $[Et_4N]_2[WS_4]$

4.2 g $[Me_4N]Br$, and 1.5 g of NaOH, are dissolved in 25 mL H_2O. This solution is added while stirring to a 60 ml solution of $[NH_4]_2[WS_4]$ (2.0 g). An excess of i-PrOH is added to obtain crystals which are filtered and washed with Et_2O and allowed to dry.

Synthesis of $[NH_4]_2[WO_2S_2]$

In a mixture of 20 mL concentrated NH_4OH and 5 mL H_2O, 5 grams of H_2WO_4 is dissolved in a 50 mL Erlenmeyer flask. This solution is filtered and cooled in an ice bath. H_2S gas is passed slowly over the surface of the reaction mixture resulting in a yellow product. The H_2S flow is maintained for 10 minutes, and the reaction flask kept in the ice bath for another 5–10 minutes. The product is isolated by filtration, washed with i-PrOH and Et_2O, dried in air, and stored in a vial. The compound is isolated in 79% (10 grams) yield.

Synthesis of $[Et_4N]_2[WO_2S_2]$

A solution (7 mL) containing 1.0 g of $[NH_4]_2[WO_2S_2]$ in 10% EtOH in H_2O is prepared. The solution is then placed under nitrogen for 1 hour to remove NH_3 gas. To this solution 40 mL i-PrOH and 80 mL Et_2O is added resulting in two distinct phases. The oil layer is collected and dissolved in 40 mL i-PrOH. To this solution, 40 mL Et_2O is slowly added resulting in a precipitation. Excess i-PrOH and Et_2O were added and the solution cooled to cause precipitation of product. The crystals were filtered and washed with Et_2O and allowed to dry.

RESULTS AND DISCUSSION

Syntheses of Complexes

Synthesis of ammonium salts of tetrathiometallates $[MS_4]$, and dithiometallates $[MO_2S_2]$; M = Mo and W, follow the methods described by McDonald et al.[5] An exhaustive use of H_2S gas is required in these reactions. The synthesis of $[NH_4]_2[MoS_4]$ is kinetically favorable and it requires less time (~30 min) than the synthesis of $[NH_4]_2[WS_4]$ (> 8 hrs). Sluggish formation of $[NH_4]_2[WS_4]$ complex leads to contamination with the oxo-substituted $[NH_4]_2[WOS_3]$ complex, therefore a steady flow of H_2S should be maintained for a prolonged period of time at an elevated temperature.

For $[NH_4]_2[MO_2S_2]$ (M = Mo or W), H_2S gas is passed over the reaction mixture (not through the solution) at a low temperature. Upon completion of the reaction more H_2S gas comes out of the reaction flask which is indicative of the completion of the reaction. Immediate filtration of precipitate under low temperature increases the yield.

In general, tetraalkyl ammonium salts of $[MoS_4]$ are obtained by following the method described by Alonso et al.[6] An overall reaction for the syntheses of tetraalkyl ammonium thiometallates can be written as according to the reaction (1):

$$[NH_4]_2[MoS_4] + 2R_4NCl + 2NaOH \rightarrow [R_4N]_2[MoS_4] + 2NH_4OH + 2NaCl \quad (1)$$

This reaction is setup in two steps: in the first step R_4NCl is treated with stoichiometric amount of aqueous sodium hydroxide to produce Me_4NOH as shown in Equation (2).

$$R_4NCl + NaOH \rightarrow R_4NOH + NaCl \quad (2)$$

In the second step this solution is slowly added to the ammonium salt of the metal sulfide yielding the target alkyl salt of the sulfide (Equation 3).

$$[NH_4]_2[MoS_4] + 2R_4NOH \rightarrow [R_4N]_2[MoS_4] + 2NH_4OH \quad (3)$$

There are some differences in the general procedure described above. For example, $[n\text{-}Bu_4N]_2[MoS_4]$ initially forms as a gel, from which a precipitate is isolated by adding i-PrOH at a low temperature. In the case of $[Ph_4P]_2[MoS_4]$, Ph_4PBr is insoluble in water, therefore, it is first dissolved in ethanol. Then an aqueous solution of NaOH is added into it to form Ph_4NOH. Regardless, these compounds were prepared in good yields. In solid state the color of the samples varies from dark red to light yellow. These compounds are isolated in crystalline state with different morphology.

Infrared Spectra

Infrared spectra of all complexes are recorded in KBr pellet from an energy range of 400 cm^{-1} to 3500 cm^{-1}. Typical M=O and M=S vibration are found in the range from 400 cm^{-1} to 900 cm^{-1} and the values are listed in Table 1. In the solid state $[R_4N]_2[MoS_4]$ complexes, the Mo=S vibration depends on the associated cation $[R_4N]^+$. This is an indication of a cation-anion interaction in the complexes, which affects the crystal packing and ultimately the metal-ligand bond energies. A consistent decrease in the energy of Mo=S vibration going from R=H to bulky R=*n*-Bu indicates a loose crystal packing in $[n\text{-}Bu_4N]_2[MoS_4]$ then $[NH_4]_2[MoS_4]$. The steric effect of $[n\text{-}Bu_4N]^+$ and $[Ph_4P]^+$ is similar as indicated by the same energy of Mo=S vibrations.

Comparison of M=S stretching vibrations in $[NH_4]_2[MoS_4]$ and $[NH_4]_2[WS_4]$ shows a 20 cm^{-1} decrease from Mo to W. This feature is consistent in other congener complexes. For example $[NH_4]_2[MoO_2S_2]$/$[NH_4]_2[WO_2S_2]$ exhibit a similar change in M=S stretching frequency.

Table 7.1. Important metal ligand vibrations.

Compound	M=S	M=O
$[NH_4]_2[MoS_4]$	480	
$[Me_4N]_2[MoS_4]$	473	
$[Et_4N]_2[MoS_4]$	470	
$[n\text{-}Bu_4N]_2[MoS_4]$	468	
$[Ph_4P]_2[MoS_4]$	468	
$[NH_4]_2[WS_4]$	460	
$[NH_4]_2[MoO_2S_2]$	490	860, 840
$[NH_4]_2[WO_2S_2]$	470	885, 845
$[NH_4]_2[MoOS_3]$	485	835
$[NH_4]_2[WOS_3]$	470	860

www.ebook3000.com

Electronic Spectra

Electronic spectra of aqueous solutions of all complexes, except $[Ph_4P]_2[MoS_4]$ for which a methanolic solution was used, were recorded. The peak positions with molar absorptivities are tabulated in Table 7.2.

The electronic spectra showed no peaks higher in energy that 470 nm suggesting that there are no d–d transitions. This is consistent as in all cases the metal ions are in a highly oxidized +6 state. As mentioned, often synthesis of $[WS_4]^{2-}$ salts have $[WS_3O]^{2-}$ as an impurity. Such contamination is easily identified by the UV spectra of $[WS_4]^{2-}$. The major peak for $[WS_3O]^{2-}$ compounds comes at a 334 nm, which corresponds to a minimum in the spectra of $[WS_4]^{2-}$.

Electronic spectra of different salts of $[MoS_4]^2$ exhibit similar band positions, suggesting that in solution the anion is not influenced by the counter ion. The presence of the phenyl groups in $[PPh_4]_2[MoS_4]$ is manifested by a strong transition ~200 nm. However, a change in the metal ion has significant effect on the electronic spectra of the salts. As expected the bands in the tungsten compounds are shifted towards lower energy. Similarly, replacing the oxo-groups with sulfide groups changes the electronic transitions at lower energies.

X-ray Powder Diffractometry

Powder X-ray diffraction is a technique that can be used in characterizing crystalline materials. Where available the experimental data should be compared with the powder diffraction pattern deposited in the International Centre for Diffraction Data (ICDD) powder Diffraction File database. The 2θ (two theta) values of the peaks are indicative of inter-planar spacings. For the series of $[RA_4N][MoS_4]$ compounds the values are quite different indicating the interplanar spacings are different. In addition, the intensity of the individual peaks are found to be different. This suggests that the different counter ion results in different lattice parameters, and perhaps a change in the space group as well. There is very little difference between the molybdenum and the corresponding tungsten compounds. However, a change in the terminal sulfido group with terminal oxo group results in a change in the peak pattern suggesting these units have different solid state structures.

Table 7.2. Electronic spectral data.

Compound	Peak Position, nm (ε, M^{-1} cm^{-1})
$[NH_4]_2MoS_4$	241(40100), 315(18700), 467(13400)
$[Me_4N]_2MoS_4$	240(25300), 315(17000), 467(12900)
$[Et_4N]_2MoS_4$	239(24700), 315(17550), 465(12850)
$[n\text{-}Bu_4N]_2MoS_4$	240(28200), 316(16700), 468(12550)
$[Ph_4P]_2MoS_4$	226(79000), 265(13700), 315(8600), 467(4700)
$[NH_4]_2WS_4$	216(35800), 277(28400), 392(18700)
$[Et_4N]_2WS_4$	215(32100), 276(24200), 393(16400)
$[NH_4]_2MoO_2S_2$	220(12550), 319(8000), 393(4000)
$[Et_4N]_2MoO_2S_2$	223(13250), 311(6050), 393(6050)
$[NH_4]_2WO_2S_2]$	246(5600), 272(6500), 326(3200)
$[Et_4N]_2WO_2S_2$	246(5800), 272(7700), 326(4000)

PROBLEMS

What are differences between kinetically controlled product and thermodynamically controlled product?

How is the powder diffraction pattern of a compound indicative of the solid state structure of the material?

Given that the ionic radii of Mo(VI) and W(VI) are very similar, why are the M=S vibrations different for the similar complexes of the two metals?

What is the electronic configuration of Mo(VI) and W(VI)?

Define the symmetry elements in $[MS_4]^{2-}$, and draw the ligand field diagram.

INSTRUCTOR'S RESOURCE

Depending on the available time the following compounds can be synthesized.

Synthesis of $[NH_4]_2[MoOS_3]$

Place 750 mL of EtOH in a 1L beaker in the ice bath. Prepare a solution of concentrate NH_4OH (50 mL) and H_2O (30 mL) in a 200 mL Erlenmeyer flask. Dissolve $Na_2MoO_4 \cdot 2H_2O$ (10 g) into the solution. Filter the solution and cool it in an ice bath for 15 min. Pass H_2S gas slowly over the surface of the reaction mixture, which will cause a precipitate formation. Continue the gas flow over the surface of the reaction mixture until most of the precipitate redissolves into the fluid and then filter the reaction mixture rapidly. Add the filtrate

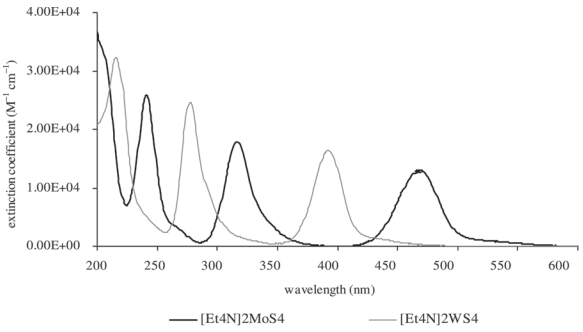

Figure 7.1. The electronic spectra of molybdenum and tungsten complexes.

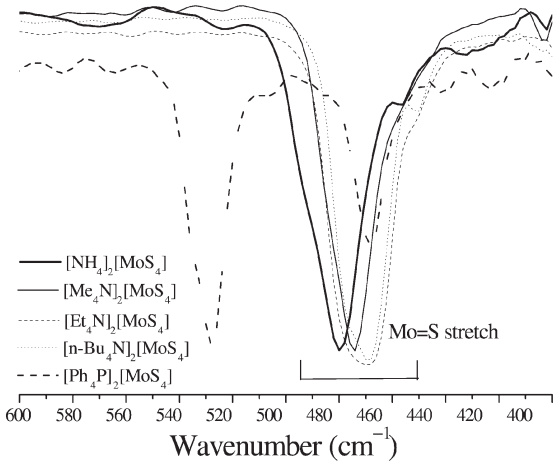

Figure 7.2. The differences in the metal- sulfide vibration.

into ice cold EtOH. Isolate the product by filtration and wash with EtOH and Et_2O. Dry this product in a N_2–flushed desiccator overnight and store in a vial. Yield = 75% (7.5 g).

Synthesis of $[NH_4]_2[WOS_3]$

Place 500 mL of i-PrOH in a 1 L beaker in an ice bath. Prepare a solution of concentrate NH_4OH (20 mL) and H_2O (5 mL) in a 200 mL Erlenmeyer flask. Dissolve H_2WO_4 (5 g) into the solution. Filter the solution and pass H_2S gas through the reaction mixture for 15 min. Filter the reaction mixture and add the filtrate into ice-cold i-PrOH. Isolate the yellow product by filtration and wash with i-PrOH and Et_2O. Dry this product in a N_2-flushed desiccator for overnight and store in a vial. Yield = 81%.

Syntheses of $[NH_4]_2[MOS_3]$ (M=Mo or W) complexes need careful monitoring of the reaction. In the case of $[NH_4]_2[MoOS_3]$ a rapid flow of H_2S gas gives a precipitate of $[NH_4]_2[MoO_2S_2]$, which redissolves into the reaction media. Filtration of the reaction mix-

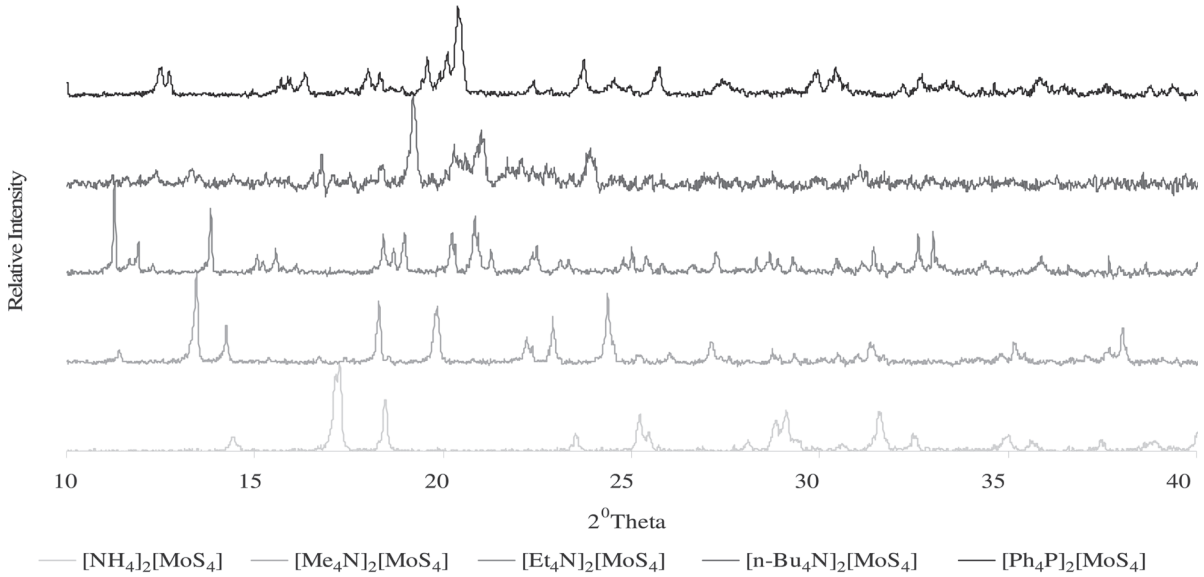

Figure 7.3. X-ray diffraction patterns of synthesized complexes.

www.ebook3000.com

ture and the addition of filtrate to i-PrOH give the precipitate of the product. It must be noted that the H_2S delivery tube should not be immersed into the reaction mixture as it will produce $[NH_4]_2[MoS_4]$ complex as an impurity. In the tungsten analogue $[NH_4]_2[WOS_3]$, the sluggish reaction requires the bubbling of H_2S gas directly into the reaction mixture. Filtration of the reaction mixture followed by the addition of filtrate into the i-PrOH gives the precipitate of the product.

A common pitfall in synthesizing the compounds is not drying the samples free from H_2S. It is very important to maintain the temperature and the flow rate for H_2S. One can also expand this module to include symmetry. For more advanced students, one can also compute the force constants for the M=S vibrations providing more quantitative information. In addition, the powder data can be used for calculating the lattice parameters. This exercise is also for advanced students.

REFERENCES

1. Stiefel, E.I. ACS Symposium Series, **1996**, 653, 2–37.
2. Hille, R. *Chem Rev.*, **1996**, 96, 2757.
3. Basu, P.; Stolz, J.F. *ChemBioChem*, **2002**, 3, 198–206.
4. Basu, P.; Stolz, J.F.; Smith, M.T. *Current Sci.* **2003**, 84, 1412–1418.
5. McDonald, J. W.; Friesen, G. D.; Rosenhein L. D.; Newton, W. *E. Inorg. Chim. Acta* **1983**, 72, 205–210.
6. Alonso, G.; Aguirre, G.; Rivero, I. A.; Fuentes, S. *Inorg. Chim. Acta* **1998**, 274, 108–110. Alonso,G.; Yang, J.; Siadati, M. H.; Chianelli, R. R. *Inorg. Chim.* Acta **2001**, 325, 193–197.

ADDITIONAL READING

B.N. Figgis and M.A. Hitchman, in Ligand Field Theory and Its Applications, Wliey-VCH, New York, 2000.

R. Jenkins and R.L. Snyder, in Introduction to X-ray Powder Diffractometry, John Wiley and Sons, New York, 1996.

www.ebook3000.com

Cloning of the β-galactosidase Gene

KRISTINA O. PAZEHOSKI[1] and CHARLES T. DAMERON[2]
[1]*Natural Sciences Division, University of Pittsburgh at Greensburg, Greensburg, PA 15601*
[2]*Department of Chemistry, Saint Francis University, P.O. Box 600, Loretto, PA 15940-0600*

LEARNING OBJECTIVES: Over a series of four laboratory experiments, students will learn the skills required to carry out basic molecular biology techniques. Techniques include bacterial cell culture, DNA purification, digestion of DNA with restriction enzymes for the purposes of "plasmid mapping" and for insertion of a gene of interest into a plasmid vector, agarose gel electrophoresis, PCR, and blue-white color selection to verify insertion of a gene of interest. All techniques covered are commonly used in molecular biology research, thus this laboratory exercise will serve to thoroughly prepare students for future studies in this field.

Description of Experiment

Due to time constraints, the experiment is carried out over the span of 4 lab periods. The procedure below is presented with specific stopping points which may be adjusted to fit the needs of the particular class.

GENERAL PREPARATIONS FOR CARRYING OUT BACTERIAL CELL CULTURE

MOST undergraduate laboratories that accompany lecture based classes provide the materials necessary to start a bacterial cell culture, or even provide the finished cell culture, at the moment the students walk into the day's lab session. Many of these students will be continuing their education in graduate school where they will be expected to prepare these materials on their own. Thus, this laboratory session is designed to introduce the students to these methods in order to equip them with skills for their future studies.

THEORETICAL ASPECTS

The fields of Molecular Biology and Biochemistry are mostly focused on studying the DNA and proteins of living organisms. In order to study the DNA and proteins, it is desirable to have the molecules of interest in large amounts that are separated from other cellular components. The bacterium *Escherichia coli* is one of the most commonly used microbes for producing large amounts of DNA or a protein of interest.[1] A gene encoding for a particular protein can be easily incorporated into plasmid DNA, which is subsequently inserted into the *E. coli* cells (this process is called transformation). The transformed *E. coli* cells can then be grown relatively quickly in either liquid or solid nutrient rich media. The final cells are harvested, broken open, and the DNA or protein is isolated through common purification techniques.

Liquid cultures of bacteria are employed by scientists when large volumes of cells are required for experiments. Large volumes are typically necessary when the scientist is attempting to isolate (purify) a specific protein. Large liquid cultures are typically grown from a single, isolated bacterial cell colony in order to minimize the occurrence of contaminants. To obtain isolated colonies, bacteria are grown on solid growth media, usually an agar plate. *E. coli* cells containing the gene of interest are "streaked" on an agar plate (procedure outlined below) and incubated until growth appears. Streaking effectively spreads cells out across the plate, so that single cells are

separated from each other. When one single *E. coli* cell multiplies during the incubation period, a single, round, visible colony forms. Using this single colony to start a large liquid culture ensures that the large culture contains descendents of the same, single *E. coli* cell. Students will both prepare agar plates and streak *E. coli* cells onto them to obtain single colonies. The second lab session will involve the growth of a large liquid culture from one of the single colonies. To speed up the process of growing the large culture, it is necessary that each lab group come into the lab one day prior to the next lab session to start a small "overnight" liquid culture.

Equipment/Chemicals Needed

Tryptone, yeast extract, NaCl, 1 M NaOH, agar, several 1 L autoclavable glass bottles, disposable sterile Petri dishes, ampicillin, chloramphenicol, glycerol stock of *E. coli* cells that express the β-*galactosidase* gene, sterile inoculating loop for streaking cells, autoclaved 500 mL Erlenmeyer flask, autoclave, 37°C incubator

Preparing Growth Media

Liquid Media

Use the following recipe to prepare 1 × LB (Luria-Bertani) media. For 1 × LB media (for 1 L total volume)—10 g tryptone, 5 g yeast extract, 5 g NaCl, 1 mL 1 M NaOH. All 4 components should be added to one 1L autoclavable glass bottle. Do not add any water to the bottle yet.

Each lab group should also prepare 1 bottle of 5 × LB media. Do the math to figure out how much of each component to add. Check with your instructor to ensure accuracy.

Autoclave (sterilize) the media. Immediately before placing the media into the autoclave, add deionized water to approximately 1 L final volume. Be sure to leave the bottle cap loose to prevent bottle explosions. (Your instructor will operate the autoclave.)

Solid Media

Use the following recipe to prepare 1 × LB agar media. 1 × LB agar media (for 1 L total volume)—10 g tryptone, 5 g yeast extract, 5 g NaCl, 15 g agar, 1 mL 1 M NaOH. All 5 components should be added to ONE 1 L autoclavable glass bottle. Autoclave the agar media, as described for the liquid media.

Pouring Agar Plates

**This section may be carried out with 1 × LB agar media that had been prepared and autoclaved by the instructor prior to class.

1. Obtain a bottle of freshly autoclaved 1 × LB agar media.
2. Allow the media to cool to a temperature at which the bottle can be comfortably held. Be careful not to let the media cool to a point of solidification.
3. While the media is cooling, prepare the following antibiotic solutions:
   - 25 mg/mL ampicillin (in DI water)—100 mL total volume
   - 40 mg/mL chloramphenicol (in ethanol)—50 mL total volume
4. Add the antibiotic to the cool media to the following final concentrations:
   - ampicillin final concentration = 100 µg/mL
   - chloramphenicol final concentration = 20 µg/mL

   (When calculating how much volume of the stock antibiotics to add, assume a final volume of 1000 mL for the media. Check with your instructor for accuracy.)
5. Obtain one stack of 5 empty Petri dishes for each student. The smaller diameter dish should be on the bottom and will contain the media, while the larger diameter dish serves as the cap. Starting from the bottom of the stack, pour the media into the dish so that it is approximately 1/2 full. Gently swirl the dish to ensure even distribution of the media. Quickly pass the flame of a Bunsen burner over the dish to pop any bubbles on the surface of the media. Continue working up the stack of dishes.
6. After pouring media into all the dishes in the stack, leave the stack on the bench to cool and solidify. The dishes can sit on the bench overnight, then should be stored in a cold room or refrigerator the following morning.

www.ebook3000.com

Streaking Agar Plates with Bacterial Cells to Obtain Isolated Colonies

**The instructor will have to prepare 1 x LB agar plates with ampicillin and chloramphenicol prior to the lab session in order for students to carry out this procedure on the first day.

1. Obtain a pre-made 1 × LB agar plate containing the ampicillin (amp) and chloramphenicol (cam) antibiotics.
2. Obtain a glycerol *E. coli* cell stock that expresses the β-*galactosidase* gene from the −80°C freezer.
3. Use a Bunsen burner to "flame" the inoculating loop. Place the metal wire of the loop directly into the flame until it turns a bright orange color.
4. Allow the loop to cool (touch the loop to the surface of the solid agar to speed up the cooling). Dip the loop into the glycerol cell stock. Only a small amount of cell stock is necessary.
5. To begin "streaking", make a single swipe with the loop onto the agar plate. See Figure 1(a).[2]
6. Place the inoculating loop back into the flame as done in Step 3, and allow it to cool.
7. Touch the loop to the plate and drag it through the first cell streak at an angle that is nearly perpendicular to the initial streak. Continue by moving the loop in a zig-zag manner toward the center of the plate. See Figure 1(b).
8. Re-flame the loop and allow it to cool.

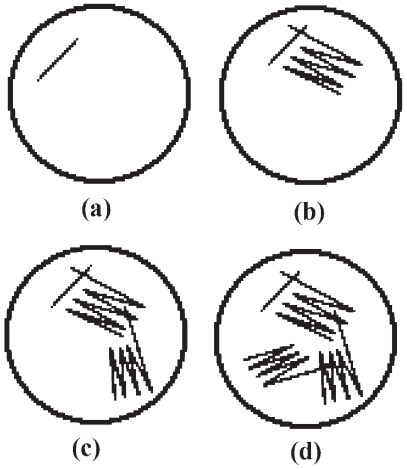

Figure 8.1.

9. Drag the loop through the second streak and zig-zag toward the center as done in Step 7. See Figure 1(c).
10. Re-flame the loop, let it cool and streak one additional time. See Figure 1(d).
11. After streaking, place the plates upside down in a 37°C incubator. The cells will incubate overnight.
12. Check for cell growth the following morning. If growth is apparent, store the plates in a cold room or refrigerator. Several individual colonies should be visible on the plate. If no growth has appeared, leave the plates in the incubator and check again in the afternoon.

Growing an Overnight Liquid Cell Culture

**This section should be started the night before the second lab period.

1. Obtain 1 L of autoclaved 1 × LB media. Add the amp and cam antibiotics to it as done for the agar media.
2. Obtain a 500 mL autoclaved Erlenmeyer flask. Place approximately 100 mL of the liquid media into the flask (1/5 the total volume of the flask).
3. Obtain the agar plates streaked with the β-*galactosidase* cells.
4. Flame an inoculating loop, let it cool and pick one colony of cells from the streaked plate.
5. Transfer the colony into the flask containing the liquid media.
6. Place foil on top of the flask, label it, and place it into a 37°C shaking incubator. Incubate the culture overnight with constant shaking at 250 rpm.

BACTERIAL CELL CULTURE AND DNA PURIFICATION

Having prepared the liquid growth media and having started an overnight liquid cell culture, students are now set up to begin the process of growing a large liquid cell culture. Students will learn how to carry out a liquid cell culture for the purpose of protein expression. Students will also gain experience in purifying the plasmid DNA (containing the β-galactosidase gene of interest) from the liquid cell culture.

Theoretical Aspects

E. coli are commonly used for producing large amounts of DNA or a protein of interest for several reasons. Bacterial cultures of *E. coli* can very easily be grown in a controlled laboratory setting. The cell growth is very rapid, allowing the researcher to obtain a sufficient amount of DNA or protein in a matter of hours. With each cell division of the *E. coli*, the recombinant DNA (otherwise known as plasmid DNA) containing the gene of interest is replicated, and thus multiplies at the same exponential rate at which the cells grow. Expression of the protein of interest can be easily induced in bacterial cell cultures, particularly when the gene of interest has been inserted into a specially designed plasmid DNA called an "expression vector". Expression vectors allow the scientist to insert the gene of interest directly after a strong promoter region of DNA.[3] Typically, the promoter is the "lac promoter", which under normal cellular conditions, is bound by a protein called the "lac repressor." As the name implies, the lac repressor prevents transcription of the gene(s) following the lac promoter. It is advantageous in the early stages of bacterial cell culture growth to keep the expression of the gene of interest repressed, as the foreign protein can potentially be toxic to the cells. Once the cells have reached a sufficient level of growth, gene expression can be induced by an "inducer molecule" binding to the lac repressor, thus releasing the repressor from the promoter DNA. The lac system is found naturally in prokaryotic cells, where it is used to control the expression of genes involved in the metabolism of lactose.[4] Lactose is the inducer molecule in these cells. When growing a bacterial cell culture under laboratory conditions, the preferred inducer molecule is iso-propyl-thio-galactopyranoside (IPTG), a synthetic molecule that is able to bind to the lac repressor as lactose does, but cannot be consumed by the *E. coli* (as lactose is). Adding IPTG at the appropriate point of cell growth will "induce" the culture to express the protein of interest in yields high enough to facilitate the subsequent analysis of structure and/or function of the protein.

When biochemists carry out protein studies, the amount of protein made by one bacterial cell culture is usually not enough to supply their entire research effort. Studies on one particular protein may extend for years as new results provide ideas for fresh experiments. Also, inevitably, mistakes are made and the scientist must purify more protein to replenish the supply. For this reason, it is important to always keep a back-up stock of *E. coli* cells that have been transformed with the plasmid containing the gene of interest. The most common method of storing these cells is to prepare a "glycerol stock" consisting of a small volume of slightly saturated liquid cell culture thoroughly mixed with an equal volume of glycerol. The glycerol stock is frozen at –80°C for storage, and can be easily used at a later time to begin a fresh cell culture. A sterilized utensil is used to scrape out a small amount of the still-frozen glycerol stock, which is then transferred to fresh LB media containing the appropriate antibiotic.

Another way for scientists to ensure that their gene of interest is safe in long term storage is to store the plasmid DNA itself. Plasmid DNA can be isolated from a saturated cell culture through a procedure referred to as a "DNA Miniprep." The DNA Miniprep involves first lysing the *E. coli* cells with a solution of sodium hydroxide (NaOH) and sodium dodecyl sulfate (SDS). The SDS dissolves the cell membrane of the bacteria and denatures the proteins and chromosomal DNA within the cell. The process is helped by the high pH (~12) provided by the NaOH. To separate the denatured proteins, membrane debris and chromosomal DNA from the plasmid DNA, and to neutralize the solution, a potassium acetate buffer is added. The SDS, denatured proteins, membrane debris and chromosomal DNA precipitate into a solid form and are easily separated from the plasmid DNA, still in a soluble form, by centrifugation. The solution containing the soluble plasmid DNA is then passed through a silica-based resin, which the plasmid DNA selectively adheres to, while all contaminants are flushed through. The final pure plasmid DNA is released from the resin by the addition of nuclease-free water. The purity and concentration of the isolated plasmid DNA can be assessed spectrophotometrically. DNA efficiently absorbs UV light at the wavelength of 260 nm. Using the approximation that 50 g/mL of DNA give an absorbance at 260 nm of 1, the concentration of your DNA sample can be obtained from the following formula:

$$[\text{plasmid DNA}]\ (\mu\text{g/mL}) = A_{260} \times \text{dilution factor} \times 50\ \mu\text{g/mL}$$

The purity of the DNA sample can be measured by

www.ebook3000.com

comparing the absorbance values at 260 nm and 280 nm. Pure DNA has a ratio of A_{260}/A_{280} within the range of 1.8–2.0. A ratio higher than 2.0 indicates RNA contamination, while a ratio lower than 1.8 indicates protein contamination. The miniprep procedure should be carried out on an un-induced portion of cell culture. Isolated plasmid DNA can be stored in the –80°C freezer. If desired, a portion of the purified plasmid DNA can be sent to a DNA sequencing facility to confirm that the sequence of the β-*galactosidase* gene of interest is correct.

Equipment/Chemicals Needed

Overnight culture of cells containing the β-galactosidase plasmid, 1 × LB media with amp and cam added (1 L), autoclaved 2 L erlenmeyer flasks (2), autoclaved 500 mL Erlenmeyer flask (1), shaking platform incubator set at 37°C, IPTG, Centrifuge, Scale, –20°C freezer, Glycerol, Sterile storage tubes (1.5 mL) with screw-top, –80°C freezer, Promega Wizard Miniprep Kit (or comparable kit), Microfuge tubes (1.5 mL), UV-Vis spectrophotometer, Quartz cuvettes, Sequencing primers.

Growing a Large Culture

**Steps 1–5 should be started approximately 2 hours before the lab usually starts.

1. Obtain 1 L of the 1 × LB media containing ampicillin and chloramphenicol.
2. Obtain two 2 L autoclaved Erlenmeyer flasks. Place approximately 500 mL of the media into each flask.
3. Add approximately 50 mL of the saturated overnight cell culture to each flask.
4. Place the flasks into a shaking platform incubator set at 37°C and 250 rpm.
5. Incubate the culture until the cells grow enough to reach an optical density at 600 nm (OD_{600}) within the range of 0.6–1.0. The incubation will typically last for approximately 2 hours.
6. During the incubation period, prepare the following solution:
   - 100 mM IPTG (in DI water) –20 mL final volume
7. When the cell culture has reached an appropriate growth level (as evidenced by the OD_{600}), set aside approximately 100 mL of the culture in a 500 mL autoclaved Erlenmeyer flask, to be used for glycerol stocks and for DNA purification later. Place this flask back into the incubator.
8. Add IPTG to the large cell culture (in the 2 L flasks) to a final volume of 1 mM.

   (When calculating how much volume of the IPTG to add, assume a final volume of 500 mL for the culture. Check with your instructor for accuracy.)
9. Incubate the induced cell culture in the shaking incubator for 2 additional hours.
10. Centrifuge the cell culture at 5000 × g for 10 minutes to harvest the cell pellet.
11. Discard the supernatant, weigh the cell pellet and store the pellet in a –20°C freezer.

Glycerol Stocks

**Be sure to use an un-induced cell culture to prepare glycerol stocks.

1. Allow the 100 mL of culture that was set aside from the large culture prior to addition of IPTG to grow to an OD600 of approximately 1.0.
2. Obtain a sterile storage tube capable of holding 1.5 mL of total volume. The tube should have a screw-top lid.
3. Place approximately 0.5 mL of glycerol into the storage tube.
4. Add 0.5 mL of the cell culture to the tube.
5. Close the tube and invert several times to ensure thorough mixing of the cells with the glycerol.
6. Label and date the tube, then store in a –80°C freezer.

Part 3—DNA Purification

**Be sure to use an un-induced cell culture for the DNA minipreps

1. Place the cell culture that was used for glycerol stocks back into the shaking incubator for 1 hour longer.
2. Remove a 5 mL aliquot of the saturated cell culture and centrifuge it at 5000 × g for 5 minutes.
3. Discard the supernatant.

4. Follow the Miniprep kit instructions provided in the kit manual.
5. The Miniprep kit will provide 50 µL of final purified DNA. Remove 20 µL for purity and concentration measurements. Store the remaining 30 µL in a –80°C freezer.
6. Dilute the 20 µL of pure DNA with 380 µL of DI water.
7. Using a UV-Vis spectrophotometer, record the absorbance of the diluted DNA solution at 260 nm and 280 nm.
8. Calculate the purity of your DNA by dividing the A_{260} by the A_{280}. The result should be within the range of 1.8–2.0 to be considered pure.
9. Calculate the concentration of the DNA by the equation provided above. What is the dilution factor? Check with your instructor for accuracy.
10. Obtain sequencing primers from your instructor and prepare the DNA for sequencing according to the guidelines set forth by your sequencing facility.

"MAPPING" PLASMID DNA AND PERFORMING PCR

"Mapping" plasmid DNA is a procedure used to verify the plasmid in use. Restriction enzymes are used to cut the plasmid DNA, and the digested fragments are visualized through agarose gel electrophoresis. Students will carry out a mapping procedure to verify the plasmid in use, and will subsequently gain experience at PCR. The amplified β-galactosidase gene will be used in the fourth section of this series as the "insert" in a cloning reaction.

Theoretical Aspects

Thus far, discussions of the background and procedures of this molecular biology experiment have focused on "plasmid DNA containing the gene of interest," but the process of inserting the gene into the plasmid vector has not yet been explained. A gene of interest can easily be inserted into plasmid DNA through the use of restriction enzymes and DNA ligase. Restriction enzymes are endonucleases that bind to a specific DNA sequence, usually 6–8 base pairs long, and break phosphodiester bonds on both strands of DNA at a specific point. These enzymes are native to bacteria, which use them as a protective measure against infection by foreign DNA.[5] The enzymes digest foreign DNA and restrict it from affecting the bacterial cell, hence the name "restriction" enzymes. Restriction enzymes can cut the double stranded DNA symmetrically, leaving blunt-ended DNA fragments (Figure 8.2, Srf I) or unsymmetricaly, leaving DNA fragments with "sticky ends." (Figure 8.2, Hind III) To date, over 3500 restriction enzymes with have been discovered and are readily available for use in the laboratory.[6] The usefulness in the laboratory is apparent as a "cut and paste" tool. A gene of interest can be cut out of the chromosome of an organism and pasted into plasmid DNA that has also been cut. The pasting procedure is facilitated by cutting the gene of interest and the plasmid DNA with the same restriction enzymes in order to generate the same sticky ends. The complementary nature of the sticky ends allows base pairing between two DNA fragments, and the phosphodiester bonds of the DNA backbone are re-sealed by the enzyme DNA ligase (Figure 8.3).

Both the gene of interest and the plasmid DNA are cut with Bam HI and Hind III to generate complementary sticky ends. The sticky ends anneal to each other and the phosphodiester bonds of the DNA backbone are re-formed by DNA ligase.

Scientists have found another use for restriction enzymes as a validation tool for the plasmid under study. In a process called "mapping", specific restriction enzymes are used to cut the plasmid DNA at one or more points, and the digested DNA fragments are separated from one another through agarose gel electrophoresis. The sizes of the digested DNA fragments are determined by comparison to a standard mixture of DNA fragments with known sizes (also run on the same electrophoresis gel). The scientist can compare the fragment sizes observed on the gel to the expected sizes based on the known DNA sequence of

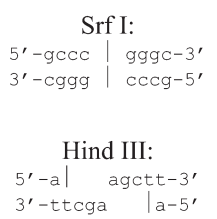

Figure 8.2. Restriction enzymes; Srf I = blunt ends, Hind III = sticky ends.

www.ebook3000.com

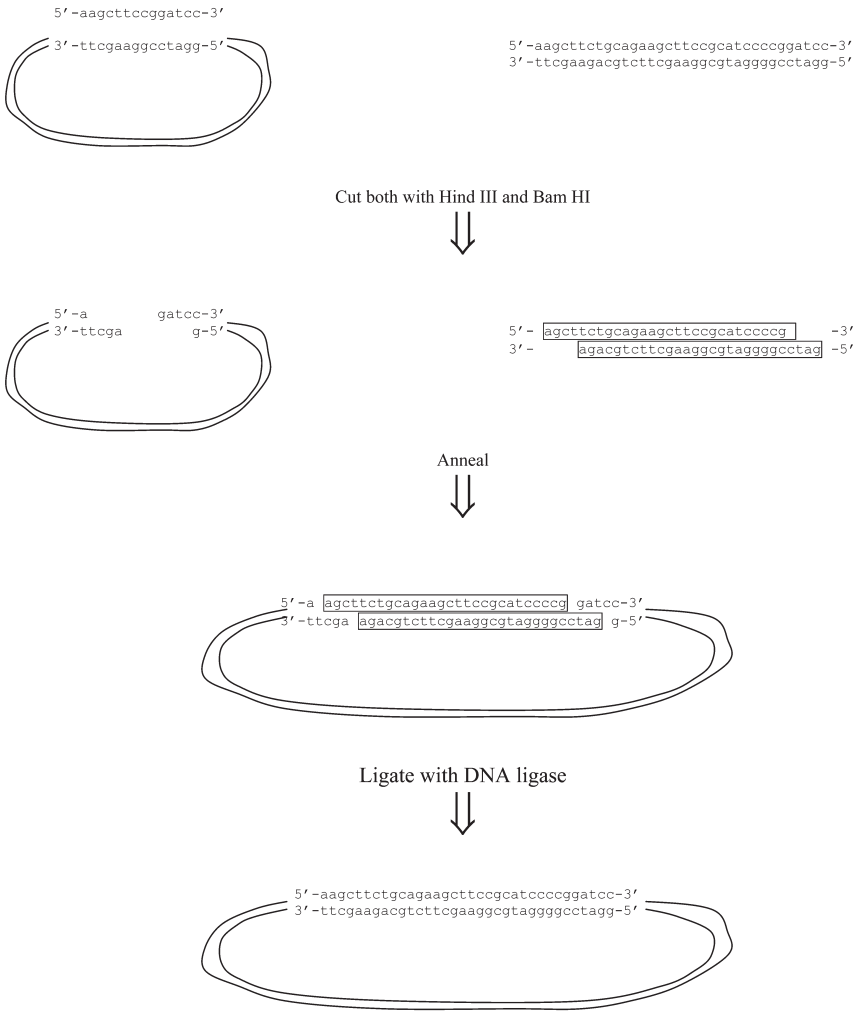

Figure 8.3. Inserting a gene of interest into a plasmid DNA.

the plasmid. Observation of the expected sizes on the gel assures the scientist that the proper plasmid is in use. Mapping can also be used to demonstrate the correct insertion of a gene of interest into a plasmid. Often, the gene of interest will have a recognition sequence for a restriction enzyme that does not normally cut the plasmid DNA. Treatment of the recombinant DNA with the specific restriction enzyme will result in a band at a size corresponding to the plasmid and the gene added together only if the gene has been successfully inserted. If the gene insertion failed, the plasmid DNA will be observed on the agarose gel as a diffuse series of bands on the large end of the size scale, characteristic of plasmid DNA that has not been cut.

Agarose gels are used to separate DNA fragments based on size and charge. Gels are prepared as a certain "percentage" of agarose, depending on the size of fragments that require separation. A general rule used for the preparation of agarose gels is that smaller DNA fragments require higher percentages of agarose. Higher percentages of agarose result in a more solid gel matrix, with smaller spaces for the DNA to pass through within the gel matrix. Small DNA fragments will pass through these spaces easily, while movement of large DNA fragments will be hindered. Lower agarose percentages will allow the large DNA fragments to move through the gel matrix, but the smaller fragments may run off the end of the gel. After running the electrophoresis gel, the DNA bands are

visualized by staining, usually with ethidium bromide. Extreme care must be taken while handling ethidium bromide, as it is a carcinogen. Gloves and safety goggles must be worn at all times.

Upon validating that the proper plasmid is in use (through the plasmid mapping), a PCR reaction can be carried out in order to amplify the β-galactosidase gene. The amplified gene will subsequently be inserted into a different plasmid during a cloning experiment in the fourth section of this series. PCR, or polymerase chain reaction, is a process that was invented in the mid 1980's to produce large amounts of a specific portion of DNA in a relatively short amount of time.[7] The process works by cycling a reaction mixture of DNA, primers, deoxynucleotides (dNTPs), and a thermostable DNA polymerase through a series of temperature changes. One reaction cycle consists first of a high temperature stage, usually approximately 95°C, which serves to separate the double strand of the original DNA. The temperature is then decreased to the range of 50–55°C in order to allow two primers, complementary to the 3′ ends of each strand of the DNA of interest, to anneal to the original DNA. The annealing of primers provides a starting point for DNA polymerase to begin catalyzing the addition of dNTPs according to the template provided by the original DNA. The extension step usually occurs within the range of 70–75°C. Typically, 20–30 of these cycles consisting of the 3 different temperatures are carried out, resulting in exponential amplification of the DNA sequence between the 2 primers. The process can be carried out by setting up 3 separate water baths at the 3 different temperatures and manually moving the reaction tubes from one bath to another, but the preferred method is to use a machine called a "thermocycler." Thermocyclers automate the process, allowing the scientist to set the desired temperatures, times at each temperature, and number of cycles, then allow the machine to carry out the reaction until it is done. Depending on the length of DNA fragment to be amplified, PCR reactions can be completed in approximately 2–4 hours.

Equipment/Chemicals Needed

Selection of restriction enzymes with appropriate reaction buffers, Plasmid DNA containing the β-galactosidase gene (the result of the mini-prep from the previous lab period), 0.6 mL microfuge tubes, PCR machine (thermocycler), Agarose, Tris, Boric Acid, EDTA, Agarose gel apparatus with well combs, Power supply, Glycerol, Bromophenol blue, DNA ladder (size marker/standard), Ethidium bromide, UV light box, Camera.

Materials for PCR Reaction

Pfu DNA polymerase, PCR reaction buffer (100 mM Tris-HCl, pH 9.0, 500 mM KCl), $MgCl_2$, dNTPs, Two primers that are complementary to the 3′ ends of the β-gal gene.

Restriction Digestions of Plasmid DNA

1. Obtain a plasmid map of the plasmid vector you were assigned to work with. These can be obtained from the manufacturer's website. For example, if you were told that you are working with the pET-14b plasmid vector from Novagen, you can visit Novagen's website and search for "pET-14b." The map will indicate which restriction enzymes cut the plasmid and the location at which they cut.
2. Obtain the sequence of the β-galactosidase gene with restriction enzyme recognition sites indicated.
3. Choose one or more enzymes (depending on the supply of your laboratory) to digest the plasmid DNA. Choose at least one enzyme that cuts the β-gal gene, but does not cut the plasmid. Common restriction enzymes include HindIII, BamHI, EcoRI and NdeI.
4. Keep all restriction enzymes and their appropriate reaction buffers on ice at all times.
5. Set up a restriction enzyme digestion reaction according to the instructions provided with the particular restriction enzyme. Use 1 μg of plasmid DNA. Refer to the concentration of DNA you calculated from the absorbance measurements to determine what volume of the plasmid DNA will contain 1 μg. Add the restriction enzyme to the mixture last. All reaction components should be mixed in a 0.6 mL microfuge tube.
6. Place the reaction mixture into a PCR machine set at the appropriate reaction temperature (usually 37°C). Alternatively, a water bath can be used.
7. Incubate the restriction digestion for 1 hour.

www.ebook3000.com

Agarose Gel Electrophoresis

1. Prepare 1 L of Tris-Borate-EDTA (TBE) buffer, pH 8.3 (in DI water) –90 mM Tris, 90 mM Boric Acid, 2 mM EDTA.

   *The pH should be near 8.3 upon dissolving the 3 components in water. Add HCl or NaOH to adjust the pH if needed.

2. Obtain an agarose gel apparatus from your instructor.
3. Use the chart below to determine what percentage of agarose gel should be made.[8] Verify your choice with your instructor before continuing.
4. Refer to the manual for the gel apparatus to determine what volume of liquid agarose should be used.
5. Determine how much solid agarose should be weighed out and dissolved in that volume of TBE buffer. The percent agarose found in the chart is given as "weight-by-volume." As a guideline, remember that 1% w/v means that 1 g of the solid compound is dissolved in 100 mL of liquid.
6. Place the correct volume of TBE buffer into an Erlenmeyer flask. Add the correct amount of solid agarose to the flask. Place the flask in a boiling water bath or in a microwave and heat until all of the solid agarose is dissolved. Swirl the flask to ensure even mixing.
7. Remove the flask from the heat source and allow it to cool enough that you are able to touch the flask with your bare hand. The agarose should still be liquid. If it solidifies, you can melt it by placing back into the heat source.
8. While the agarose is cooling, assemble all of the components of the gel apparatus according to the instructions in the manual. Be sure the well comb is placed in an appropriate position.
9. Pour the liquid agarose into the gel apparatus (the well comb should be in place before pouring). As the agarose continues to cool, it will change from a clear liquid to a cloudy white solid.
10. As the gel is setting, prepare 10 mL of Sample Loading Buffer (in DI water)
    - 0.2 M EDTA, pH 8.3
    - 50% (v/v) glycerol
    - 0.05% (w/v) bromophenol blue

    Mix well.
11. Add 4 µL of the Sample Loading Buffer directly to 20 µL of each of the restriction digestion samples. Prepare an undigested DNA sample by mixing the same components that you did for the restriction digestion, but leave out the restriction enzyme.
12. Prepare a DNA ladder by mixing with Sample Loading Buffer.
13. Ensure that the agarose gel is solidified by gently pressing on it with a pipet tip.
14. Fill the gel apparatus chamber, containing the solidified agarose gel (with the well comb still in place), with TBE buffer. The agarose gel should be completely covered with buffer.
15. Remove the well comb from the gel.
16. Load the restriction digestion samples, the DNA ladder and the uncut DNA sample into the wells.
17. Place the cap on the gel apparatus, connect the red and black electrodes to a power supply and run the gel at 120 V. Before turning on the power supply, check to make sure the gel is situated in the correct direction. Use the phrase "run to red" to remind yourself which direction the DNA will move in the electric field. The sample wells should be situated closest to the black electrode.
18. While the gel is running, prepare 50 mL of a 5 µg/mL ethidium bromide solution in a Tupperware container. *Caution:* ethidium bromide is toxic—gloves, safety goggles and a lab coat must be worn at all times when handling this chemical.
19. Run the gel until the blue tracking dye (bromophenol blue) has moved about two-thirds of the way down the gel. Turn off the power

Table 8.1. Mobility range of DNA in different percentage agarose gells.

Agarose % (w/v)	Approximate range of separated DNA fragments (kb)
0.3	60 to 5
0.5	30 to 1
0.7	12 to 0.8
1.0	10 to 0.5
1.2	7 to 0.3
1.5	4 to 0.2
2.0	3 to 0.1
3.0	< 0.1

supply, remove the cap of the gel apparatus and transfer the gel to the ethidium bromide solution.

20. Allow the gel to soak in ethidium bromide for approximately 1 hour.
21. View the gel in a UV light box to see the DNA bands. Be sure to shield your eyes and skin from exposure to the UV light, since it is carcinogenic.
22. Take a picture of the gel to include in your lab report.
23. Analyze the gel: compare the bands that appear in the sample lanes to the DNA ladder. Do the bands appear at the predicted sizes?

PCR

**A 50 µL PCR reaction mixture should be prepared according to the table below. Reaction components should be added to the PCR tube in the order shown in Table 8.2.[9]

1. The plasmid DNA containing the β-galactosidase gene will be the "template" DNA for the PCR reaction. Use 200 ng of template DNA for the reaction. Using the DNA concentration obtained from the absorbance at 260 nm, calculate the volume of this DNA that is necessary to include 200 ng.
2. The instructor will provide PCR primers. The primers should be provided as stock solutions of approximately 20 µM concentration. The final primer concentration in the 50 µL reaction volume should be 1 µM. Calculate how much of the stock primer should be added to attain a final concentration of 1 µM.
3. The amount of $MgCl_2$ can affect the efficiency of the polymerase enzyme. If the supply of reaction components permits, set up 3 PCR reactions with varying amounts of $MgCl_2$. If only 1 PCR reaction is set up, use a final concentration of 1.5 mM $MgCl_2$ in the 50 µL reaction volume.
4. After calculating the volumes of each component to be added, determine how much water should be added to end with a final reaction volume of 50 µL.
5. Add all components to a 0.6 mL microfuge tube (PCR tube) in the order listed in the table above.
6. Place the tubes into the thermocycler. If the thermocycler does not have a heated lid, add a drop of mineral oil directly to the reaction mixture. The oil will sit on top of the liquid and prevent evaporation of the reaction mixture during the PCR.
7. Program the thermocycler according to the cycle steps shown in Table 8.3.
8. Program the thermocycler to go to 4°C for an indefinite amount of time when the PCR cycling is finished. This will allow you to start the program in the lab and let the PCR machine work overnight.
9. The following morning, retrieve the PCR reaction tubes from the thermocycler and store in a refrigerator until the next lab period.

Table 8.2.

Reaction Component	Volume
PCR Qualified Water	X µL
PCR buffer	5 µL
dNTP mix (10 mM each dNTP)	1 µL
Forward Primer	0.5–2.5 µL
Reverse Primer	0.5–2.5 µL
25 mM $MgCl_2$	0–8 µL
Pfu DNA polymerase (2.5 U/ µL)	0.5 µL
Template DNA	Y µL
Total reaction volume	50 µL

Table 8.3.

Cycling Guidelines	
Initial denaturation	94°C for 3 minutes
Perform 30 cycles of the following 3 steps	
Denaturation	94°C, 30 seconds
Annealing	60°C, 30 seconds
Extension	72°C, 3 minutes

"Cloning" the PCR Product (β-galactosidase gene) into a New plasmid DNA Vector

Students will learn how to insert the PCR product (amplified β-galactosidase gene) from section 3 into plasmid DNA. Successful insertion of the gene will be verified by blue-white color selection of bacterial colonies.

Theoretical Aspects

The idea of "cloning," which is the process of inserting a gene of interest into plasmid DNA, was introduced at the beginning of the third lab period in

www.ebook3000.com

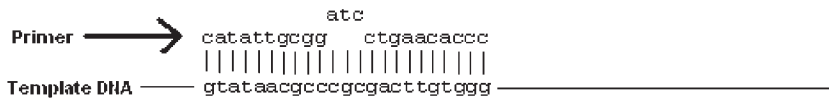

Figure 8.4. PCR primer design. The PCR primer with a three-base mismatch will result in a PCR product that contains the recognition sequence 5′-ggatcc-3′ for the restriction enzyme Bam HI.

this series. To summarize, the scientist performing the procedure digests both the gene of interest and the plasmid DNA vector with appropriate restriction enzymes. If restriction enzyme recognition sequences do not naturally exist at each end of the gene of interest, the scientist can "engineer" suitable sequences at the proper locations. PCR primers can be designed to include the desired recognition sequence. The primers may not exactly match the original template DNA, but the PCR reaction will occur as usual provided that the mismatch is located in the middle of the primer (Figure 6.4). The PCR reaction is carried out (as done in the third lab period of this series), and the PCR product is digested with the appropriate enzymes. The plasmid DNA vector to be used is digested with the same enzymes. The plasmid and gene insert are mixed together and incubated with DNA ligase to seal the two DNA fragments together.

The issue of engineering the gene of interest to contain the restriction enzyme recognition sequences can be avoided if the scientist is able to use "blunt-end" cloning. The method involves carrying out the PCR with *Pfu* DNA polymerase (as was done in the third lab period), which results in a PCR product with blunt ends, or no single stranded overhangs. The plasmid DNA vector can then be cut with one restriction enzyme that cleaves the double stranded DNA symmetrically. The plasmid and gene insert are mixed as before with DNA ligase to seal the fragments together. The major disadvantage of this method is that the gene of interest can be incorporated into the plasmid DNA vector in either direction, forwards or backwards. If the scientist desires the gene of interest to be inserted in a specific direction, each end of the gene must be digested with different restriction enzymes that leave different sticky ends. The plasmid DNA vector must be digested with the same two restriction enzymes. Only the sticky ends that are complementary to each other are able to anneal to each other, thus ensuring the directionality of the gene insert in the plasmid DNA vector. It is especially important that this method be used when inserting a gene into an expression vector, since insertion of the gene in the wrong direction after the promoter will result in the production of the wrong protein.

Blunt-end cloning will be used. It is recommended that a cloning kit be used, such as Stratagene's PCR-Script® Cam Cloning kit.[10,11] The cloning vector included in the kit has a single recognition sequence for a restriction enzyme called Srf I, which cuts the DNA symmetrically, leaving blunt ends. (The PCR product already has blunt ends since it was PCRed with *Pfu* DNA polymerase.) The Srf I sequence in the cloning vector is located within a DNA sequence that encodes for β-galactosidase, situated after a *lac* promoter. The *lac* promoter allows for expression of the β-galactosidase gene upon addition of IPTG to a cell culture. Despite the presence of the *lac* promoter, the plasmid is not considered to be an expression vector because the insertion site for the gene of interest does not lie immediately after this promoter. Rather, the insertion site is some distance away from the promoter, in the middle of the β-galactosidase gene, so that proper insertion of the gene of interest (the PCR product from lab period #3) will result in the disruption of the native β-galactosidase gene. What is the importance of this? The β-galactosidase enzyme catalyzes the cleavage of the glycosidic bond between galactose and glucose in the compound lactose [Figure 8.5(a)]. β-galactosidase will also cleave a synthetic compound that is similar to lactose called "X-gal" [Figure 8.5(a)]. Cleavage of X-gal results in a blue colored product. Bacterial colonies that have been transformed with a plasmid containing the intact β-galactosidase gene will appear blue in color when grown on an agar plate containing X-gal and IPTG. Recall that it was previously mentioned that proper insertion of the gene of interest results in the disruption of the β-galactosidase gene. In this scenario, the β-galactosidase gene would not be expressed as a protein, therefore the X-gal would not be cleaved and no blue color would appear. Bacterial colonies will appear white when grown on an agar plate. Using this blue-white color system is very common in molecular

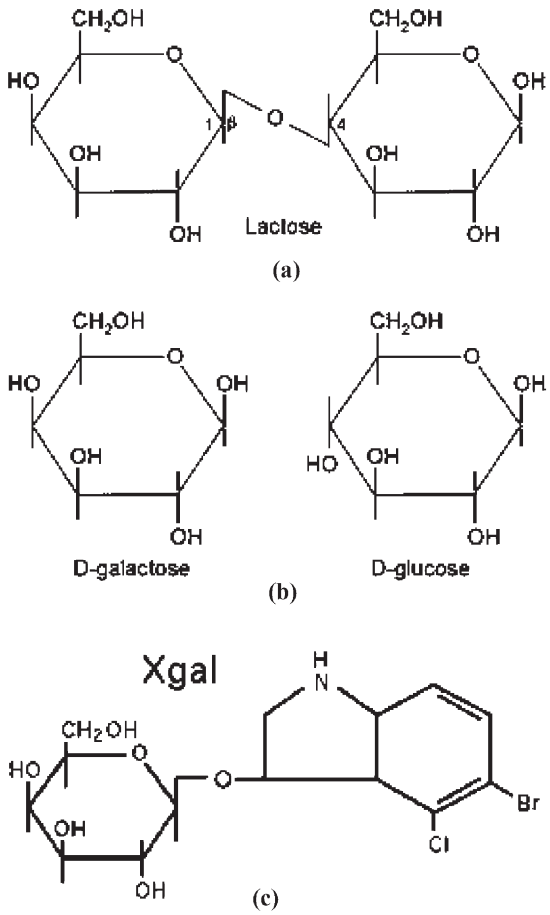

Figure 8.5. Structures of lactose and X-gal; (a) Lactose, (b) Lactose cleaved by b-galactosidase, (c) X-gal.

biology as a selection method.[12] It gives the scientist an easy way to verify that the cloning experiment as been successful. It may seem somewhat confusing that this particular lab involves inserting the β-galactosidase gene (the PCR product from lab #3) into the cloning vector that already contains a β-galactosidase gene. However, successful insertion of the gene of interest will still be observed as white bacterial colonies since the gene will be inserted at a distance away from the promoter.

Equipment/Chemicals Needed

PCR product from lab period #3, PCR purification kit, including DNA binding solution, microspin cups, receptacle tubes, and PCR wash buffer, microfuge, DI water, cloning components, cloning vector, reaction buffer, purified PCR product, Srf I, DNA ligase, DI water, 65°C water bath, competent *E. coli* cells, 42°C water bath, LB broth (no antibiotic included), shaking platform incubator set at 37°C, LB agar plates containing chloramphenicol, X-gal, IPTG, glass rod cell spreader (sterile), 37°C incubator

Purifying the PCR product

1. Mix an equal volume of the DNA binding solution with the PCR product, and place the mixture into a microspin cup that is inside a receptacle tube.
2. Microfuge at full speed for 30 seconds with the cap of the receptacle tube closed.
3. Discard the solution that passed through the microspin cup. The DNA is contained within the white solid visible in the microspin cup.
4. Place 750 µL of PCR wash buffer (2 mM Tris, pH 7.5, 20 mM NaCl, 80% ethanol v/v) into the microspin cup and microfuge for 30 seconds as done before.
5. Discard the solution that passed through the microspin cup. To remove any additional moisture, microfuge for 30 seconds as done before, and discard the flow through.
6. Place the microspin cup into a 1.5 mL microfuge tube, add 50 µL of DI water, and let sit for 5 minutes.
7. Microfuge at full speed for 30 seconds with the cap of the 1.5 mL microfuge tube closed.
8. Discard the microspin cup—the purified PCR product is in the 1.5 mL microfuge tube.

Cloning

1. Cloning reactions can be optimized by using a proper insert-to-vector ratio. Typical ratios are within the range of 40:1–100:1. A simple formula can be used to determine the amount of insert (PCR product) that gives a 1:1 insert-to-vector ratio. The formula assumes the use of 10 ng of cloning vector DNA:

www.ebook3000.com

$$\text{X ng of PCR product} = \frac{(\text{number of bp in PCR product})(10 \text{ ng of cloning vector DNA})}{3399 \text{ bp in cloning vector DNA})}$$

**The number of bp in the β-galactosidase PCR product is 3000 bp.

2. Calculate how much PCR product (in ng) is needed to have an insert-to-vector ratio of 100:1.
3. Record the absorbance value of the PCR product DNA solution at 260 nm. Use the recorded value to calculate the DNA concentration, as done for the DNA minipreps in lab period #2.
4. Covert the amount of PCR product calculated in Step 2 into a volume, using the concentration determined in Step 3 as a conversion factor.
5. Set up the ligation reaction in the following order:
   - 1 µL cloning vector (10 ng/mL)
   - 1 µL reaction buffer
   - X µL purified PCR product (volume calculated in Step 4)
   - 1 µL Srf I restriction enzyme (5 U/mL)
   - 1 µL DNA ligase (4 U/mL)
   - DI water to a final reaction volume of 10 µL
6. Incubate the ligation reaction at room temperature for 1 hour, then heat at 65°C for 10 minutes.
7. During the incubation period, prepare the competent *E. coli* cells for transformation. Competent cells must be kept on ice at all times! The cells are normally stored in the –80°C freezer. Removing a tube of cells from the freezer and placing it into an ice bath will allow the cells to thaw gently. If the cells must be aliquoted into smaller portions, place the empty tubes on ice for a few minutes before transferring cells into them. A portion of 40 µL should be used for this transformation procedure.
8. Add 2 µL of the ligation reaction to 40 µL of competent cells. Swirl gently and incubate on ice for 30 minutes.
9. During the incubation period, heat a few milliliters of LB broth (without antibiotics) at 42°C.
10. After the cells have incubated on ice, apply a heat shock by placing the tube into a 42°C water bath for 30 seconds. Immediately return the cells to ice for a 2 minute incubation.
11. Add 0.45 mL of heated LB broth to the heat shocked cells, and incubate the mixture at 37°C while shaking at approximately 250 rpm for 1 hour.
12. During the incubation period, prepare the LB-chloramphenicol plates. Place 100 µL of LB broth into the middle of the plate. Add 100 µL of 2% X-gal and 100 µL of 10 mM IPTG into the broth and spread with a sterile glass rod spreader, at least 30 minutes prior to plating the transformed cells. (Precipitation of chemicals can occur if X-gal and IPTG are mixed together prior to plating.)
13. Ensure the plates are dry, then spread 200 µL of the transformed cells onto the plate after the incubation period is over.
14. Place the plates upside down in a 37°C incubator overnight.
15. Check for cell growth the following morning. If growth is apparent, store the plates in a cold room or refrigerator. Several individual colonies should be visible on the plate. Most of the colonies should be white, indicating successful insertion of the gene of interest. If no growth has appeared, leave the plates in the incubator and check again in the afternoon.

REFERENCES

1. Studier, F. W., and Moffatt, B. A. (1986) Use of bacteriophage T7 RNA polymerase to direct selective high-level expression of cloned genes, *J Mol Biol FIELD Full Journal Title:Journal of molecular biology 189,* 113–130.
2. Kreuzer, H., and Massey, A. (2001) *Recombinant DNA and Biotechnology: A Guide for Teachers and Students,* Second ed., American Society of Microbiology.
3. Alberts, B., Johnson, A., Lewis, J., Raff, M., Roberts, K., and Walter, P. (2002) *Molecular Biology of the Cell,* Fourth ed., Garland Science.
4. Burstein, C., Cohn, M., Kepes, A., and Monod, J. (1965) Role of lactose and its metabolic products in the induction of the lactose operon in Escherichia coli, *Biochimica et Biophysica Acta, Nucleic Acids and Protein Synthesis 95,* 634–639.
5. Meselson, M., and Yuan, R. (1968) DNA restriction enzyme from E. coli, *Nature FIELD Full Journal Title:Nature 217*, 1110–1114.
6. Martin, P., Boulukos Kim, E., and Pognonec, P. (2006)

REtools: a laboratory program for restriction enzyme work: enzyme selection and reaction condition assistance, *BMC Bioinformatics FIELD Full Journal Title:BMC bioinformatics 7*, 98.

7. Mullis, K. B., and Faloona, F. A. (1987) Specific synthesis of DNA in vitro via a polymerase-catalyzed chain reaction, *Methods in Enzymology 155*, 335–350.
8. Boots, S. (1989) Gel electrophoresis of DNA, *Anal Chem FIELD Full Journal Title: Analytical chemistry 61*, 551A-553A.
9. Williams, J. F. (1989) Optimization strategies for the polymerase chain reaction, *Biotechniques FIELD Full Journal Title: BioTechniques 7*, 762–769.
10. Costa, G. L., Sanchez, T., and Weiner, M. P. (1994) Stratagies *7*, 52.
11. Bauer, J. C., Deely, D., Braman, J., Viola, J., and Weiner, M. P. (1992) *Stratagies 5*, 62–64.
12. Zabarovskii, E. R., Turina, O. V., Nurbekov, M. K., and Kiselev, L. L. (1989) SK18 diphasmid for constructing genomic libraries with blue/white selection, multiple cloning sites, and with the M13 and l ori, *Nucleic Acids Research 17*, 3309.

www.ebook3000.com

Investigating Protein Expression in Bacteria Grown Under Different Growth Conditions

PARTHA BASU, COURTNEY SPARACINO, PETER CHOVANEC and JOHN F. STOLZ
Departments of Chemistry and Biochemistry, and Biological Sciences, Duquesne University, Pittsburgh, PA 15282

LEARNING OBJECTIVES: This module will introduce senior undergraduate students to microbial physiology and differential protein expression, as well as methods involved in proteomic analysis. Using the metabolically versatile bacterium *Sulfurospirillum barnesii* as the model organism, the students will explore the formulation of the culture medium, methods for growing bacteria anaerobically, preparation of cellular proteins, two dimensional (2D) gel electrophoresis and sample preparation for mass spectroscopy and bioinformatics analyses. In principle, a similar method can be applied the more common bacterium, *Escherichia Coli.*

INTRODUCTION

Versatility of Bacterial Metabolism

BACTERIA have survived billions of years primarily by their ability to adapt to changes in the environment. Many bacteria can grow aerobically, while others grow anaerobically, and in some cases the same bacterium can grow both aerobically and anaerobically depending on the conditions. They can utilize a variety of substrates for growth and respiration, and in doing so dramatically alter the expression of different proteins in the cell. For example, the haloalkaliphilic gammaproteobacterium *Alkalilimnicola ehrlichii* grows aerobically as a heterotroph utilizing acetate as the electron donor and carbon source. In the absence of oxygen, however, it grows as a chemolithoautotroph, coupling the oxidation of arsenite (electron donor) to the dissimilatory reduction of nitrate (electron acceptor) while using carbon dioxide as its carbon source.[1] Thus, while growing aerobically it has a respiratory chain that includes a terminal oxidase, whereas anaerobically it has nitrate reductase and Calvin cycle enzymes.

The soil bacterium, *Sulfurospirillum barnesii*[2], that is used in this laboratory has quite the versatile metabolism as it is capable of using hydrogen, lactate, formate, and pyruvate as electron donors and nitrate, nitrite, selenate, thiosulfate, fumarate, arsenate, and dimethylsulfoxide as electron acceptors. Depending on the growth conditions (what electron donor or acceptors are provided), the organism will express specific types of dehydrogenases, oxidases and reductases[3]. For this experiment, the proteome (protein profile) of cells grown with fumarate or nitrate as the terminal electron acceptor will be compared.

Bacterial Physiology

How an organism generates energy and obtains its carbon and reducing equivalents define its physiology. Energy can be derived from either inorganic or organic compounds (*chemo*) or light (*photo*). Phototrophic organisms use specific wavelengths of light and possess distinct light harvesting pigments (e.g., chlorophyll a, bacteriochlorophylls a, b, c, d, e, and g) and photosynthetic apparatus. Reducing equivalents are essential for the many processes in the cell (including energy generation) that involve oxidation/reduction reactions, and may come from inorganic compounds (*litho*) or organic compounds

(*organo*). Organisms that obtain their carbon from organic compounds are known as *heterotrophs*. *Autotrophs* can generate organic compounds and cellular carbon directly from carbon dioxide. Cyanobacteria, bacteria that grow via oxygenic photosynthesis, obtain energy from light, reducing equivalents from water (H_2O), and carbon from CO_2, and thus are known as "photolithoautotrophs". Photosynthetic bacteria that get both their reducing equivalents and carbon from organic compounds are known as "photoorganoheterotrophs". Sulfur oxidizing bacteria like *Beggiatoa,* are chemolithoauthotrophs as they gain energy by oxidizing hydrogen sulfide with oxygen, and get their carbon from CO_2.

Heterotrophs generate energy through either respiration or fermentation. In respiration, ATP is generated via an ATP synthase by pumping hydrogen ions that were created through a proton motive force (described by the chemiosmotic theory). The latter involves an electron donor complex (typically a dehydrogenase) and a terminal electron acceptor complex, linked by a set of electron transfer complexes embedded within the cytoplasmic membrane. In aerobic respiration, $NADH^+$ is commonly the electron donor and oxygen is the terminal electron acceptor. In anaerobic respiration, other terminal electron acceptors, such as nitrate, Fe^{3+}, or sulfate, substitute for oxygen. For chemoorganoheterotrophs, organic compounds (e.g., acetate, formate, lactate, pyruvate) serve as electron donors. Chemolithoheterotrophs use inorganic electron donors such as hydrogen or hydrogen sulfide. Suitable electron acceptors for anaerobic respiration include oxyanions of nitrogen (i.e., nitrate, nitrite) and sulfur (sulfate, sulfite, thiosulfate), elemental sulfur, Fe^{3+} (i.e., FeOOH), Mn^{4+}, Cr^{6+}, As^{5+}, Se^{6+}, Se^{4+}, fumarate, trimethylamine oxide (TMAO), dimethylsulfoxide (DMSO), and carbon dioxide are suitable electron acceptors. Interestingly, inorganic electron acceptors and donors can be coupled to generate energy, for example, nitrate reduction coupled to sulfide oxidation or arsenite oxidation. When hydrogen or a reduced inorganic compound is used as the electron donor, it is necessary to provide a carbon source (unless the organism is capable of carbon fixation).

In fermentation, ATP is generated through the phosphorylation of an organic substrate and occurs in the cytoplasm. Energy generation does not involve an exogenous electron acceptor and ATP is generated via substrate level phosphorylation. Fermentations are named after the main end product they produce (i.e., lactic acid, ethanol, butyric acid, propionic acid, homoacetic acid, and mixed acid fermentation).

Growth Media Formulation

The nutritional requirements of a bacterium are a reflection of its mode of metabolism, chemical composition, and the biosynthetic (anabolic) pathways present. The chemical composition of a "typical" bacterium is shown in Table 9.1, which highlights that carbon is the most abundant, followed by oxygen, nitrogen, hydrogen, and phosphorous. With the addition of sulfur, these major elements need to be provided to the organism in significant quantity. Additional elements, such as potassium, calcium, magnesium, and iron, are usually needed in lesser amounts and are thus known as macronutrients. Micronutrients are elements (trace) e.g., Mn, B, Se, Cu, Co, Mo, W, and Zn that are needed only in trace amounts and may be toxic at higher concentrations. They are often found in cofactors as part of metalloenzymes. Regardless of the concentration, these basic elements are required by the organism and must be provided in the growth medium. Sodium and chlorine are also important, however these two elements may be provided as counter ions for other elements in the medium (e.g., $MgCl_2$, $NaHCO_3$). Unless the organism has an obligate requirement for sodium, such as marine and halophilic (salt loving) bacteria, specific addition of NaCl may not be necessary.

Growth factors, such as vitamins, are compounds that are not made by the organism but are essential for cell growth and metabolism. Vitamin B_{12} is essential

Table 9.1. Typical chemical composition of bacteria.[4]

Wet weight—70–85% water (9.5×10^{-13} g)
Dry weight: (2.8×10^{-13} g)
55% protein
10–20% cell wall
5% polysaccharide
9% lipid
3.4% lipopolysaccharide
20% RNA
3% DNA
C - 50%; O - 20%; N - 14%; H - 8%; P - 3%; S - 1%; K - 1%; Ca - O.5%; Mg - 0.5%; Fe - 0.2%

www.ebook3000.com

for phototrophic bacteria although many lack the pathway for its synthesis (thus it needs to be added to the medium). Yeast extract (1 g/L), which essentially is yeast cells that have been lysed and heated, is often used as it contains many different nutrients and cofactors. Other supplements are beef extract, casein, and proteose peptone. Medium made with these general supplements is known as "non-defined" as the exact composition is unknown. Medium for which all the ingredients are known is called "defined" or "synthetic".

During growth and metabolism bacteria can change the pH of the medium. Thus finding a suitable buffer is very important. Phosphate and bicarbonate are common buffers used in growth media. Organic buffers such as MOPS and HEPES are used in certain media, however, organisms may be able to use them as a source of carbon. Bicarbonate buffer is sensitive to CO_2 and phosphate come outs of solution at concentrations higher than 0.1 M. The pH of the medium should be adjusted prior to sterilization, but may need to be adjusted again after autoclaving especially if additional constituents are added.

The specific growth conditions may require additional ingredients or greater concentrations of specific elements. Photosynthetic organisms have a greater need for magnesium and iron as these elements are parts of crucial cofactors (i.e., chlorophyll). Anaerobic microbes are often sensitive to oxygen. In some cases (e.g., sulfate-reducing bacteria) addition of reducing agents such as sodium dithionite, thioglycolate, or sodium sulfide is sufficient. However, some organisms and electron acceptors e.g., Fe^{3+} are sensitive to reducing agents and thus the use of the latter should be avoided. In this case it is also necessary to remove the oxygen in the medium prior to sterilization, via "degassing". This is done by bubbling the medium for several minutes with a mixture of CO_2 and N_2 (typically 20:80) deoxygenated gas.

The most common method of sterilization is autoclaving (121°C at 15 psi, for 20–30 min/l). However, heating complex medium can cause some components to react and can cause precipitation (e.g., sulfide reacts with metals). Vitamins, growth factors, and antibiotics are also heat labile. The solution to precipitation is to autoclave the reactive constituents (i.e., the solution of bicarbonate, trace metals) separately. Heat labile compounds should be filter-sterilized and aseptically added to the sterile medium after it has had a chance to cool.

Cell Fraction Preparation

Proteins are the most abundant macromolecule in cells, making up approximately 55% of the dry weight (Table 9.1). Proteins can be structural or functional (enzyme). Most proteins are present in the cytoplasm; however there are many proteins in the membrane (e.g. receptors, integral membrane proteins) and on the surface (pili, adhesions). When preparing proteins for analysis, the cell integrity must be compromised to release the soluble constituents (e.g., cytosolic proteins). Cells can be "lysed" by a variety of methods including osmotic stress, cavitation (sonic dismembranator), and pressure (e.g., French Pressure Cell). In Gram negative cells proteins may be localized to the cytosol, cytosolic membrane, periplasm, or outer membrane. Using a combination of chemical treatments (e.g., lysozyme, detergent) and centrifugation steps, proteins from the four compartments can be separated. However, for the purposes of this lab, only cell lysates will be used. Once the cell fraction is prepared, the proteins can be resolved either by molecular mass alone (1D electrophoresis) or by their charge (isoelectric focusing) and molecular mass (2D electrophoresis).[5]

An important aspect of reproducible protein preparation is determining the protein content of the sample at each step. The method for determining protein concentration must be precise and reproducible. Three popular methods will be investigated: Bradford[6], Lowry[7,8,9] and 280 nm spectroscopy[10,11].

Proteomic Analysis

Proteome analysis is a powerful approach for the identification of gene products expressed in various cells and tissues under different conditions. Depending on the conditions, an organism can express a multitude of proteins at any given time. Two-dimensional electrophoresis (2D-E) is a technique for the reliable separation of hundreds of proteins in a single gel. This protocol describes a method for performing the first and second dimension separations for two large-format 2D-gels simultaneously in a single vertical electrophoresis unit. In the first dimension

proteins are separated based on their isoelectric points (pIs) and the second dimension separation is based on the molecular weight. Once separated, they can be excised from the gel, digested and analyzed by mass spectrometry. The better the separation, the more reliable are the mass spectral results. Better separation means the proteins are better resolved, and often larger format gels provide better resolution. In most cases, protein samples are excised from the gel and digested with a proteolytic enzyme (e.g., trypsin) to make smaller fractions. These fragments are analyzed by matrix-assisted laser desorption/ionization time-of-flight mass spectrometry (MALDI-TOF-MS), generating a profile of the different peptide fragments of each protein, which is then matched with to profiles in a existing database. This approach, called peptide fingerprinting mapping (PFM), is generally used for identifying proteins. However, in some cases this may not be sufficient for identification, requiring more advanced tandem mass spectrometric approaches. In any event, using robust MS-based proteomics approaches, one can obtain an inventory of cell proteins of the organism of choice, providing insight into the physiology of the organism.

EXPERIMENTAL PROCEDURE

This experiment is broken into the five individual steps for simplicity: growth, cell harvesting, cell fractionation, protein concentration determination, and electrophoresis. All are of equal importance and care should be taken in each step to ensure an equivalent comparison of the two samples, nitrate and fumarate grown cells. *All students should wear proper attire including safety goggles, lab coats and gloves, and take proper precautions.*

Growth of Sulfurospirillum barnesii *Strain SES-3*

The following ingredients are to be dissolved in 3920 mL dH_2O: 0.9 g K_2HPO_4, 0.9 g KH_2PO_4, 1.8 g NaCl, 0.9 g $(NH_4)_2SO_4$, 0.47 g $MgSO_4 \cdot 7H_2O$, 2.0 g yeast extract, 16.3 g $NaHCO_3$, 2.0 g cysteine, 40 mL trace element mixture, 40 mL vitamin mixture, 9.0 mL sodium lactate (60%). After they are thoroughly mixed, the solution is separated into two 2 L screw top appropriately labeled bottles. 20 mM of terminal electron acceptor (sodium nitrate *or* sodium fumarate) is to be added to the media bottles, and the pH of the solution is to be adjusted to 7.3 with HCl while stirring magnetically. Once the pH is adjusted, the solutions are to be degassed by passing purified N_2-gas for 20-30 min. The stir bar is to be removed before degassing the air at the top for 10 min. The bottle can be sealed by covering the opening of the bottle and removing the syringe simultaneously. A dithionite solution (2 g in 10 mL nanopure degassed water) is to be prepared separately. All bottles are to be autoclaved on slow exhaust for 55 min, and cooled to room temperature. Once all the components are at RT, the amendments are added aseptically to the medium. Lastly, a 15 mL of stock *S. barnesii* and the dithionite solution are added taking care to avoid introduction of oxygen into the media. If properly done and the cells in the inoculum were at log growth phase, the cultures should grow in approximately 1–3 days. Prior to harvesting, a sample of the culture should be examined microscopically to assure that no contamination has occurred.

Harvesting Cells

Log growth phase cultures are harvested by centrifugation. Access to a centrifuge that can handle large scale (1 L) volumes will facilitate efficient cell harvesting. However, smaller scale volumes (250–500 mL) can be done in batches and subsequently pooled. Most bacterial cells are readily pelleted by centrifugation at 7,000 × g for 15 min. The supernatant is poured off and the cell mass resuspended in a small volume (10 mL) of lysis buffer (150 mM Tris- HCl with 300 mM NaCl of pH, 7.5) and transferred to a pre-weighed 50 ml volume centrifuge tube. The cells are then centrifuged at 8000 rpm for 15–30 minutes and once again the supernatant discarded. The wet weight of the cells can be determined by subtracting the weight of the tube from the weight of the tube with the cells. The cell pellet should then be rinsed with lysis buffer and centrifuged one additional time. At this point the cell pellet can be frozen at –80°C, as needed.

Cell Lyses: French Pressure Cell Press

To prepare the sample for lyses the cell pellet should be resuspended in cold lysis buffer. The pellet is further homogenized using a 40 mL douncer until clumps

www.ebook3000.com

are no longer present. The homogenized sample is placed into a French press cell that has been pre-cooled. The directions for operation of the cell should be followed carefully and care taken not to release the pressure too quickly. The protease inhibitor cocktail (1 mL/10 mL) DNase (1 mg/10 mL) is immediately added to the cell lysate. The lysate is then centrifuged at 8,000 rpm for 5 min to remove any unbroken cells. The supernatant is collected in a labeled 50 mL centrifuge tube. The pellet of unbroken cells can be weighed (to determine the efficiency of cell lyses) and discarded.

Determination of Protein Concentration

Protein concentrations will be estimated in three different ways. Depending on the class size, it is prudent to divide the class into three smaller groups and have each group perform a specific method. Again, the purpose of this part of the exercise is to demonstrate the benefits as well as the limitations of the different methods.

Spectroscopy. A bovine serum albumin (BSA) solution (3 mg/mL) in 2% SDS is prepared for establishing a standard curve. From this stock solution standards of differing concentrations (e.g., 5, 10, 25, 50, 100 μg/mL) including a blank (buffer alone), are prepared via serial dilution. The absorbance at 280 nm of each of these solutions is measured and used to plot a standard curve. The cell fractions from the nitrate and fumarate grown samples are then measured at 280 nm (note: dilution in the tris buffer may be necessary if the concentration proves to lie outside the standard curve) with the absorption value used to determine the protein concentration from the standard curve. In both cases, the concentration should be determined in triplicate from independent samples.

Lowry. An equal volume of 0.25% $CuSO_4 \cdot 5H_2O$ containing 0.2% potassium tartrate, and 20% sodium carbonate are mixed together. In addition, a 0.8 M NaOH solution and a 10% SDS solution are needed. Equal volumes of the three solutions and distilled water are mixed to make copper tartrate reagent (CTC) solution, which is stable for a week at room temperature. A 3 mg/mL BSA in 20 mL of the 2% SDS is prepared as stock standard solution from which five different concentrations were generated via serial dilution to a final volume of 1 mL. A 50 μL aliquot of fumarate or nitrate sample is diluted appropriately with 2% SDS to a final volume of 1 mL. 1 mL of the CTC solution is added to both the samples and the standards, and the solutions are incubated at room temperature for 5 minutes. 500 μL of Folin-Ciocalteu reagent (20%, v/v in water) is then added in each solution, and the final solutions are vortexed for 1 min and incubated for 5 minutes. The absorbance of the samples and standards is measured at 750 nm. Again, a standard curve is plotted and the protein concentration of the samples determined using the absorbance values.

Bradford. Two stock solutions are made first, a Coomassie Blue solution and 0.1 M NaCl. The Coomassie Blue solution contains Coomassie dye (100 mg of Coomassie brilliant blue G-250 per liter distilled water) and 8.5% phosphoric acid. The Coomassie solution should be filtered through a Whatmann no. 1 filter paper and stored at 4°C. The protein standard is prepared by dissolving BSA (3 mg/mL) in 0.1M NaCl. The BSA standard concentrations are prepared from a solution containing 3 mg/mL BSA in 0.1M NaCl. The samples are diluted appropriately to 1 mL with 0.1 M NaCl. 1 mL of the Coomassie solution is added (to all samples and standards) and mixed thoroughly by vortexing. The absorbance of the solutions are determined at A_{595} for all standards and samples from which the concentration of the unknown protein is determined.

1D Electrophoresis

One liter of each of the following solutions is to be made prior to the electrophoresis experiments: 10× running buffer, destaining solution and Coomassie brilliant blue. The Coomassie brilliant blue solution contains 0.05% w/v Coomassie brilliant blue (R), 50% v/v isopropyl methanol, 10% v/v glacial acetic acid in distilled water. Running buffer (10×), is to be made of 500 mM tris (60.5 g/L), 1.96 M glycine (147.1 g/L) and 1% lauryl sulfate. Destaining solution is prepared by mixing a 10% glacial acetic acid, 5% methanol and distilled water. Laemmeli sample buffer is to always be made fresh and according to manufacture's instructions.[12]

The total protein content of nitrate and fumarate samples is equalized by diluting the samples with Laemmli sample buffer (e.g., Biorad, 161-0737) in micro centrifuge tubes to a final amount of 10–20 μg total protein/20 μl of sample buffer. The sample is then immersed in boiling water bath for 10 minutes to

denature the proteins. The denatured samples are centrifuged at low speed (3,000–5,000 g) for 3 min while assembling the gel electrophoresis apparatus and filling with 1× running buffer according to manufacture's directions. The samples are loaded onto the gel by pipetting 20 µL into each well. The molecular weight standards solution is also placed into a central well for reference. The gel is run at 150 V for about 70 min or until the dye front reaches the bottom of the gel. The gels are removed from the apparatus, separated from the glass plates, and placed into a glass dish with Coomassie blue stain. The gels should stain in about 60 min. The Coomassie stain is disposed of in a proper container and the gel is incubated in destaining solution overnight. A sponge should be placed in a corner, not touching the gel to remove the leftover dye. Once the gel has properly destained, photo documentation can be done. Avoid allowing the gel to dehydrate.

2-D electrophoresis (2D-E). Two-dimensional gel electrophoresis has several distinct steps and is more involved than one-dimensional gel electrophoresis. The overall procedure is shown schematically in Figure 9.1.

Protein sample preparation and rehydration. The cell lysates are precipitated with trichloroacetic acid (TCA) at a final concentration of 10%, on ice for 60 min. The protein pellet obtained by subsequent centrifugation is washed with acetone in order to remove residual TCA. Immobiline Drystrips (13 cm, pH 3–10, Bio-Rad) are rehydrated in 250 µL rehydration solution containing 500 µg solubilized proteins for isoelectric focusing (IEF). The rehydration solution consists of 8 M urea, 2% (w/v) CHAPS, 20 mM DTT and 1% (v/v) ampholytes and also contains a trace of bromphenol blue as the tracking dye. Urea is used to disrupt the hydrogen bonds; CHAPS is used to solubilize lipids and it disrupts membranes and hydrophobic interactions; DTT reduces disulfide bridges and ampholytes helps solubilization, scavenging and inhibiting interactions between sample proteins and Immobilines of the IPG strips.

1st Dimension-Isoelectric Focusing (IEF). IEF is an electrophoretic method that separates proteins according to their isoelectric points (pI). The pI is the specific pH at which the net charge of the proteins is zero. In a pH gradient, under the influence of an electric field, a protein will move to the position in the gradient where its net charge is zero.

A dry strip to be removed from the freezer and allowed to equilibrate at room temperature for 15 min. The sample is loaded into the rehydration tray and the IPG strip is then carefully placed gel side down and covered with mineral oil. Normally the rehydration is conducted overnight (12–16 hours) to ensure maximal diffusion. The rehydrated strips are then moved to the electrophoresis unit and placed in a lane. Paper wicks that have been soaked in distilled water, are then placed at each end of the strip (these will make contact

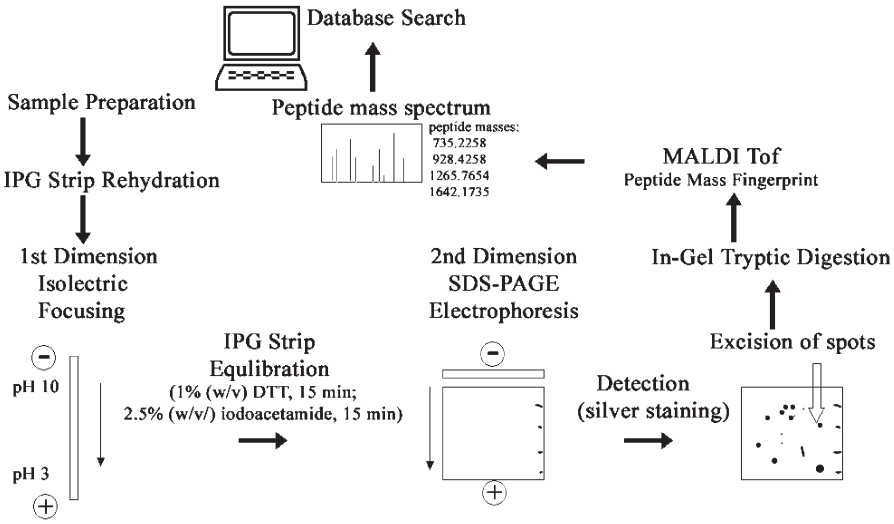

Figure 9.1. Schematic representation of 2D Gel electrophoresis.

www.ebook3000.com

Table 9.2. Gel electrophoresis conditions.

Step	Voltage	Time	Volt-Hours	Ramp
1	30	20 min		Linear
2	8000	2 h		Linear
2	8000		25,000	Rapid

with the electrodes). Make sure that your strips have been properly aligned with the (+) end at the cathode and (–) end at the anode. A layer of Drystrip cover fluid is then added to the wells, the cover of the unit is closed, and the strips are electrophoresed at 20°C. The system used in this exercise is the BioRad Protean IEF Cell isoelectric focusing system; however, systems from other manufacterers can also be used with the appropriate conditions described in their manual. Focusing is carried out first at 300 V for 20 min, then 8000 V for 2 h, followed by additional focusing at 8,000 V until a total of 25 kVh has been reached. Table 9.2 shows a typical case for the Protean system.

Equilibration. Following IEF, the mineral oil is poured off and the strips are equilibrated twice for 15 min each time with gentle shaking, first in 30% (v/v) glycerol, 6 M urea, 2% (w/v) SDS, 50 mM Tris-Cl, pH 8.8, 1% (w/v) DTT and a trace of bromphenol blue as tracking dye. The second time the equilibration is done in this same solution, except that DTT is replaced by 2.5% (w/v) iodoacetamide.

SDS-PAGE-2nd Dimension. After equilibration, each IEF strip is drained on a filter paper and immersed in SDS running buffer (25 mM Tris base, 0.192 M glycine and 0.1% SDS). The strips are then carefully positioned at the top of the second dimension PAGE gel and sealed with a solution containing 1% agarose (w/v) in SDS running buffer. Electrophoresis is performed at 4°C and 60 V/gel for 15 min and then at 200 V/gel, until the tracking dye has reached the bottom of the gel.

Staining. For proteomic analysis, protein spots are visualized employing Coomassie brilliant blue R-250. The gels are fixed for 20 min in a methanol-acetic acid solution (4 parts methanol, 1 part acetic acid, 5 parts distilled water), and then stained with 0.1% (w/v in 25 parts methanol, 8 parts acetic acid, 67 parts water) Coomassie Blue R-250 solution. After the staining is complete, the gel is destained overnight in destain solution (25 parts methanol, 8 parts acetic acid, 67 parts water). When destaining is complete, the gels are photographed. Differences in the protein expression are analyzed by densitometry to understand differential expression of the protein under different growth conditions such as fumarate and nitrate. Once spots (i.e., proteins) of interest are identified they are excised from the gel and subjected to tryptic digest, followed by mass spectrometric analysis for the identification of the protein. Depending on the goals and the resources of the experiment, the mass spectrometric aspect can be included in another module. A representative gel is shown in Figure 9.2.

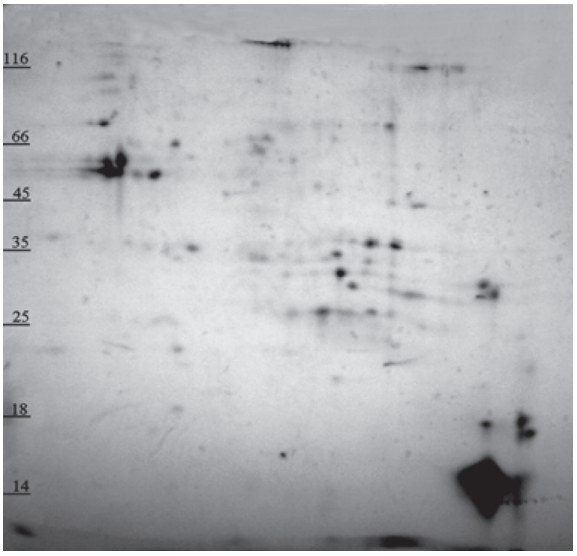

Figure 9.2. 2D Gel for S. barnesii grown on nitrate. Bacteria were broken using French pressure cell press after 24 h growth. Cell lysate was precipitated with TCA, and run on pH 3–11 IEF strip and stained with Coomassie blue.

INSTRUCTOR'S RESOURCES

Almost any facultative bacterium for which the complete genome is available can be used in this exercise. Both *Pseudomonas aeruginosa* and *Escherichia coli* are capable of growing anaerobically using nitrate as the terminal electron acceptor. Aerobic cultures are grown on standard LB medium in flasks on a shaker (100 rpm). Anaerobic cultures are grown on LB medium supplemented with 20 mM sodium nitrate in screw capped tubes or bottles. The end product of nitrate respiration in *E. coli* is ammonia and the pathway involves a nitrate reductase, (NarGHI),

and nitrite reductase (NrfAH). *P. aeruginosa* is a denitrifier with nitrate being converted to dinitrogen gas. Nitrite, nitric oxide, and nitrous oxide are intermediates in the pathway. Nitrate reductase (NarGHI), nitrite reductase (NirSCM), nitric oxide reductase (NorCB), and nitrous oxide reductase (NosZ).

SUGGESTED READING

Scopes R K. *Protein Purification Principles and Practices* (1993)

REFERENCES

1. Hoeft, S.E., et al., IJSEM 57:504-512, 2007.
2. a. Oremland RS, et al. Isolation, growth, and metabolism of an obligate anaerobic, selenate-respiring bacterium, strain SES-3. *Appl. Environ. Microbiol.* 60: 3011–3019, 1994. b. Laverman AM, et al. Growth of strain SES-3 with arsenate and other diverse electron acceptors. *Appl. Environ. Microbiol.* 61: 3556–3561, 1995. c. Stolz JF, et al. Sulfurospirillum barnesii sp. nov. and Sulfurospirillum arsenophilum sp. nov., new members of the Sulfurospirillum clade of the epsilon Proteobacteria. *Int. J. Syst. Bacteriol.* 49: 1177–1180, 1999.
3. Martinez Murillo, F. et al 1997 Differential protein content in Geospirillum barnesii. Arch. Microbiol.
4. G. Gottschalk 1986 *Bacterial Metabolism 2nd Ed.* Springer-Verlag, New York, 380 pgs.
5. Schägger H; von Jagow G (Nov 1987). "Tricine-sodium dodecyl sulfate-polyacrylamide gel electrophoresis for the separation of proteins in the range from 1 to 100 kDa". *Anal Biochem* **166** (2): 368–379.
6. Bradford, MM. A rapid and sensitive for the quantitation of microgram quantitites of protein utilizing the principle of protein-dye binding. *Analytical Biochemistry 72*: 248–254. 1976.
7. Lowry, OH, NJ Rosbrough, AL Farr, and RJ Randall. Protein measurement with the Folin-Phenol reagents. *J. Biol. Chem. 193*: 265. 1951.
8. Stoscheck, CM. Quantitation of Protein. *Methods in Enzymology 182*: 50–69 (1990).
9. Hartree, EF. *Anal Biochem 48*: 422–427 (1972).
10. Layne, E. Spectrophotometric and Turbidimetric Methods for Measuring Proteins. *Methods in Enzymology 3*: 447–455. 1957.
11. Scopes R K. *Protein Purification Principles and Practices* 46–48 (1993).
12. Laemmli U K. (Aug 1970). "Cleavage of structural proteins during the assembly of the head of bacteriophage T4". *Nature* **227** (5259): 680–5.

www.ebook3000.com

Understanding the Electronic Structure of Hydrated Metal Complexes

PARTHA BASU, ERANDA PERERA, RAGHVENDRA S. SENGAR, EILEEN M. CHESTNUTT and LAUREN M. MATOSZIUK

Department of Chemistry and Biochemistry, Duquesne University, Pittsburgh, PA 15282

LEARNING OBJECTIVES: This experimental module utilizes the preparation of hydrated metal complexes, recording their electronic spectra and detailed analysis of the electronic spectral data. The purpose of this experiment is to isolate hydrated complexes of chromium, record their electronic spectra and determine the ligand field strength of water. In the next phase, the students are to design methods to synthesize a hydrated complex of a 1st row transition metal of their choice and analyze its electronic spectra. In the process the students develop a detailed understanding of ligand field theory, d-d transition, and crystal/ligand field stabilization energy.

INTRODUCTION

LIGAND field theory provides a strong conceptual basis for understanding the metal-ligand interaction that underpins the properties of transition metal complexes.[1,2] Such interaction defines the properties of the metal complex, e.g., reactivity, and spectroscopic signature. Quantitative determination of ligand field stabilization energy (LFSE), one objective of this experiment, is rarely covered in an undergraduate curriculum. Here we will study the kinetics of ligand exchange on the Cr(III) ion, where a water molecule replaces a chloride ion. The starting Cr(III) complex is Cr(III) chloride, usually designated as $CrCl_3 \cdot 6H_2O$, which is crystallographically determined to be a *trans*-$[CrCl_2(H_2O)_4]Cl \cdot 2H_2O$ complex.[3] In solution, where a water molecule can replace chloride ions, it is important to separate different hydrated species i.e., $[CrCl_2(H_2O)_4]Cl$; $[CrCl(H_2O)_5]Cl_2$; $[Cr(H_2O)_6]Cl_3$.[4] As all species are ionic, ion exchange chromatography is to be used in separation by varying the strength of the acid in the mobile phase.[5] The differentially hydrated species absorb light differently thus providing a means to identify the species present in solution.

PREPARATION OF STUDENTS

Students must be introduced to the possible hazards of perchlorate and chromium before they perform experiments and must be instructed in proper waste disposal. Proper labeling and storage of synthesized compounds with the appropriate name (or formula) of chemical should be the part of general laboratory practice. The required apparatus includes Erlenmeyer flasks, measuring cylinders, test tubes, beakers, and pipettes. Training on the UV-visible spectrophotometer and requisite software may be helpful to students, so that they can work independently on the project. This module works well as a group project where individual students perform specific tasks and share the information, which also increases collaboration.

CHEMICAL AND EXPERIMENTAL HAZARDS

Perchlorates are explosives, especially when heated. Some chromium compounds are carcinogenic and should be treated with caution. All waste should be disposed appropriately. Due to the toxic nature of chemicals used in the reactions, rubber gloves, suitable

goggles for eye protection, and laboratory coats must be worn during the experimentations.

EXPERIMENTAL PROCEDURE

Preparation of a Dowex Ion-exchange Column

A slurry of Dowex 50 × 8 H^+ resin in water is to be added to a glass column, equipped with a frit, to a height of 15 inches. Deionized water is to be passed through the column until the eluent becomes colorless. The water is to be subsequently drained to the top of the resin.

Preparation of the Cr(III) Solution

2.33 g of $CrCl_3 \cdot 6H_2O$ will be dissolved in 25 mL of 0.002 M $HClO_4$. Precautions to be taken in handling perchloric acid include heat and contact with organic solvents. The solution is to be stirred without heat until all solid chromium complexes dissolve.

Preparation of $[CrCl_2(H_2O)_4]Cl$

5 mL of the Cr(III) solution is to be added to a newly prepared Dowex ion-exchange column and drained to the top of the resin, with the time of addition being noted. The column is to be eluted with 0.10 M $HClO_4$ and a green band to be collected, and the time of collection is to be noted. (*Note:* The green band should be collected in a series of test tubes rather than a beaker in order to prevent other species in the Cr(III) solution from contaminating the entire collection) UV-visible spectra (350–800 nm) of the green fractions are to be collected in a spectrophotometer.

Isolation of $[CrCl(H_2O)_5]Cl_2$

5 mL of the Cr(III) solution is to be placed in a test tube and incubated in warm water for ~3 minutes. This solution should be added to a fresh Dowex column and eluted with 0.20 M $HClO_4$ until the eluent becomes colorless. This should elute all residual $[CrCl_2(H_2O)_4]^+$ from the column. The molarity of the perchloric acid is to be increased to 1.0 M in order to elute $[CrCl(H_2O)_5]^{2+}$ from the column. Again the fractions are collected in test tubes and the UV-visible spectra of the solutions are to be recorded. The times of addition and elution are to be noted.

Isolation of $[Cr(H_2O)_6]Cl_3$

5 mL of water are to be added to 5 mL of the Cr(III) solution and the solution heated in a warm water bath for 5 minutes. This mixture is added to the column and eluted with 1.0 M $HClO_4$ until the eluent becomes colorless and the remaining dark band is eluted from the column with 3.0 M $HClO_4$. The fractions are to be collected in test tubes as before and their UV-visible spectra (350–800 nm) to be recorded. Again the times of addition and elution are noted.

Separation of $[CrCl_2(H_2O)_4]Cl$, $Cr(H_2O)_5]Cl_2$, and $[Cr(H_2O)_6]Cl_3$

5 mL of a fresh Cr(III) solution is diluted with 5 mL of water and the resulting solution added to a fresh Dowex column. The $[CrCl_2(H_2O)_4]Cl$ species eluted with 0.1 M $HClO_4$ till the eluent become colorless. This is to be followed up by elution of $[CrCl(H_2O)_5]Cl_2$ with 1.0 M $HClO_4$ and finally $[Cr(H_2O)_6]Cl_3$ to be eluted with 3.0 M $HClO_4$. UV-visible spectra of each fraction are to be recorded. Total volume of each fraction is to be noted.

Fitting the Absorption Bands

All absorption spectra should be saved as spreadsheet ASCII files. The data will be imported into graphics software and the data are plotted, using the following equation:

$$f(x) = ae^{-(x-b)^2/(2c^2)} \quad (1)$$

as absorbance versus wavelength. In this case, the software, Origin, has been used. Generally a Gaussian function of generic formula (Equation 1), (where a is the height of the peak, b, is the location of the center of the peak and c, is related to the full width at half height) is employed. The Gaussian function results in a normal or bell-shaped curve which is symmetrical about the mean or center. It is based on the assumption that independent random errors occur on a normal distribution and this distribution can be represented by the bell-shaped curve. For deconvoluting overlapping bands for accurate determination, multiple peak options are to be used.

www.ebook3000.com

RESULTS AND DISCUSSION

Preparation of Complexes

All complexes are prepared in solution, and characterized in solution. Ion exchange chromatography is used to separate the three Cr(III) complexes. Because all three complexes are of Cr(III), different hydration levels change the overall charge as each chloride is replaced with a water molecule. An increase in overall charge increases the overall binding to the column that requires stronger acid for elution.

Coordination Geometry about Cr in $CrCl_2(H_2O)_4^+$, $CrCl(H_2O)_5^{2+}$ and $Cr(H_2O)_6^{3+}$

Each of these compounds has octahedral geometry about the central metal ion, with six ligands coordinated to a central Cr(III). $CrCl_2(H_2O)_4^+$ can exist in two geometric isomeric forms: cis and trans that are defined based on the relative arrangements of the chloride ligands. Although all structures in Figure 10.1 possess overall octahedral *geometry*, strictly speaking their geometry is lower than that of O_h due to the different ligand types e.g., Cl and H_2O. The ground state electronic configuration of elemental chromium(0) is $[Ar]3d^54s^1$; and that for Cr(III) as in $CrCl_2(H_2O)_4^+$, $CrCl(H_2O)_5^{2+}$, and $Cr(H_2O)_6^{3+}$, is $[Ar]3d^34s^0$ due to a decrease in the shielding of the 3d electrons as a result of the removal of electrons from the 4s orbital. This decrease in shielding results in a more tightly bound d electrons, which in effect lowers the energy of the 3d orbital compared to the 4s orbital. Thus, in each case the central metal ion has three electrons and they are arranged according to Hunds rule of maximum multiplicity.

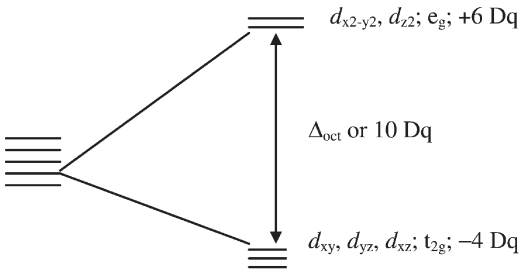

Figure 10.2. Schematic representation of d-orbital splitting in octahedral field.

The crystalline field can be depicted as an array of negative point charges. In the case of an octahedral arrangement of ligands around a central metal ion, such as that seen in the $CrCl_2(H_2O)_4^+$, $CrCl(H_2O)_5^{2+}$, and $Cr(H_2O)_6^{3+}$ complexes, this array can be described as six point charges, one on each face of a cube centered around a central metal ion. In an octahedral field the degeneracy of the five d-orbitals is lost as they have different geometric disposition. Thus, the t_{2g} orbitals (d_{xy}, d_{yz}, and d_{xz}) are energetically equivalent and lower in energy, and the e_g (d_{x2-y2} and d_{z2}) orbitals are also equivalent, and are higher in energy. The octahedral field splitting energy is labeled as 10 Dq, and represents the difference in energy of the two subsets of *d* orbitals with respect to the crystal field (Figure 10.2). The discussion up until now has dealt with only single electron wave functions (for instance, a metal ion with a d^1 configuration).

Crystal Field Splitting in d^3 Complexes. In the previous discussion of ligand field splitting, a single electron example was used. For a multiple *d* electron configuration, such as the d^3 configuration encountered in $CrCl_2(H_2O)_4^+$, $CrCl(H_2O)_5^{2+}$, or in $Cr(H_2O)_6^{3+}$, many electron wave-functions can be de-

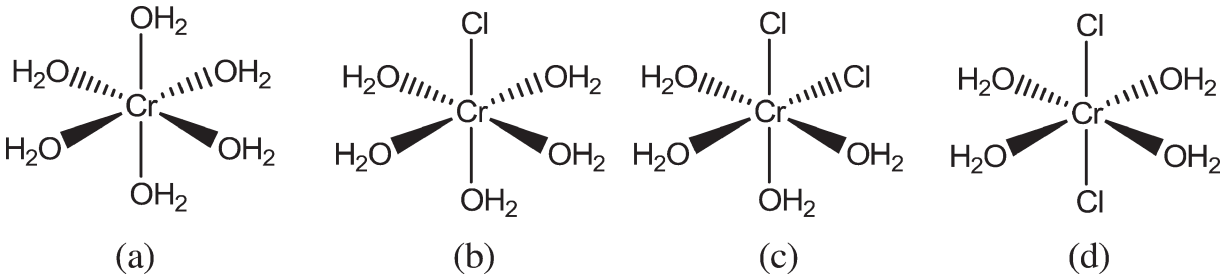

Figure 10.1. The octahedral geometry of; (a)$Cr(H_2O)_6]^{3+}$; (b)[$CrCl(H_2O)_5]^{2+}$; (c) cis $[CrCl_2(H_2O)_4]^+$ and (d) trans-$[CrCl_2(H_2O)_4]^+$.

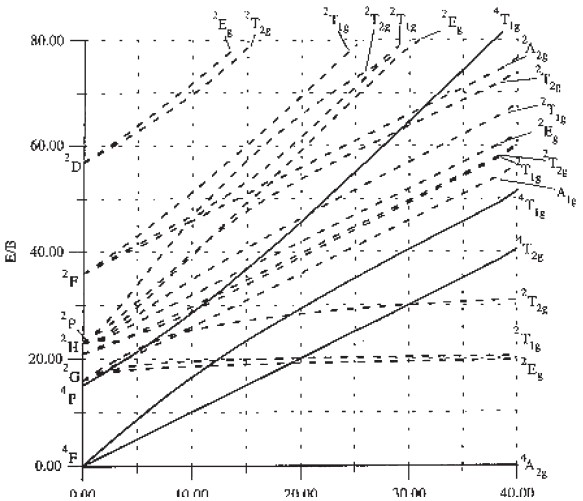

Figure 10.3. A Tanabe Sugano diagram for the d^3 electron configuration. The ^4F ground state is split by the crystal field to generate the $^4A_{2g}$, $^4T_{2g}$, and $^4T_{1g}$ states, with $^4A_{2g}$ being the ground term.

scribed by an ensemble of term symbols in the form ^{2S+1}L where S represents the spin angular momentum, 2S+1 represents the spin multiplicity, and L represents the orbital angular momentum.[3] For the d^3 configuration, the term symbols are ^2H, ^2G, ^4F, ^2F, ^2D, ^2D, ^4P, and ^2P. A summary of the elucidation of these term symbols is provided in Table 10.3 including a table of microstates (Table 10.4). The ground state, according to Hund's rules is ^4F.[3] This ground ^4F term, when split by the crystal field yields the states $^4A_{2g}$, $^4T_{2g}$, and $^4T_{1g}$ with $^4A_{2g}$ being the ground term, as shown in Figure 10.3, the Tanabe Sugano diagram for a d^3 electronic configuration.[1] For d^3 electrons, three different peaks, corresponding to the three possible '*d–d*' transitions should occur; however, for this experiment we focused on only transitions arising from the aforementioned F terms.

Table 10.1. Absorption maxima of each peak in cm^{-1}.

Cr(III) Complex	Absorption Maxima of Peak #1 (cm^{-1})	Absorption Maxima of Peak #2 (cm^{-1})
$[CrCl_2(H_2O)_4]^+$	22400	15600
$[CrCl(H_2O)_5]^{2+}$	23850	16400
$[Cr(H_2O)_6]^{3+}$	24800	17400

Selection Rules for Electronic Transitions

There are several selection rules for electronic transitions. One of these is the *spin selection rule* which denies the possibility of an electronic transition between states of different spin multiplicity. The reasoning behind this rule is that as light has no spin properties, it is not able to change electronic spin. Another selection rule is the result of the *parity rule*. This rule involves the symmetry of wave-functions and states that transitions between orbitals or states of different parity are forbidden. This implies that '*d–d*' transitions are forbidden, which, however, is not necessarily the case. An additional selection rule for electronic transitions is that the two orbitals involved in a transition must have orbital angular momenta that differ by only one unit. This rule implies that $s \rightarrow p$ transitions are allowed; however, $s \rightarrow d$ transitions are not allowed.

"Violation" of Selection Rules

For spin allowed transitions, although the parity rules imply that pure '*d–d*' transitions should not occur, they still do as a result of the vibrations of octahedral metal complexes. Some of these vibrations actually eliminate the center of inversion, and thus *d–p* mixing may occur, which in turn allows '*d–d*' transitions to take place. Spin forbidden '*d–d*' transitions may also occur due to the fact that the electronic wave function cannot be cleanly separated into spatial and spin components, but rather the spin and orbital angular momenta of the electrons are coupled by a magnetic interaction known as spin-orbit coupling. In this experiment, absorption spectra of 3 octahedral Cr(III) complexes, $[CrCl_2(H_2O)_4]Cl$, $[CrCl(H_2O)_5]Cl_2$, and $[Cr(H_2O)_6]Cl_3$ with d^3 electronic configurations are to be recorded. These spectra are then analyzed using ligand field theory and the background developed herein, in order to determine the 10Dq values of each complex, and the ligand field strengths of water and Cl^-.

Data Analysis and Discussion

The objective of the first part of the experiment is to determine the absorption maxima of the three Cr(III)

www.ebook3000.com

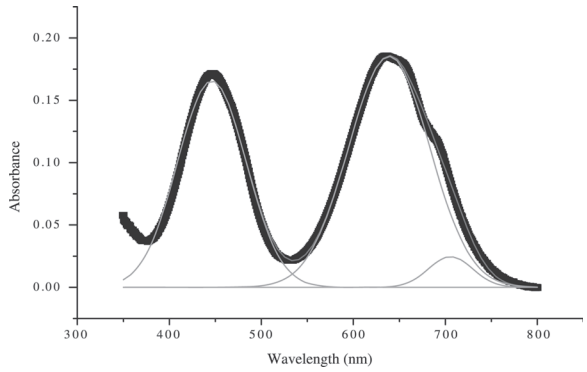

Figure 10.4. An example of Gaussian peak fit for multiple peaks using Origin software for $[CrCl_2(H_2O)_4]Cl$. Note that the data are shown with thick black line and thin lines show the fit.

complexes, $[CrCl_2(H_2O)_4]Cl$, $[CrCl(H_2O)_5]Cl_2$, and $[Cr(H_2O)_6]Cl_3$, using the Origin software. The multi-peak Gaussian fit was used to determine the exact peak maxima (Figure 10.4). Three peaks were selected for analysis, but only the two higher energy peaks are of importance as mentioned previously. These band positions are to be listed in a table (an example is given below). The positions are listed in nanometers and they need to be converted to wave numbers, and averaged for each band, as listed in Table 10.2.

Using this maximum peak data and a Tanabe Sugano diagram, it is possible to identify ligand field splitting in the three different Cr(III) coordination complexes. Tanabe Sugano diagrams are correlation diagrams that are particularly useful in the interpretation of the electronic spectra of coordination complexes. The absorption peaks for each complex of higher energy correspond to the $^4T_{1g}$ electronic state, and the peaks of lower energy correspond to the $^4T_{2g}$ electronic state. Using this knowledge, it is possible to calculate the 10Dq value of each Cr(III) coordination complex as well as of water and chlorine in the octahedral complexes. Examples of these calculations are below.

Representative Calculations for $^4A_{2g} \rightarrow {}^4T_{1g}$ Transition

Finding 10Dq value of $[Cr(H_2O)_6]Cl_3$: From the Tanabe-Sugano diagram, E/B = 32.32. We know that E is equal to the energy of the higher energy peak of the complex in cm^{-1}. Therefore: 24687.82 cm^{-1}/B = 32.32. We find that B = 763.86 cm^{-1}. Following that 10Dq/B = 22.76, the 10Dq value of the complex and also of water itself is 17385 cm^{-1}.

The 10Dq values of the $[CrCl_2(H_2O)_4]^+$ and $[CrCl(H_2O)_5]^{2+}$ complexes can be calculated in a similar manner. These values can then be used to calculate the 10Dq value of chlorine. This can be done using either of the following equations:

$$10Dq\ [CrCl_2(H_2O)_4]^+ = (2/6)10Dq\ [Cl] + (4/6)10Dq\ [H_2O]$$

or

$$10Dq\ [CrCl\ (H_2O)^5]^{2+} = (1/6)10Dq\ [Cl] + (5/6)10Dq\ [H_2O]$$

The values obtained from all previous calculations are to be presented as in Table 10.2 and then calculate the 10 Dq value for the individual ligands and compare them with literature values.

Look for any trends in the 10 Dq data within the Cr(III) complexes. With each hydrolysis (replacing of a Cl ligand with a H_2O ligand), the 10Dq value should change. From this one can quantitatively understand the LFSE values for the water and chloride ligand.

Because the total volume was noted in each of the separated fractions, knowing the extinction coefficient of each transition, concentration of the species can be calculated. In the absence of the exact extinction

Table 10.2. This table illustrates the 10Dq values calculated for each Cr(III) complex according to each transition state possible on the Tanabe Sugano diagram.

Cr(III) Complex	10Dq from $^4A_{2g} \rightarrow {}^4T_{1g}$, cm^{-1}	10Dq from $^4A_{2g} \rightarrow {}^4T_{2g}$, cm^{-1}	Average 10Dq Value
$[CrCl_2(H_2O)_4]Cl$	15640	15920	15780
$[CrCl(H_2O)_5]Cl_2$	16470	16380	16425
$[Cr(H_2O)_6]Cl_3$	17385	17860	17622

Table 10.3. Microstates for d^3 electrons. There are 120 microstates total. Those boxes denoted by a * are the combinations which would be violations of the Pauli Exclusion Principle.

M_L/M_S	3/2	1/2	1/2	−1/2	−1/2	−3/2
6	*	*		*		*
5	*	$1^+\ 2^+\ 2^-$a		$1^-\ 2^+\ 2^-$a		*
4	*	$1^+\ 1^-\ 2^+$a $0^+\ 2^+\ 2^-$b		$1^+\ 1^-\ 2^-$a $0^-\ 2^+\ 2^-$b		*
3	$0^+\ 1^+\ 2^+$c	$0^+\ 1^+\ 2^-$a $0^-\ 1^+\ 2^+$b	$0^+\ 1^-\ 2^+$c $-1^+\ 2+\ 2^-$d	$0^+\ 1^-\ 2^-$a $0^-\ 1^-\ 2^+$b	$0^-\ 1^+\ 2^-$c $-1+\ 2^+\ 2^-$d	$0^-\ 1^-\ 2^-$c
2	$-1^+\ 1^+\ 2^+$c	$-2^+\ 2^+\ 2^-$a $-1^+\ 1^-\ 2^+$b $0^+\ 0^-\ 2^+$d	$-1^+\ 1^+\ 2^-$c $-1^-\ 1^+\ 2^+$e $0^+\ 1^+\ 1^-$e	$-2^-\ 2^+\ 2^-$a $-1^-\ 1^+\ 2^-$b $0^+\ 0^-\ 2^-$d	$-1+\ 1^-\ 2^-$c $-1^-\ 1^-\ 2^+$e $0^-\ 1^+\ 1^-$e	$-1^-\ 1^-\ 2^-$c
1	$-2^+\ 1^+\ 2^+$c $-1^+\ 0^+\ 2^+$f	$-2^+\ 1^+\ 2^-$a $-2^-\ 1^+\ 2^+$b $-1^+\ 0^+\ 2^-$d $-1^-\ 0^+\ 2^+$g	$-2^+\ 1^-\ 2^+$c $-1^+\ 1^+\ 1^-$e $-1^+\ 0^-\ 2^+$f $0^+\ 0^-\ 1^+$e	$-2^+\ 1^-\ 2^-$a $-2^-\ 1^-\ 2^+$b $-1+\ 0^-\ 2^-$d $-1^-\ 0^-\ 2^+$g	$-2^-\ 1^+\ 2^-$c $-1^-\ 1^+\ 1^-$e $-1^-\ 0^+\ 2^-$f $0^+\ 0^-\ 1^-$e	$-2^-\ 1^-\ 2^-$c $-1^-\ 0^-\ 2^-$f
0	$-1^+\ 0^+\ 1^+$c $-2^+\ 0^+\ 2^+$f	$-2^+\ 0^+\ 2^-$a $-2^-\ 0^+\ 2^+$b $-1^+\ 0^-\ 1^+$d $-1^+\ -1^-\ 2^+$g	$-2^+\ 0^-\ 2^+$f $-1^+\ 0^+\ 1^-$c $-1^-\ 0^+\ 1^+$e $-2^+\ 1^+\ 1^-$e	$-2+\ 0^-\ 2^-$a $-2^-\ 0^-\ 2^+$b $-1^-\ 0^+\ 1^-$d $-1^+\ -1^-\ 2^-$g	$-2^-\ 0^+\ 2^-$f $-1^+\ 0^-\ 1^-$c $-1^-\ 0^-\ 1^+$e $-2^-\ 1^+\ 1^-$e	$-1^-\ 0^-\ 1^-$c $-2^-\ 0^-\ 2^-$f
−1	$-2^+\ -1^+\ 2^+$c $-2^+\ 0^+\ 1^+$f	$-2^+\ -1^+\ 2^-$a $-2^-\ -1^+\ 2^+$b $1^+\ 0^+\ -2^-$d $1^-\ 0^+\ -2^+$g	$-2^+\ -1^-\ 2^+$c $-1^+\ -1^-\ 1^+$e $1^+\ 0^-\ -2^+$f $0^+\ 0^-\ -1^+$e	$-2^+\ -1^-\ 2^-$a $-2^-\ -1^-\ 2^+$b $1^+\ 0^-\ -2^-$d $1^-\ 0^-\ -2^+$g	$-2^-\ -1^+\ 2^-$c $-1^+\ -1^-\ 1^-$e $1^-\ 0^+\ -2^-$f $0^+\ 0^-\ -1^-$e	$-2^-\ -1^-\ 2^-$c $-2^-\ 0^-\ 1^-$f
−2	$-2^+\ -1^+\ 1^+$c	$-2^+\ -2^-\ 2^+$a $-2^+\ -1^-\ 1^+$b $0^+\ 0^-\ -2^+$d	$-2^+\ -1^+\ 1^-$c $-2^-\ -1^+\ 1^+$e $0^+\ -1^+\ -1^-$e	$-2^+\ -2^-\ 2$-a $-2^-\ -1^+\ 1^-$b $0^+\ 0^-\ -2^-$d	$-2^+\ -1^-\ 1^-$c $-2^-\ -1^-\ 1^+$e $0^-\ -1^+\ -1^-$e	$-2^-\ -1^-\ 1^-$c
−3	$-2^+\ -1^+\ 0^+$c	$-2^+\ -1^+\ 0^-$a $-2^-\ -1^+\ 0^+$b	$-2^+\ -1^-\ 0^+$c $-2^+\ -2^-\ 1^+$b	$-2^+\ -1^-\ 0$-a $-2^-\ -1^-\ 0^+$b	$-2^-\ -1^+\ 0^-$c $-2^+\ -2^-\ 1^-$d	$-2^-\ -1^-\ 0^-$c
−4	*	$-2^+\ -1^+\ -1^-$a $-2^+\ -2^-\ 0^+$b		$-2^-\ -1+\ -1^-$a $-2^+\ -2^-\ 0^-$b		*
−5	*	$-2^+\ -2^-\ -1+$a		$-2^+\ -2^-\ -1^-$a		*
−6	*	*		*		*

[a]Corresponds to the ^{2}H state.
[b]Corresponds to the ^{2}G state.
[c]Corresponds to the ^{4}F state.
[d]Corresponds to the ^{2}F state.
[e]Corresponds to the two ^{2}D states.
[f]Corresponds to the ^{4}P state.
[g]Corresponds to the ^{2}P state.

coefficient, assuming a similar value for the extinction coefficient for these bands allows one to understand the relative amount of each species. Upon studying this data, it should be evident that some sample would contain only the $[CrCl_2(H_2O)_4]Cl$, others $[CrCl(H_2O)_5]Cl_2$, and finally $[Cr(H_2O)_6]Cl_3$. The amount of each species would be suggestive of the rate of hydrolysis. If the rate is found to be slow, it can be increased by increasing the temperature. Regardless $[Cr(H_2O)_6]Cl_3$ appears to be the most stable species which forms slowly at a lower temperature and faster at a higher temperature.

Table 10.4. A summary of the orbital multiplicities, spin multiplicities, and total multiplicities for each term symbol. The sum of the total multiplicities is 120, as predicted.

State	Orbital Multiplicity	Spin Multiplicity	Total Multiplicity
^{2}H	11	2	22
^{2}G	9	2	18
^{4}F	7	4	28
^{2}F	7	2	14
^{2}D	5	2	10
^{2}D	5	2	10
^{4}P	3	4	12
^{2}P	3	2	6

www.ebook3000.com

SUMMARY

In this experiment, three Cr(III) species ($[CrCl_2(H_2O)_4]Cl$, $[CrCl(H_2O)_5]Cl_2$, and $[Cr(H_2O)_6]Cl_3$) were prepared (both individually as well as in a mixture), and their absorption spectra analyzed. With the help of a Tanabe Sugano diagram, and term symbols, the 10Dq value of each complex was calculated, which help lead to the 10Dq value of H_2O and Cl^-.

QUESTIONS

1. Identify a reasonable mechanism for Cl-displacement by water. Explain the fact that $[CrCl_2(H_2O)_4]^+$ hydrolyzes to $[CrCl_2(H_2O)_4]Cl$ faster than $[CrCl(H_2O)_5]C_{l2}$ hydrolyzes to $[Cr(H_2O)_6]C_{l3}$.
2. Why would HCl be an inappropriate solvent to elute the Cr(III) complexes from the column?
3. Why acid is used in the procedure?
4. Why did you increase the strength of the acid rather than conduct the experiment in reverse i.e., use the stronger acid first?
5. Which species is expected to bind the column most strongly?
6. Which species is the thermodynamically controlled product and which species is the kinetically controlled product?
7. Why is $^4A_{2g}$ taken to be lowest in energy?

INSTRUCTOR'S RESOURCE

This module can be extended to include an independent study component where students are to design their own hydrated metal complex, measure their electronic spectra and calculate the LFSE. One can then compare how the LFSE vary as a function of metal ions. For a reference please see the review article: Bussiere, G.; Beaulac, R.; Cardinal-David, B.; Reber, C., "Coupled electronic states in trans-$MCl_2(H_2O)_4^{n+}$ complexes (M: Ni^{2+}, Co^{2+}, V^{3+}, Cr^{3+}) probed by absorption and luminescence spectroscopy." *Coord. Chem. Rev.,* **2001**, 219–221, 509–543. Some advanced students conducted single point density functional calculations using Gaussian to understand the shape of the orbitals.

REFERENCES

1. Gerloch, M. and E.C. *Constable. Transition Metal Chemistry: the valence shell in d-block chemistry.* Weinheim, Germany: VCH Publishers, 1994.
2. Figgis, B. N.; Hitchman, M A. *Ligand Field Theory and Its Applications.* Wiley-VCH, New York, N.Y.USA. 2000.
3. Nyburg, S. C.; Soptrajanov, B.; Stefov, V.; Petrusevski, V. M. Dicesium trans-Tetraaquadichlorochromium(III) Chloride: Redetermination of the Crystal Structure and Infrared Study of the Water Spectrum. *Inorg. Chem.* **1997**, 36, 2248–2251.
4. McCarthy, P.J.; Lauffenburger, J. C.; Skonezny, P. M.; Rohrer, D. C. Crystal structure and low-temperature crystal spectra of dicesium dichlorotetraaquachromium(III) chloride. *Inorg. Chem.,* **1981**, 20, 1566–70.
5. Finholt, J. E.; Caulton, K. G.; Libbey, W. J. Synthesis of monochloropenta aquochromium(III) ion by displacement ion exchange. *Inorg. Chem.* **1964**, 3, 1801–2.

www.ebook3000.com

Solid Phase Extraction of Lipids from a Cellular Lysate on a Microfluidic Device

MITCHELL E. JOHNSON, SEAN PAWLOWSKI, KEVIN E. BARRY, MEDHAVI BOLE, EILEEN M. CHESTNUTT, JENNA L. DAGGETT, STEVEN L. LEPISH, LAUREN M. MATOSZIUK, MELISSA P. MEREDITH, SCOTT G. SAJDAK, LAUREN E. SLOMKA, CORINNE F. STALZER, RYAN TADISCH, ADAM T. WASILKO and JULIE N. WONG-CHONG

Duquesne University, Department of Chemistry and Biochemistry, 600 Forbes Ave., Pittsburgh, PA 15282

LEARNING OBJECTIVES: The experiment brings together elements of microfluidics and lipidomics, two major research areas in chemistry and biochemistry. One objective of this experiment is to give students a basic foundation in microfluidic chip design and construction; another is to introduce them to the "omics" sciences (lipidomics, proteomics, metabolomics, etc.) in a meaningful way. Students also learn electrospray mass spectrometry for the analysis of lipids, giving them exposure to a major analytical technique. Sample preparation is often overlooked as a separate sub-discipline of chemical analysis, but practicing chemists know that sample preparation is the most time consuming part of any procedure, and is the largest source of error. Consequently, this experiment provides an excellent way to focus on sample preparation issues in the analysis of real samples, while introducing students to a very timely research direction, namely, the integration of sample preparation on microchips, part of the necessary development of lab-on-a-chip. Students also learn some basics of working with cells. In terms of pedagogy, this experiment is designed to teach the students how to cooperate between groups, and how to coordinate the efforts of several groups to achieve a broad goal. Communication and data sharing are important for the success of this experiment, as the need for both is built into each step in the experiment. Finally, this is essentially a research project with unknown outcomes, and so serves well as a capstone-type laboratory experience in which students are transitioned to a research environment.

INTRODUCTION

Lipidomics and the 'Omics Technologies

THE central theme of the 'omics technologies-genomics, proteomics, metabolomics, lipidomics, glycomics, etc. is the acquisition of a profile of the genes, proteins, small molecule metabolites, lipids, or oligosaccharides, respectively, in a biological system. The system itself can be an organism or a single cell or anything in between. The "profile" can be a quantitative list of every single gene, protein, etc., or it can be a list of a subset thereof-for example, soluble proteins or eicosanoid lipids. The technology of obtaining the genome differs substantially from the other 'omics technologies: the genome is measured by combining molecular biology techniques with capillary gel electrophoresis and laser-induced fluorescence spectroscopy to measure DNA fragment lengths and base identities. This approach works because, chemically, genomic material has very little chemical diversity, it is very carefully packaged, and only the order of the bases is important in understanding its function. Furthermore, enzymes exist that can manipulate DNA at the single base level in a very reproducible manner. On the other hand, the thousands of proteins that are produced in cells from the DNA blueprint have a very wide array of sizes, functions, charges, surface properties, and three-dimensional structures. In addition, the

proteome is complicated by the fact that many proteins are modified after they have been constructed, by cutting them up and/or modifying their side-chains with methyl groups, lipids, saccharides, phosphates, and many other species. The same kind of diversity is manifested in of all of the products of the genome and the proteome. Consequently, the technology for profiling such a hugely diverse set of compounds remains an incredible challenge. Two branches of chemical analysis play an important role in 'omics: separation science and mass spectrometry. Proteins are separated, usually, according to surface charge (isoelectric focusing or ion exchange) and by size (gel electrophoresis or size exclusion chromatography) in two separate dimensions and then subjected to reversed phase liquid chromatography and one or more dimensions of mass spectrometry. In lipidomics, distinct subclasses of lipids, obtained by liquid extraction from a cell or tissue mass, are isolated by solid phase extraction, liquid chromatography, or thin-layer chromatography and then analyzed by a further dimension (or two) of liquid chromatography and two or more dimensions of mass spectrometry. Mass spectrometry is the central technique for all of the 'omics technologies except for genomics. The variety of available techniques and the power of software that comes with modern instruments make it imperative that chemistry and biochemistry students be exposed to at least the basics of electrospray mass spectrometry.

Microfluidics and Lab-on-a-Chip

Many techniques in chemistry have at least one dimension that is on the micrometer scale. The analytical technique of gas chromatography is one example, where the micrometer dimensions are the column inner diameter (250 μm) and film thickness (0.25 μm). In most cases, however, the remainder of the experimental apparatus is on the meter scale, or at least the decimeter scale. The idea of "lab-on-a-chip" has been one of shrinking an entire experimental apparatus to the scale of a microscope slide. The major areas of focus have been in chemical analysis and in chemical synthesis. The advantages in shrinking the laboratory come from scaling laws, which predict that either the same performance will be achieved in a small fraction of the time compared to the traditional scale, or performance will be greatly enhanced on the same time scale. Many of these concepts were brought to fruition in the early '90's by the application of basic photolithography to the creation of channels in glass microchips[1–5]. The channels were used for simple chemical reactions and for separations based on electrophoresis and chromatography. The ability to fabricate more complex features on chips-valves, pumps, optics, electronics-has been the key to creating chips that approach whole laboratory functions on a single chip. The Suggested Reading section gives references of a number of recent reviews that demonstrate the power of the microfluidic approach-namely, that there are experiments that can only be done on a chip.

Solid Phase Extraction on Microchips: "Extracting" Lipids for Lipidomics on Small Cell Populations

One difficulty in profiling the chemical population of a small sample-for example, a few suspect cells from a pathology sample-is that the lipidome, for example, exists over a wide range of concentrations. Basic cell structural elements, such as 34-carbon phosphatidylcholines, are in relatively high abundance (mM), while signaling lipids, such as prostaglandins, are in low abundance (nM or below). The difficulty in analyzing such samples is that the less abundant species can easily get lost if the sample processing steps are inefficient and wasteful of sample. Furthermore, some techniques in common use for lipidomics, such as TLC, require a relatively large amount of sample for visualization. The logical choice is to minimize dead volume and sample transfer steps by putting all or part of the sample preparation scheme on a microchip platform. The approach used here is to use a microchip platform to simultaneously lyse cells to release their lipid content, then adsorb the lipids on a stationary (chromatography) phase. The lipids can then be washed, if necessary, to release contaminants such as protein, and they can be eluted using a strong solvent. The eluent can be directed into a mass spectrometer, or simply collected as fractions for further analysis by MS or MS/MS. In this experiment, the microchips are designed and produced using etched glass substrates, a scheme for cell lysis is developed and tested, a method for cell

www.ebook3000.com

lysis and lipid capture on the microchip is developed, the lipids are eluted from the microchip, and they are analyzed using electrospray mass spectrometry. In the experiment described herein, there are five groups, each assigned to different tasks, as outlined below. Figure 11.1 shows a workflow diagram.

EXPERIMENTAL

Cell Staining

The purpose of this part of the project was to develop and evaluate a cell staining protocol. The first

Figure 11.1. Workflow diagram for the production of microchips for the isolation of lipids from lysed cells and electrospray MS analysis of the lipids. Shading indicates tasks assigned to a particular group. Timing is roughly top to bottom, but dependencies are shown by the arrows. To test the final lysis method, for example, the microchips have to be made. Unshaded ovals represent potential additional tasks.

step in extracting lipids is to lyse the cells, or break them up (see the next section). Stained cells are easily evaluated for lysis, which must be complete. Incomplete lysis results in cell fragments, which can easily clog micrometer-sized features on the microchips. Therefore, one or two groups developed cell staining procedures using an epifluorescence microscope for evaluation, and another two groups developed cell lysis protocols using a phase contrast microscope for evaluation (see Figure 11.1). The groups then combined the best methods and evaluated lysis under the epifluorescence microscope.

Sulfurospirillum barnesii strain SES-3 cells were a generous gift from the Basu group (see Chapter 9 on cell growth and harvesting conditions). Groups developing lysis and staining procedures were provided with cells suspended in growth medium. Groups 1 and 2 developed staining methods based on the commercial dyes DiO and DiD (Invitrogen Molecular Probes, Inc., Carlsbad, CA). DiO and DiD are green and red absorbing dyes, respectively, with maximum absorbance wavelengths of 484 nm and 644 nm, respectively, when bound in the cell membrane. DiO is sold as a solid, but DiD is sold as a sticky oil (resin), and each dye needed some workup before it was suitable for cell staining. Also, cells have to be spun down to remove the growth medium, washed, and spun down again, several times, before they could be stained successfully. The following describes the procedure for DiO; DiD was similar, except that the sticky oil was manually applied to cells as well.

Preparation of DiO Stock Solution

Two hundred milligrams of the lipophillic tracer DiO [molecular structure shown in Figure 11.2 was obtained from Molecular Probes Inc (Cat. No. D275)].

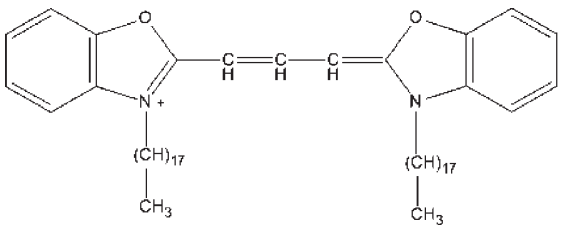

Figure 11.2. Structure of DiO, a dialkylcarbocyanine probe. The long alkyl tails insert into the membrane, anchoring the fluorophore to the membrane surface, while the charged, aromatic fluorophore remains parallel to the membrane phospholipids.

Twenty-five mg of DiO and 5 mg of octadecylamine were added to a microcentrifuge tube, followed by 0.5 mL of chloroform. The tube was heated in a 50°C water bath for five minutes. One mL of MeOH was added to facilitate precipitation, and the tube was placed on ice. After the formation of a precipitate, the tube was centrifuged for five minutes at 14,400 × *g*.

After evaporation, the pellet was diluted in 0.5 mL DMSO and the contents vortexed. Because the dye did not completely go into solution, an additional 0.5 mL of DMSO was added, for a final dye concentration of approximately 0.03 M. The solution was vortexed until it became homogeneous. The dye was frozen and protected from light to prevent photobleaching.

Staining

After thawing, the stock solution was vortexed for one minute, followed by two minutes of sonication. *S. barnseii*, cultured in nitrate and lactate enriched media were obtained. A 0.5 mL portion of live cells was placed in a microcentrifuge tube. In a separate tube, a 1:100 dilution of the DiO stock solution was prepared. One microliter of the diluted dye was added to the live cells, and the contents were vortexed. The final concentration of the dye in the cell solution was approximately 0.6 μM. The cells were then placed in a 37°C water bath for eight minutes. After heating, the tube was centrifuged for five minutes at 6,900 × *g*. A pellet formed and the supernatant was removed. The cells were then washed in 0.5 mL of 0.15 M Tris buffer, using a pipette to break up the cell pellet. The tube was vortexed for two minutes, then centrifuged for an additional five minutes at 6,900 × *g*. The supernatant was removed and the pellet resuspended in 0.5 mL 0.15 M Tris buffer. The cell pellet was broken up and vortexed, then centrifuged as before. The supernatant was again removed and the pellet resuspended in Tris buffer. Tris buffer was used to resuspend the cell pellet to prevent proteins within the media from interfering with the staining procedure. The staining procedure was tested using cells on well slides before being tested in the microfluidic device.

Imaging

The stained cells were viewed using a Nikon Eclipse E-600 microscope with a 100 W mercury lamp. The images were recorded using a RT-Slider Camera and

www.ebook3000.com

the QED Camera Standalone program. The contrast of the images was enhanced using Adobe Photoshop. A FITC-HYQ filter set (excitation bandpass filter 480 ± 20 nm, dichroic reflector 505 nm cut-on, emission bandpass filter 535 ± 25 nm) was used for all fluorescence microscopy imaging.

Cell Lysis

There are numerous ways to lyse cells. The purpose of this part of the experiment was to find a method that worked well with the cells being used, that was rapid, and that could easily be adapted for use in the microchip platform. Ultrasonication, a common technique for cell lysis, was not useful, as it would involve sonicating the whole microchip, an awkward, if not destructive, proposition. Two groups were assigned different protocols for lysing cells: a solution phase method based on lysozyme, and a solid phase method based on hydrophobic microparticles (chromatographic packing material). In order to determine whether the cell lysis procedure was successful, cells were viewed before and after the attempted lysis on a phase contrast microscope. Later, when the fluorescent staining procedure was available, the stained cells were viewed under epifluorescence illumination.

Lysis buffer was prepared by adding a pinch of Omnipur Lysozyme (Sigma) to 3 mL of 0.15 M Tris buffer. Cells in culture medium were pipetted onto standard well plates, and lysis buffer was added. The cells were imaged before and after adding the buffer using phase contrast microscopy in standard white light mode. Cells were readily lysed using this procedure, as shown by the complete lack of any identifiable features after adding the lysis buffer.

To image stained cells, cells stained with DiO (above) were injected directly into the inlet well of the microchip (see below). Two microliters of stained cells were injected into the well of the microfluidic device and imaged under the epifluorescence microscope, using the same parameters as described above for DiO imaging. Four microliters of lysis buffer was injected directly on top of the stained cells. PEEK tubing was used to connect the input well to the syringe pump, and to direct the flow from the output well to a waste beaker. Tris buffer (0.15 M) was then flowed through the microchip column for 4 minutes at a flow rate of 10 μL/min. The input well was again imaged in the fluorescence microscope to test for cell lysis.

Microchip Design and Manufacture

The design of the microchip was critical. The basic concept was to create a chip with a column in it that would be used for the extraction. A column in a microchip can be made using sol-gel techniques or by creating weir structures and packing the column created in-between the weirs with solid phase chromatographic packing[6]. One group was responsible for creating the photolithography masks for making the chips, and another was responsible for making the chips.

Photolithography

A brief description of the photolithography process is in order, as the process defines the design parameters. Figure 11.3 shows a basic conceptual diagram of photolithography using a positive photoresist. A positive photoresist is one that is solubilized where UV light strikes it, allowing the creation of features in the photoresist (and therefore the glass) wherever there is a clear spot in the mask. A negative photoresist on the other hand hardens the polymer where the light strikes. In the process described below, positive photoresist is used, so wherever channels are desired in the glass, the mask must be clear, and it must be opaque to UV light elsewhere. The basic process is shown in the figure. Glass substrates precoated with Cr (for adhesion of the photoresist) and photoresist are placed in contact with the mask and exposed to UV radiation for a specified amount of time. The solubilized photoresist is stripped off, the Cr layer is stripped off, and channels are etched in the glass using hydrofluoric acid solution. Following etching, the glass is cleaned, drilled, and the two sides of the chip are pressed together. The chips are bonded in a programmable high temperature oven for several hours. The use of HF for etching has the consequence (besides safety considerations, see below), which is that etching takes place isotropically. That is, etching rates are more or less the same in all directions, depending on glass crystallinity. Therefore, allowance must be made during mask design for the fact that the channels will be wider than the mask

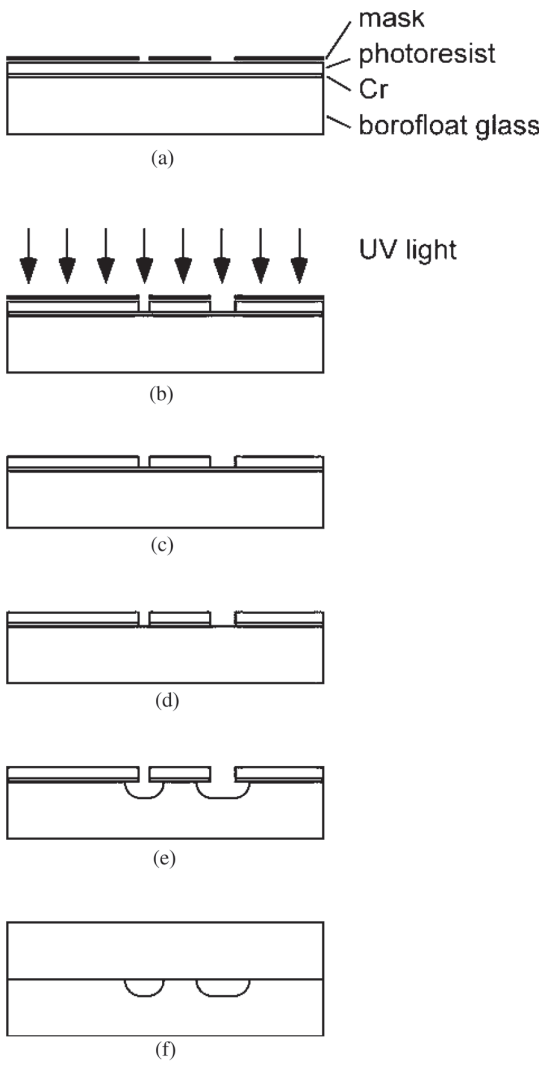

Figure 11.3. Conceptual diagram of the basic photolithography process for a positive photoresist. (a) The "sandwich" of the photomask blank (bottom), coated with a thin layer of Cr, a thin layer of photoresist, and the photomask. (b) The sandwich is exposed, solubilizing the photoresist (gray). (c) The mask is removed, the photoresist is stripped off from where it was exposed, transferring the mask design to the blank. (d) The Cr is stripped off. (e) The chip is etched with HF. (f) The plates are cleaned and the top plate is bonded in place.

feature. In addition, unless other masking techniques are used, all features will etch to the same depth.

Mask Design

The basic design for the chips used in this experiment are shown in Figure 11.4(a). Both top and

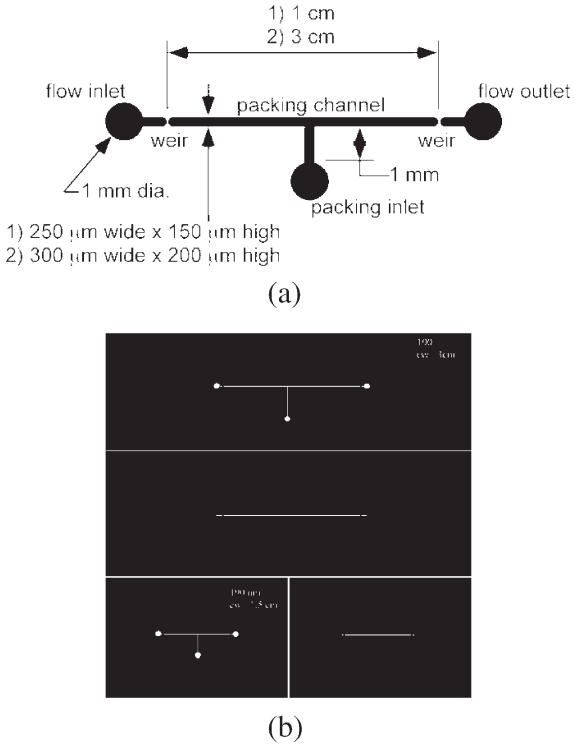

Figure 11.4. Mask design. (a) shows the design parameters for the short and long channel microchips. (b) shows the image of the actual mask for the top and bottom pieces of one long and one short channel chip. Reservoirs are only etched in one side of the chip. The total size of the mask is 3″ × 3″, same as the photomask blank. Note that it is helpful to etch design parameters in the corners of the chip itself to aid in identification of the chip. It is also helpful to make outlines of each chip piece to aid in scoring and separating the pieces.

bottom of the chip are etched, so that a symmetrical, oval channel is produced. Two masks were used; one with a 1 cm channel, one with a 3 cm channel. The smaller channel masks were printed at high resolution on photographic emulsion (Pixels, Inc., Charlottesville, VA), whereas the larger masks were printed on a high resolution ink-jet printer (Canon Pixma Pro900, 4800 × 2400 dpi). Masks for top and bottom of the larger channel chip are shown in Figure 11.4(b). Masks were produced in Adobe Illustrator (CS2, Adobe, Inc). In order to produce a 300 µm wide channel that is 200 µm deep, both top and bottom masks have line features that are 100 µm wide. Etching top and bottom 100 µm deep gives a channel that is a total of 200 µm deep, and each channel etches laterally by the same 100 µm, giving a channel that is 300 µm wide at its axis.

www.ebook3000.com

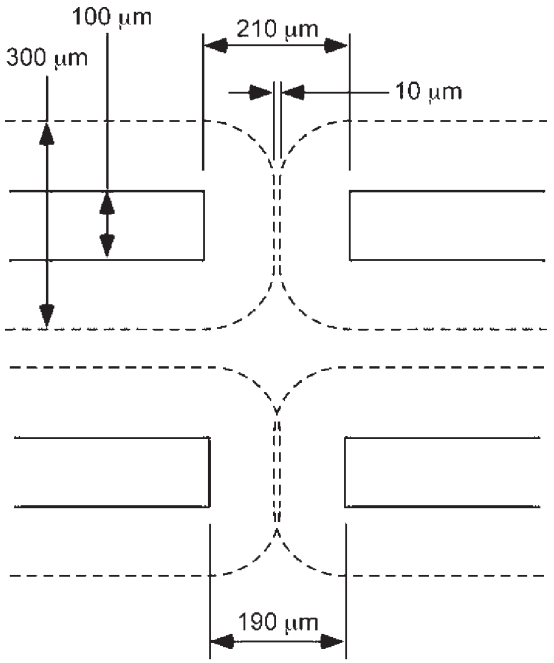

Figure 11.5. Mask design for the weir structures. The two drawings represent the top and bottom masks and chips. The mask outlines (and the final, etched outline at the bottom of each channel) are shown as solid lines, whereas the final etch lines on the surface of each chip half are shown as dashed lines. Etching depth is determined by the desired column diameter, and the separation of the mask features is determined by the etch depth (as each feature will etch laterally the same distance as it etches down) and the desired final separation or overlap.

The weirs require more careful design. The efficiency of the weir-type filter depends on the size of the filter, design of the filter, dilution of the sample, viscosity of the medium, and the filtration flow rate[7]. The principle of the weir mask design is shown in Figure 11.5. The weir is formed by etching the top plate so that the two channels almost touch, thereby leaving a sliver of glass unetched. The bottom is etched at the same time, so if the mask features for the mask for the bottom half of the chip are slightly closer together, the glass will get etched through laterally. The final outline of the etch at the surface of the glass is shown as dashed lines in Figure 11.5; the original mask features are shown as solid lines, which also represent the rough outline of the bottoms of the channels. If the two plates are then placed against each other, the weir is formed such that the etched-through part on the bottom forms a very small half-oval against the top plate that did not etch through. The size of the opening can be controlled by the etch distance (defined by the desired depth of the channel) and the distance between the two mask features. Dimensions for the 3 cm channel chip are shown in the figure.

Chip Fabrication

Schott Borofloat photomask blanks with a 520 nm layer of AZ1518 positive photoresist on 120 nm layer of chrome were purchased from Telic Co. (Santa Monica, CA). The photomask blank was placed in a laminar flow hood, AirClean 600 PCR Workstation (Raleigh, NC), and a red light was used to prevent damaging the photoresist until the photomask blank was exposed to UV light.

The mask was laid and centered on top of the photomask blank. The dull side of the mask was matched with the resist side of the photomask blank. They were then covered with a glass plate to ensure full and constant contact. The "sandwich" was then centered under a UV lamp, a Spectroline SB-100PC, with long UV wavelength of 365 nm (Spectroline, Westbury, NY). The sandwich was exposed to the UV radiation for 3 min for the photoemulsion type masks or 20 s for the ink-jet type masks, respectively, so that the image from the photomask was transferred to the photoresist. The recommended irradiance for polymerization of the positive resist is 25 mJ/cm^2 for 7 seconds[8]. The irradiance data for direct illumination of UV light was previously measured using a calibrated light meter. The maximum irradiance was 39.89 mW/cm^2 at the center of the illuminated region, and the minimum irradiance was 2.76 mW/cm^2 at the edge of the 3 × 3 cm plate. The maximum and minimum total energy were obtained by multiplying the respective irradiance with the time of exposure, 180 seconds. Therefore, the maximum total energy was calculated to be 7200 mJ/cm^2 (800 mJ/cm^2 for the 20 s exposure), and the minimum total energy was 496.8 mJ/cm^2 (55 mJ/cm^2).

The exposed photomask blank was then placed in 15 mL of AZ 300 MIF developer (AZ Electronics Materials, Somerville, NJ) contained in a 19 × 10 cm crystallizing dish. The solution was swirled over the top of the photomask blank for 30 seconds to solubilize the exposed region of the photoresist. The developed blank was then rinsed with deionized water for 40 seconds to remove the developer, after which it was placed in 25 mL of CR-9 Chromium Photomask

Etchant (Cyantek Corp, Freemont, CA). The solution was swirled over the top of the photomask blank until the chrome was removed, about 1–2 min. The mask was then rinsed again for 40 seconds with deionized water, to remove any remaining chrome in the channels.

Before the photomask blank was etched, the initial width of the channel was measured using a microscope with an optical scale, and determined to be 100 μm. The photomask blank was then etched using a 14:20:66 (v/v/v), HNO_3: HF: H_2O solution. The solution was prepared by adding 17 mL of HNO_3 (ThermoFisher, Waltham, MA) to 79 mL of deionized water and 24 mL of 40% HF (Alpha Aesar, Ward Hill, MA). The photomask blank was rinsed in deionized water to remove any particles before putting it in the etching solution. The solution was placed on a rotating plate and allowed to swirl for 40 seconds. The plate was removed from the HF solution, placed into a container with 1 L of deionized water, and swirled to remove the HF solution. The plate was then rinsed with deionized water, using the water spigot, model wp-100 (Waterpik Inc. F.T Collins, CO), after which the etching of the weirs was observed under a light microscope and a zoom stereomicroscope (Leica Wild, Wetzlar, Germany). The HF etching process was repeated 12 times, and the photomask blank was removed at intervals of time, until the weirs were barely touching and overlapping respectively for the top and bottom. After this initial trial to determine the rate of etching, for any following etching procedures, the chip would be etched for 18 minutes continuously, and then the size of the weirs would be checked under the stereomicroscope before further etching. After the etching was completed, the final width of the channel was measured to be 250 μm under the light microscope and the depth was calculated to be 75 μm (using the short column mask). The total time of etching was 21:20 min for an etch rate of 3.5 μm/min, which was fairly typical. Etch rates were monitored and recorded for each plate, and the HF solution was replaced after the etch rate slowed considerably.

Using an Accu Press drill (DynaArt Design, Lancaster, CA), and a diamond tipped drill bit (0.75 mm, Kingsley North, Norway MI) fluidic access holes were drilled in the wells at the end of each channel, for the top chips only. Water was poured onto the access holes while drilling to keep the glass from cracking. More importantly, the drill bits would vaporize from heat if not cooled with water. The glass was vigorously washed with deionized water. Chip pieces were cut from the photomask blank using a glasscutter, and then rinsed with deionized water using the water spigot.

The drilled chips were placed in 15 mL of RS-120 Resist Stripper (Cyantek Corp., Fremont, CA) at 50°C for 5 min to remove the remaining photoresist. The solution was swirled until all of the remaining resist had dissolved and then rinsed with deionized water for 2 minutes. The chips were then placed into CR-9 chrome etchant and swirled until the remaining chrome was dissolved. They were then rinsed with deionized water and placed in 15 mL of Nanostrip (Cyantek Corp., Fremont, CA, also called piranha etch) to remove any remaining organic solvents on the chips. The chips were swirled in nanostrip for 3 minutes and then rinsed again for 40 seconds in deionized water. The water spigot was used to trace the channels to remove any excess debris.

The cleaned chips were placed in RCA solution, which was made up of 75.0 mL deionized water and 15.0 mL NH_4OH mixed on a hot plate at 60°C to which 15.0 mL of H_2O_2 was added. The chips were swirled for 30 minutes in the RCA solution. The chips were removed from the solution and each piece was rinsed for 5 minutes with deionized water using the water spigot. The chips were cleaned thoroughly to ensure proper bonding.

The top and bottom chips were brought into contact while still wet and were held together by capillary action. The top chip was pressed gently from the middle to the outside to remove any trapped air pockets. The chips were then placed between two 1 cm thick Macor plates (Morgan Advanced Ceramics, Fairfield, NJ). The assembly was placed in a furnace (Lindberg/Blue Moldatherm 1100°C, from ThermoFisher) and a 400 gram stainless steel weight was placed on top of the macor plates. The temperature was raised by 10°C/min to 80°C and was held there for 30 min, after which it was ramped at the same rate to 610°C and held there for 8 hours. The temperature was then ramped down to room temperature at 10°C/min. The chips were then examined under the stereoscope to ensure proper alignment of the channels and weirs, to make sure that they were clear, and that the top and bottom chips had not shifted. If the chips did not bond completely, as indicated by interference fringes in the chips when viewed under white light, the chips were cycled through the temperature program again.

www.ebook3000.com

Microchip Packing

To pack the chips, as noted above, C18 or silica beads were used. These materials were used because of the nonpolar or polar properties of the beads. Because the membrane lipids being studied are glycerophospholipids and other types of membrane lipids, a nonpolar or polar stationary phase will attract the nonpolar or polar component, respectively, of the lipids while the lysed cells run through the column. To be able to pull the lipids off of the column, a strong polar eluent was needed. A chloroform/methanol solution was used to elute the lipids off of the C18 column and methanol was used for the silica column. The different eluents were used for the different columns because the C18 is nonpolar while silica is polar. This means that a less polar eluent was needed to pull the lipids off of the beads in the C18 column. By adding the chloroform to the methanol, a less polar eluent was made, allowing for the lipids to be eluted. Along with varying the solvents, the composition of the column can be varied and as a result the separation and retention can be affected. In this experiment, the composition remained the same through the trials.

The chips were packed using a slurry of the packing material. The packing material was mixed with enough methanol to form a viscous slurry. The slurry was introduced to the reservoir on the side-arm of the chip (see Figure 11.4) while simultaneously applying a mild vacuum to the reservoirs using pipet tips and a vacuum pump or asprirator on the other two reservoirs. Generally, it was necessary to apply the slurry repeatedly while tweaking the position of the vacuum tips to get a good pack. The packing was done under a zoom stereomicroscope. If necessary, the packing material could be drawn back out and repacked. The C18 packing material was Luna 15 μ C18(2) 100 Å (Phenomenex, Torrance, CA) meaning that it was an HPLC grade packing material consisting of spherical, 15 μm diameter particles with 100 Å pore sizes. This material is too small to hold against the weirs. Though weirs can certainly be etched that will hold such small material, the probability of clogging the weirs increases with decreasing diameter. Therefore, the chips were "pre-packed" using preparative C18 beads that measured 55 to 105 μm in diameter with 125 Å pore size (Waters, Milford, MA). A small amount of the larger packing was packed up against the weir to hold the smaller beads on the column. Once the larger C18 material was against each weir, the slurry of smaller C18 was injected to fill in the interstitial space of the larger C18 beads and the middle of the column. The silica packing material was 32–63 μm diameter silica gel with 60 Å pore size (Sorbent Technologies, Atlanta, GA). Once the chips were packed, passing water through the channel using a syringe pump tested the flow of each chip. After the chips held flow, the lower port of the T-shape was sealed with epoxy and left to dry overnight before use.

Cell Lysis and Lipid Capture on Chip

This part of the experiment was the critical part, where all of the previous experiments came together. At this point, chips had been made, chips had been packed, and cell lysis procedures had been developed and evaluated.

Once the columns were packed and appeared to contain no gaps, the chips were connected to an injection apparatus. A schematic of the apparatus is shown in Figure 11.6. Fluid was driven by a standard syringe pump (Harvard Apparatus Model 11, Holliston, MA). Reagents were injected using an HPLC type injection port (Rheodyne 7725, Rohnert Park, CA) with a 5 μL injection loop. The injection port was connected to the chip with PEEK tubing (Upchurch, Oak Harbor, WA, 1/16″ od × 0.010″ id) and either custom pressure holders or Upchurch Nanoports. Flow was driven through the system to test the packing stability and to ensure that there were no clogs, typically at 10–20 μL/min.

Tris buffer was run through the tubing and chip apparatus for several minutes at a flow rate of 10 μL per minute to flush out the system. The injector of the syringe pump was switched to "load" and 4 μL of the lysis buffer was injected onto the chip. A sample of cells (2 μL) was added immediately thereafter, followed by another 4 μL of lysis buffer. In a previous trial, the cells were injected first followed by lysis buffer; however no lipids were captured, possibly a result of the Tris buffer washing the lysis buffer away. The syringe pump was switched back to "Inject" and Tris buffer was flowed through the chip for 43 seconds to elute proteins. The time was calculated to take into account the dead volume of the column and tubing. The glass syringe on the syringe pump was replaced with either methanol (silica chip) or 2:1 chloroform:methanol (C18 chip) and this eluent was

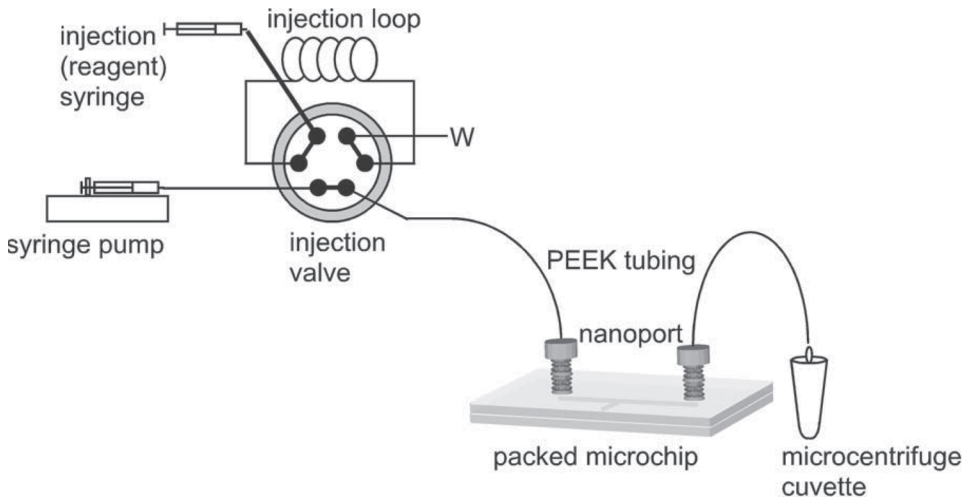

Figure 11.6. The flow apparatus for online cell lysis, lipid capture, and lipid elution on the packed microchip. The valve is a standard HPLC type injection valve. The reagent syringe is used to inject lysis buffer, cells, and more lysis buffer. W is the waste channel. The syringe in the syringe pump is filled with either Tris buffer or elution solvent.

run through the column to elute the lipids. Two samples were collected, one sample that was eluted with the Tris buffer and one sample that was eluted with eluent.

Once the samples were collected, 0.5 mL of a mixture of 8 mL chloroform, 4 mL HPLC grade methanol, and 8 µL of 10 mM ammonium hydroxide was added to each of the two collected samples. The two tubes were centrifuged for 5 minutes at 13000 rpm to separate the organic layer from inorganic layer. No layers appeared in either of the samples. After the lipids were captured, they were analyzed by electrospray mass spectrometry (ESI/MS).

Lipid Extraction from Whole Cells

In order to evaluate the mass spectra obtained from the microchip eluent, it was necessary to perform a total lipid extraction of the same cells. The basic approach was a very standard one: basically liquid extraction of lipids from the cells (see the websites in the Suggested Reading), followed by basification with ammonium hydroxide and infusion ESI/MS[9,10].

The first step in lipid extraction was the process of spinning down a 5 mL culture sample of *S. barnesii* cells in a conical centrifuge tube at 33,000 × *g* for 10 minutes. The cells were then washed with 5 ml of H_2O. The cell pellet was suspended in 5% solution of trichloroacetic acid and cooled on ice for 15 minutes. An additional 5 ml of H_2O was added and the same spinning procedure was employed as above. The supernatant was poured off and the cells were re-suspended in 5 mL of H_2O. The cells were once more spun down and the supernatant disposed of.

One mL of a solution consisting of 15 mL H_2O, 15 mL 95% EtOH, 5 mL diethylether, 1 mL pyridine, 36 µL ammonium hydroxide was added to the cell pellet. The cell suspension was heated for an hour in a 60°C water bath with occasional swirling. While still warm, this mixture was centrifuged once more. The supernatant was removed without disturbing the cell pellet and transferred to a new test tube. Next, 0.25 mL H_2O and 2.5 mL $CHCl_3$ were added and then vortexed to insure mixing. This mixture was then centrifuged at 8000 rpm for 5 minutes. Once the layers separated, the lower layer ($CHCl_3$ phase) was removed and placed in a glass vial. This vial was placed under N_2 until drying was complete. Once all of the liquid was removed, the resulting lipids were re-suspended in a solution of 2:1 chloroform:methanol and ammonium hydroxide. The final product was analyzed by ESI/MS.

Mass Spectrometry of Lipids

Two samples were run on the ESI/MS, the lipids directly extracted from the *S. barnesii* cells and the

www.ebook3000.com

lipids captured from the microchip. About 0.3 mL of the lipids directly extracted from the cells were injected by a syringe pump at a rate of 20 μL/min. About 0.4 mL of the lipids captured from the microchip were injected by a syringe pump at the same rate. The ESI/MS was a Waters ZMD single quadrupole mass spectrometer. For ESI, the capillary was held at 3.5 kV, the cone voltage was 60 V, the source temperature was 120°C, and the desolvation temperature was 350°C. For the MS, 375 scans of 1.49 s duration were collected at a cycle time of 1.6 s over a mass range of 200–800 Da. Spectra were obtained by monitoring the ion current and integrating spectra during stable ion current. All spectra were downloaded and analyzed in Igor Pro (Wavemetrics, Eugene, OR) and LipidMaps peak identification software (www.lipidmaps.org).

RESULTS AND DISCUSSION

Cell Staining and Lysis

Figure 11.7 shows photomicrographs of cells stained with DiO and viewed under epifluorescence illumination. The staining protocol worked well, provided two most important parts of the protocol were followed: the dye solution was prepared as described (dissolution of solid dye did not work well); and the cells were washed thoroughly. For cells obtained from tissue samples, if so desired, a new cell preparation protocol must be devised. Figure 11.7(a) shows the cells in a well slide; Figure 11.7(b) shows the cells in the inlet port of a complete microfluidic device. The first photomicrograph was taken during method development; the second was taken during testing of the full lysis procedure on-chip. Lysis was also tested, as noted above, using phase contrast microscopy, and the method using a pinch of lysozyme was found to work very well for cell lysis. The solid phase method did not work at all. Photomicrographs of stained cells showed completely black following lysis, both in the well slides and in the microchip. It should be noted that the *S. barnesii* cells are bacterial cells, and therefore are among the easiest cells to lyse. Eukaryotic cells would be expected to be more difficult, as would cells from yeast or sperm; therefore, other protocols might need to be developed for other types of cells.

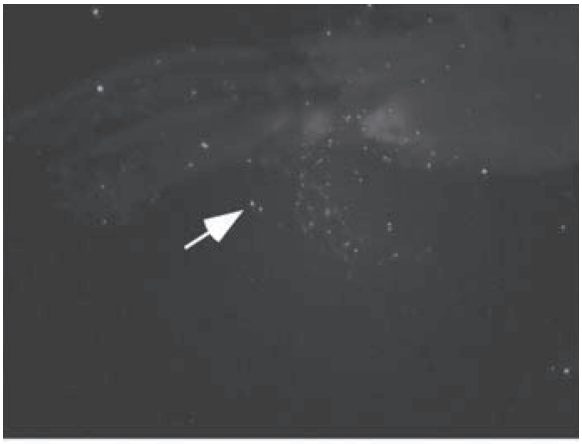

(a)

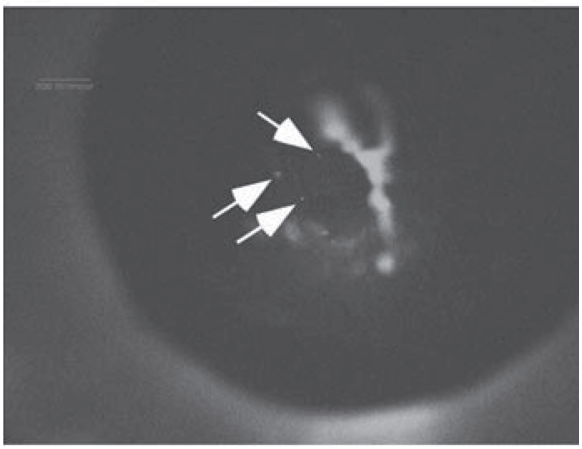

(b)

Figure 11.7. Photomicrographs of stained cells in (a) a well slide, at 20× magnification, and (b) the inlet reservoir of a packed microchip, at 10× magnification. The white arrows point to cells. The well slide contains many more visible cells than the chip. The large, Y-shaped feature in (b) is likely a solid crystal of DiO. Following lysis, images were completely black, without any features.

Chip Manufacture and Packing

The best quality chips were produced from the photographic emulsion masks. Resolution was higher, resulting in less roughness at channel edges, and there was less roughness on the surface of the chip. Either mask was usable, but for convenience, the ink-jet method was preferred, as masks could be designed and made in-house in a matter of an hour. In order to maintain the high resolution of the ink-jet printer, the

manufacturer-recommended transparency blanks had to be used to produce the masks. Therefore, it was necessary to measure the actual transmission of the masks at the wavelength of the UV lamp (365 nm). Figure 11.8 shows a plot of % transmission of a small portion of a mask that was either "clear" (i.e., not filled in the mask file) or "opaque" (i.e., filled with black in the mask file). Two features stood out-the clear or blank part of the mask was not 100% transmissive (60.8% at 365 nm), and the blocking part of the mask was not 100% opaque (8.01% at 365 nm) to UV light. Therefore, exposure had to be limited to 20 s, a figure reached through test blanks of varying exposure. Taking the transmittance of the clear region into account, the actual exposure of the photomask was 485 and 34 mJ/cm^2 for the center and fringe of the exposure pattern, respectively. For the opaque region, exposure was still 64 mJ/cm^2 at the center of the pattern, which exceeded the recommended exposure. Certainly, a 3 min exposure greatly overexposed the photoresist, leading to unusable photomask blanks. However, the 20 s exposure seemed to work well, and subsequent work has shown that this exposure level and mask combination are adequate for producing prototype chips.

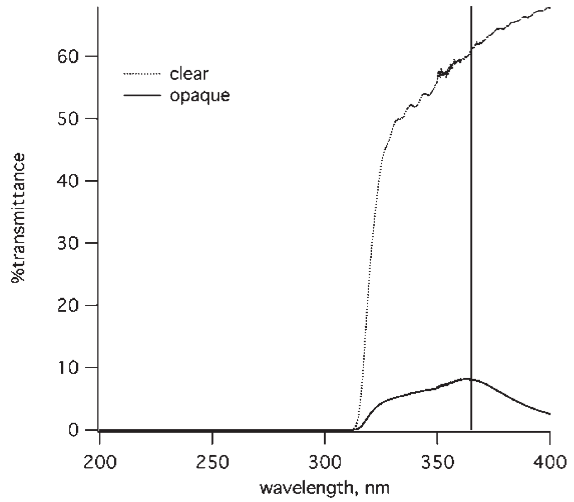

Figure 11.8. Wavelength dependent transmittance of the transparency mask material used in the ink-jet printer. "Clear" trace is the clear feature on the mask where the photomask blank will be exposed, "Opaque" is the black region (see Figure 11.4). Spectra obtained in simple transmittance mode with the film in the cuvette holder of a double-beam UV-vis spectrophotometer. The vertical line is drawn at 365 nm, the maximum emission wavelength of the UV lamp.

It was found necessary to print in black and white or grayscale, rather than color, as color printing tended to leave stray dots of colored ink at the borders of the mask features, increasing the roughness of the features. Mask resolution limits were tested for the ink-jet printer by printing bars and squares of varying sizes, alone or next to one another. Generally, features of 20–50 μm were realizable without too many roughness problems, but 10–20 μm features were not feasible. For similar reasons, features had to be at least 100 μm apart in order to have bondable glass in between the features.

The temperature ramp for bonding also required some trial and error. The initial ramp was a straight 10°C/min to 640°C. While chips bonded with this method, there was considerable frosting on the chip surface, making optical interrogation of the chips difficult. Therefore, the ramp was changed to include a half hour hold at 80°C, followed by a maximum temperature of 610°C. The low temperature hold slowly dried out the chip, such that capillary forces held the chip halves together very tightly, and the lower maximum temperature resulted in clear, well-bonded chips.

Chip packing took some experience. One group was assigned to packing, and the members became proficient at packing chips. The packing material was easily visualized under a zoom stereomicroscope, and it was easy to see when the material packed tightly against the weirs. When gaps appeared, as often happened, repeated application of vacuum was sometimes successful, but often the packing material had to be removed by vacuum and the slurry re-applied. Jemere et al. describe the use of applied voltage to help pack the beads in tightly[6], but this procedure was not attempted. Reportedly, that method results in tighter packing than vacuum alone. It was also found to be important to test the packed chip under flow under the microscope, to make certain that the packing was tightly packed and did not move under flow. Figure 11.9 shows close-ups of parts of the successfully packed chips.

Lipid Extraction the Microchip

Figure 11.10 shows a positive ESI/MS of lipids extracted directly from the S. barnesii cells (total lipid extract) and using the 1 cm silica-packed microchip. Relatively few common peaks were obtained (the peak

www.ebook3000.com

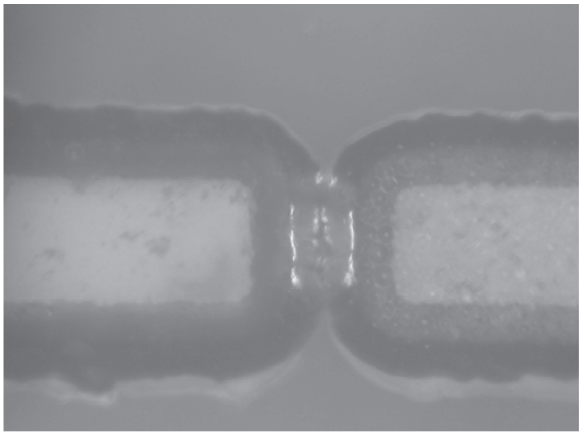

(a)

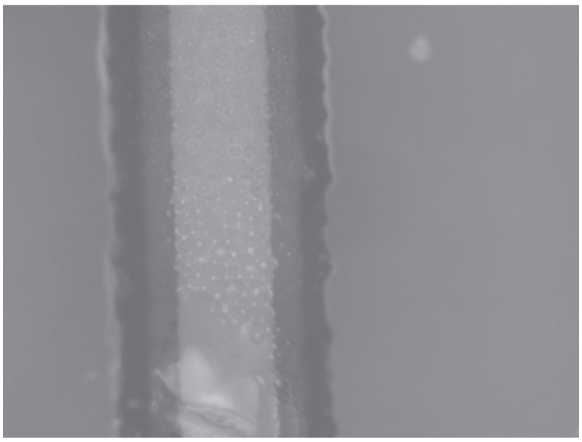

(b)

Figure 11.9. Photomicrographs of portions of a packed microchip. (a) the inlet weir. Packing material can clearly be seen to the right of the weir. See Figures 11.4 and 11.5. (b) the side arm, with epoxy sealing off the packing material. The epoxy is on the bottom in the figure, and packing material can be seen above an s-shaped boundary.

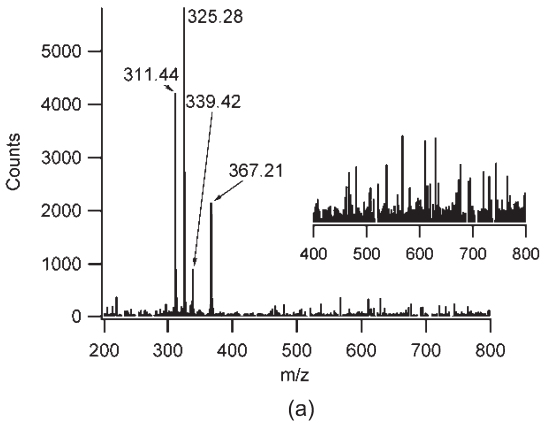

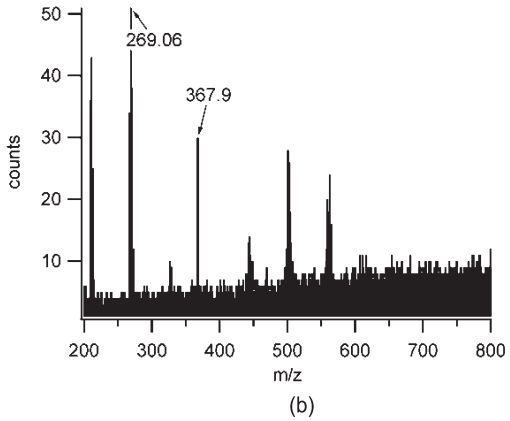

Figure 11.10. Electrospray mass spectra of lipids obtained from (a) total lipid extract, and (b) an extract obtained on the 1 cm silica microchip. Note the difference in peak intensities. The inset in (a) is scaled by 10×.

at 367 is the only common, high intensity peak). The chip extract had very poor signal strength, probably because the column was quite short (1 cm) and little lipid material was obtained. The MS shown in the inset of Figure 10a shows a number of peaks that correspond to extracted lipids, though even this spectrum has relatively low signal strength. The peak at 367 amu was identified, tentatively, as 1-tridecanoyl-sn-glycero-2-phosphate, or C13 lysophosphatidic acid. The lipids that were tentatively identified with this procedure were all C12 or C13 lyso-glycero-phospholipids, or relatively small, polar lipids. Without a second dimension of MS, or higher resolution MS, however, peak assignments were only tentative. Based on peak shapes, however, except for the peaks in the 400–500 amu range in the chip extract, it appeared that the extraction was relatively uncontaminated by peptides or proteins, or other multiply charged species.

Further experimentation has shown that the 3 cm chip with C18 packing and chloroform:methanol eluent extracts many more lipids, and in fact results in over 350 identifiable peaks in positive and negative ion mode. The chip extracts about 70% of the lipids found in the total lipid extract. The silica chip using either methanol or isopropanol also extracts about 60% of the total lipids. Interestingly, both chips extract

roughly the same range of lipids, mostly the higher molecular weights, above about 600 amu, in spite of the very different polarity of surfaces of the two packing materials.

REFERENCES

1. Jacobson, S. C.; Hergenröder, R.; Koutny, L. B.; Ramsey, J. M., High-Speed Separations on a Microchip. *Analytical Chemistry* **1994,** 66, (7), 1114–1118.
2. Jacobson, S. C.; Hergenröder, R.; Koutny, L. B.; Ramsey, J. M., Open Channel Electrochromatography on a Microchip. *Analytical Chemistry* **1994**, 66, (14), 2369–2373.
3. Jacobson, S. C.; Hergenröder, R.; Moore, A. W., Jr.; Ramsey, J. M., Precolumn Reactions with Electrophoretic Analysis Integrated on a Microchip. *Analytical Chemistry* **1994**, 66, (23), 4127–4132.
4. Jacobson, S. C.; Koutny, L. B.; Hergenröder, R.; Moore, A. W., Jr.; Ramsey, J. M., Microchip Capillary Electrophoresis with an Integrated Postcolumn Reactor. *Analytical Chemistry* **1994**, 66, (20), 3472–3476.
5. Seiler, K.; Harrison, D. J.; Manz, A., Planar Glass Chips for Capillary Electrophoresis: Repetitive Sample Injection, Quantitation, and Separation Efficiency. *Analytical Chemistry* **1993**, 65, (10), 1481–1488.
6. Jemere, A. B.; Oleschuk, R. D.; Ouchen, F.; Fajuyigbe, F.; Harrison, D. J., An integrated solid-phase extraction system for sub-picomolar detection. *Electrophoresis* **2002**, 23, (20), 3537–3544.
7. Yuen, P. K.; Kricka, L. J.; Fortina, P.; Panaro, N. J.; Sakazume, T.; WIlding, P., Microchip Module for Blood Sample Preparation and Nucleic Acid Amplification Reactions. *Genome Research* **2001**, 11, (3), 405–412.
8. Roper, M. G.; Shackman, J. G.; Dahlgren, G. M.; Kennedy, R. T., Microfluidic Chip for Continuous Monitoring of Hormone Secretion from Live Cells Using an Electrophoresis-Based Immunoassay. *Analytical Chemistry,* **2003**, 75, (18), 4711–4717.
9. Han, X.; Gross, R. W., Global analyses of cellular lipidomes directly from crude extracts of biological samples by ESI mass spectrometry: A bridge to lipidomics. *Journal of Lipid Research* **2003**, 44, (6), 1071–1079.
10. Han, X.; Gross, R. W., Shotgun lipidomics: electrospray ionization mass spectrometric analysis and quantitation of cellular lipidomes directly from crude extracts of biological samples. *Mass Spectrometry Reviews* **2005,** 24, (3), 367–412.

SUGGESTED READING

Lipidomics

www.lipidmaps.org
www.cyberlipid.org

Nicolaou, A. and Kokotos, G., Eds. *Bioactive Lipids,* The Oily Press, PJ Barnes & Assoc: Bridgewater, England; 2004.

German, J. B.; Gillies, L. A.; Smilowitz, J. T.; Zivkovic, A. M.; Watkins, S. M., Lipidomics and lipid profiling in metabolomics. *Current Opinion in Lipidology* **2007**, 18, (1), 66–71.

Han, X.; Gross, R. W., Shotgun lipidomics: electrospray ionization mass spectrometric analysis and quantitation of cellular lipidomes directly from crude extracts of biological samples. *Mass Spectrometry Reviews* **2005**, 24, (3), 367–412.

Murphy, R. C.; Fiedler, J.; Hevko, J., Analysis of nonvolatile lipids by mass spectrometry. *Chemical Reviews (Washington, D.C.)* **2001**, 101, (2), 479–526.

Tranchida, P. Q.; Donato, P.; Dugo, G.; Mondello, L.; Dugo, P., Comprehensive chromatographic methods for the analysis of lipids. *Trends in Analytical Chemistry* **2007**, 26, (3), 191–205.

Microfluidics

Landers, J. P., Ed. *Handbook of Capillary and Microchip Electrophoresis and Associated Microtechniques, 3rd Ed.*, CRC Press: Boca Raton, FL; 2007.

Geschke, O.; Klank, H.; and Telleman, P., Eds. *Microsystem Engineering of Lab-on-a-chip Devices, 2nd Rev. Ed.,* Wiley-VCH: Weinheim, Germany; 2004.

Whitesides, G. M., The origins and the future of microfluidics. *Nature* **2006**, 442, (7101), 368–373. This paper introduces a series of six more papers that comprehensively review the state of the art in microfluidic technology as of 2006.

Easley, C. J.; Karlinsey, J. M.; Bienvenue, J. M.; Legendre, L. A.; Roper, M. G.; Feldman, S. H.; Hughes, M. A.; Hewlett, E. L.; Merkel, T. J.; Ferrance, J. P.; Landers, J. P., A fully integrated microfluidic genetic analysis system with sample-in-answer-out capability. *Proceedings of the National Academy of Sciences of the United States of America* **2006**, 103, (51), 19272–19277.

Song, H.; Chen, D. L.; Ismagilov, R. F., Reactions in droplets in microfluidic channels. *Angewandte Chemie, International Edition* **2006**, 45, (44), 7336–7356.

www.ebook3000.com

INSTRUCTOR'S RESOURCE

The overall goal of this project is to effectively "capture" lipids from lysed cells on a solid chromatographic support that has been packed into a microchip, release the captured lipids, collect them, and to analyze them by mass spectrometry. There are a number of individual steps that need to come together to make this project successful: a cell lysis procedure needs to be developed, lysis needs to be verified, chips need to be made, they need to be packed with stationary phase, the capture process needs to be developed, the elution process needs to be developed, and mass spectra of the lipid extracts need to be taken. Spectra from the chip extraction are compared to a standard extract from the cells, so a lipid extraction procedure needs to be followed as well. With many "sub-goals" or sub-projects, it is quite easy to divide the project among a number of groups, as this format promotes communication among groups and necessitates data sharing for success of individual modules.

The lab is broken down into a series of tasks for five groups; it can be modified to suit other numbers of groups, though there will be redundancy if larger numbers of groups are used. The goal is to provide each group with a unique set of tasks all tending towards one end: a protocol for cell lysis and lipid extraction on microchips. Figure 11.1 shows a task flow diagram. Each task is described in detail above. The way it has been presented makes it a complex experiment, and consequently each group has to perform well in order to get a successful outcome. It is probably suitable only for advanced, highly capable students in a sizable group. The workflow implied in Figure 11.1 is deliberate. The bubbles corresponding to each task are shaded according to the group to which they are assigned. Roughly speaking, all but one group starts out by working with the cells and developing staining and lysis protocols. Another group starts the chip making process by beginning with the masks. Once staining and lysis conditions are worked out, groups split off to make the chips and to pack them, while two other groups start testing the lysis protocols on the first batch of chips. While they are doing that, and working out the flow system, the manufacturing groups switch to learning to run the ESI/MS and to extracting the cells with standard protocols for a control sample. Part of the design for the way groups are arranged is to keep everyone moving forward, and part of the design is to force groups to share data. For example, the chip-making group needs to know how the masks were designed in order to estimate the etching time.

There is some redundancy built in. For example, two lysis methods and two staining methods are evaluated in the hopes that one of each will work successfully. It should be noted here that if different cell or tissue types are used, it is likely that some amount of new development will have to take place. Conversely, if the instructor is looking to start this experiment with a set of experiments that are almost certain to work well "up front," the staining and lysis of bacterial cells, as described above, can be taken as cookbook experiments or sub-tasks. As another example of redundancy, two chips are made and packed, with different types of stationary phase, and each is evaluated for its efficacy.

The project can be modified in some obvious ways. For example, with fewer groups there could be less emphasis on developing lysis and staining methods, or less emphasis on testing the mask-making protocols. With more students or more groups, thin-layer chromatography could be added as a means of screening fractions. There are numerous protocols for TLC of lipid extracts (see the cyberlipid website). If the protocols developed in this project become widely used, the project can shift to cell metabolism projects. It is also possible to do this project with a combination of TLC and gas chromatography with mass spectrometry using standard transesterification protocols instead of using electrospray MS. Smaller groups and less experienced students can be accommodated by adopting a subset of the experiment. For example, the focus could be on the microfluidic portion: making microfluidic chips. There are a variety of useful experiments that could be devised simply by having the students make a few basic chip designs. Examples include: making a simple extraction chip that demonstrates preconcentration of hydrophobic dyes (see the Jemere, et al. references); making a simple chip that demonstrates electrophoresis of charged fluorescent dyes (see early Ramsey and Manz references); or making chips and studying simple chemical reactions or mixing on chips (see the Song, Chen and Ismagilov reference). It is also possible to alter the experiment by using pre-lysed cells. This approach can be used to cut down on the number of

groups doing different things, and it simplifies the procedures for adsorbing the lipids on the chip. A similar experiment could be done by extracting DNA on a microchip, though the analysis would be by gene chip or the like (see the Easely, et al. reference). It is also possible that this lab could be developed across biology, chemistry, and biochemistry departmental boundaries.

A final word on equipment. There are several pieces of equipment for making microchips that have moderate price tags: the laminar flow hood and the programmable furnace are about $2k each. However, a "chip lab" as described here costs about $8k, including enough supplies to produce chips from a dozen 3″ × 3″′ photomask blanks. The only cost that is not included in that figure is the cost of the inspection microscope(s); zoom stereomicroscopes are common equipment, and we refurbished a standard brightfield microscope from a biology lab castoff. A good zoom stereomicroscope costs about $4500. The cost figure includes fittings for making a useable chip, but does not include supplies for using the chip, such as electrophoresis power supplies, optical detection equipment, or syringe pumps. It is assumed that common acids and a supply of ultrapure water are available. Many chip labs have clean room facilities, dedicated ultrapure water supplies, and expensive mask alignment and exposure facilities, and therefore cost in excess of $100k. However, unless very fine features or complicated structures are desired, such facilities are unnecessary, as long as care is taken in cleaning the chips before bonding. Except for mask exposure, all of the operations described above take place in an ordinary fume hood or in a standard laboratory environment.

SAFETY CONSIDERATIONS

Most of the processes described above are such that ordinary laboratory precautions are adequate. However, usage and handling of HF is extremely dangerous, and is best performed by a graduate teaching assistant or the instructor. The reader is referred to their local environmental safety and health professionals. All HF operations are performed in a fume hood. HF is stored in well labeled plastic, sealable containers. Attire consists of latex gloves, acid resistant gloves of elbow length (ThermoFisher), liquid repellant coveralls with elastic wrists and ankles and a hood, face shield, and, when handling HF, neoprene gloves and apron. The chips are handled with stainless steel forceps. Disposal should be according to local environmental safety and health personnel. It is recommended that calcium gluconate gel be kept on hand in case of accidental exposure, and that a plan worked out with local emergency facilities in case of gross exposure. Users are also cautioned that the cleaning solutions contain highly concentrated sulfuric acid and hydrogen peroxide, and extra care should be exercised when handling these solutions. They should be disposed of immediately following use.

ACKNOWLEDGEMENTS

All of the equipment and supplies purchased for creating the chip making laboratory and for carrying out the experiments described above (with the exception of ESI/MS) were purchased with support from the Spectroscopy Society of Pittsburgh and the Society for Analytical Chemists of Pittsburgh under the auspices of the Joseph A. Feldman Equipment Grant.

www.ebook3000.com

Preparation, UV-Vis and MCD Spectroscopy, and Molecular Modeling of Zinc Phthalocyanine: Confirmation of Degeneracy of the First Excited State

VICTOR N. NEMYKIN and PAUL KIPROF
Department of Chemistry and Biochemistry, University of Minnesota Duluth, Duluth MN 55812

LEARNING OBJECTIVES: This laboratory is divided into three sections. In the first section the students are to synthesize 2(3),9(10),17(18),23(24)-tetra-tert-butylphthalocyanine-zinc(II), in the second part the students are to investigate the UV-Vis and MCD spectra of 2(3),9(10),17(18),23(24)-tetra-tert-butylphthalocyanine-zinc(II), and in the final part the students are to understand the electronic spectra through theoretical modeling. The students are to learn how to synthesize macrocycle ligand and its zinc complex. The students are to learn about the rich UV-visible and magnetic circular dichroism (MCD) spectra of the Zn-phthalocyanine complex, their symmetry. They are to learn about higher level spectroscopy such as MCD spectroscopy. The students are to learn about theoretical modeling of transition metal complexes.

INTRODUCTION

PHTHALOCYANINES (Pcs, Figure 12.1) belong to an important class of macrocyclic compounds because of their wide range of applications that vary from the traditional use as blue or green dyes[1] to new applications in catalysis,[2] photodynamic therapy of cancer,[3] nanotechnology,[4] and non-linear optics.[5] The majority of these applications exploit unique optical properties of Pcs, and thus, a variety of spectroscopic techniques such as UV-Vis spectroscopy, magnetic circular dichroism (MCD), and fluorimetry as well as time-resolved fluorescence spectroscopy can be used in the characterization of the excited states of Pcs and their analogues.

Among different Pcs and their analogues, PcZn is often used as a good starting model for the understanding of phthalocyanine-based excited state properties because of closed-shell d^{10} configuration of the central atom (which simplifies UV-Vis and MCD spectra due to the absence of additional MLCT and LMCT transitions) and the high symmetry (D_{4h}) of the complex.[6] The first UV-Vis data on transition-metal phthalocyanines (PcM) were reported by Linstead and co-workers more than sixty years ago.[7] Since then, spectra of different phthalocyanines, including the closed-shell zinc phthalocyanine complex (PcZn), have been recorded at high temperature in the gas-phase,[8,9] in different solvents,[10,11] in cryogenic matrices at low temperatures,[12] and in supersonic jet expansions.[13] It has been found that the bright blue color of phthalocyanines originates from the intense absorption band (historically called the Q-band) typically located in the 650–680 nm region of the visible spectrum (Figure 12.2). The molecular extinction coefficient observed for the Q-band in first-row transition metal phthalocyanine complexes (i.e. zinc phthalocyanine) is close to the theoretical limit for single-electron excitation processes and varies in the range of 120,000–250,000 L mol^{-1} cm^{-1}.[1]

The first spectral assignments of PcZn were provided by Edwards *et al.* for gas-phase high-temperature spectra in which the Q, B, N, L, and C (earlier known as M) bands were identified in the UV-Vis spectrum.[8] Based on PPP-CI calculations, it had been suggested that the Q, B, N, and L bands

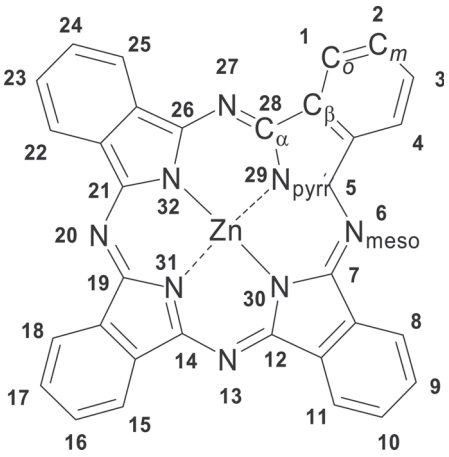

Figure 12.1. Labeling schemes in PcZn.

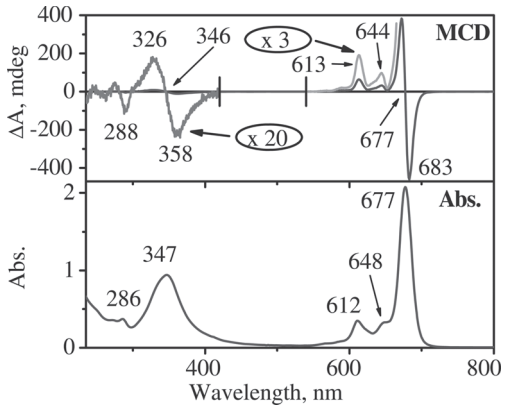

Figure 12.2. Room-temperature experimental MCD and UV-Vis spectra of zinc phthalocyanine (10^{-5} mol/L) recorded in dichloromethane.

consist of almost pure π – π* single electron transition configurations.[8] Specifically, the Q-band was assigned to the single electron transition from the highest occupied molecular orbital (HOMO) of a_{1u} symmetry to the doubly degenerate lowest unoccupied molecular orbital (LUMO) of e_g symmetry (Figures 12.3 and 12.4). In addition, low intensity bands observed in UV-Vis spectra of phthalocyanine complexes at ~650 nm and ~610 nm were assigned to the 0-1 and 0-2 vibronic components of the Q-band (Figure 12.4).

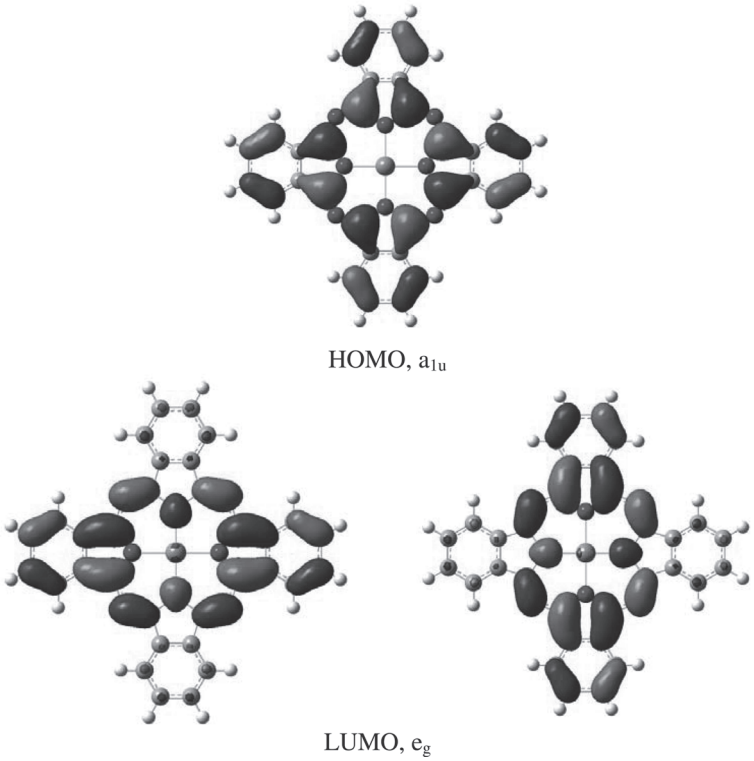

Figure 12.3. Frontier π-orbitals of zinc phthlocyanine calculated at Density Functional Theory (DFT) level of theory using B3LYP exchange-correlation functional.

www.ebook3000.com

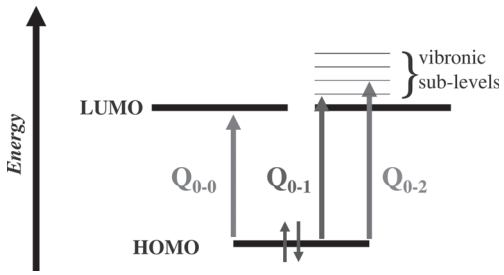

Figure 12.4. Simplified overview on the single-electron transitions observed in the Q-band spectral envelope of zinc phthalocyanine. $Q_{0\text{-}0}$ band observed at 677 nm, $Q_{0\text{–}1}$ band observed at 648 nm, and $Q_{0\text{-}2}$ band observed at 612 nm.

The promotion of a single electron from the HOMO of a_{1u} symmetry to the doubly degenerate LUMO of e_g symmetry leads to the transformation of $^1A_{1g}$ ground state of zinc phthalocyanine into a doubly degenerate first excited state of ^1E_u symmetry.[1]

The aim of this laboratory work is to confirm the degeneracy of the first excited state (1^1E_u) using experimental and theoretical approaches.

SAFETY RECOMMENDATIONS

4-*tert*-butyl-phthalonitrile (CAS No. 32703-80-3): *Skin Contact:* May cause skin irritation. *Skin Absorption:* May be harmful if absorbed through the skin. *Eye Contact:* May cause eye irritation. *Inhalation:* Material may be irritating to mucous membranes and upper respiratory tract. May be harmful if inhaled. *Ingestion:* May be harmful if swallowed. *Sensitization:* Possible sensitizer.

N,N-dimethylethanoamine (CAS No. 108-01-0): *Skin Contact:* Causes burns. *Skin Absorption:* Harmful if absorbed through skin. *Eye Contact:* Lachrymator. Causes burns. *Inhalation:* Harmful if inhaled. Material is extremely destructive to the tissue of the mucous membranes and upper respiratory tract. *Ingestion:* Harmful if swallowed. ORL-RAT LD50: 2000 mg/kg.

Lithium (CAS No. 7439-93-2): Flammable! Avoid contact with water and moisture! *Skin Contact:* Causes burns. *Skin Absorption:* May be harmful if absorbed through the skin. *Eye Contact:* Causes burns. *Inhalation:* Material is extremely destructive to the tissue of the mucous membranes and upper respiratory tract. May be harmful if inhaled. *Ingestion:* May be harmful if swallowed. INT-MOUSE LD50: 1 g/kg.

N,N-dimethylformamide (CAS No. 68-12-2): This product is or contains a component that is not classifiable as to its carcinogenicity based on its IARC, ACGIH, NTP, or EPA classification. May cause congenital malformation in the fetus. ORL-RAT LD50: 2.8 g/kg.

Zinc(II)acetate dihydrate (CAS No. 5970-45-6): *Skin Contact:* May cause skin irritation. *Skin Absorption:* May be harmful if absorbed through the skin. *Eye Contact:* Causes eye irritation. *Inhalation:* Material may be irritating to mucous membranes and upper respiratory tract. May be harmful if inhaled. *Ingestion:* Harmful if swallowed. ORL-RAT LD50: 794 mg/kg.

Diethyl ether (CAS No. 60-29-7): Flammable! *Skin Contact:* Causes skin irritation. *Skin Absorption:* May be harmful if absorbed through the skin. *Eye Contact:* Causes eye irritation. *Inhalation:* Material is irritating to mucous membranes and upper respiratory tract. May be harmful if inhaled. *Ingestion:* Harmful if swallowed. ORL-RAT LD50: 1215 mg/kg.

Required Equipment

Magnetic stirring hot plate, sand bath, magnetic stirring bar, 50 mL one-neck round bottom flask, 100 mL beaker, 50-mL two-neck Schlenk flask or three-neck round bottom flask, nitrogen source, oil bubbler, water condenser, inlet/outlet gas adaptor.

Time required for experiment: Synthesis of metal-free ligand—1.5h. Metallation reaction—4h. Isolation—2h.

Table 12.1. Chemical Data.

Compound	FW	Amount	mmol	mp, °C	bp, °C	Density
4-*tert*-butyl-phthalonitrile	184.24	500 mg	2.7	49–51	165–168 (6 mmHg)	
lithium	6.94	100 mg	14	180	1342	0.534
zinc(II)acetate dihydrate	219.5	220 mg	1	237		1.840

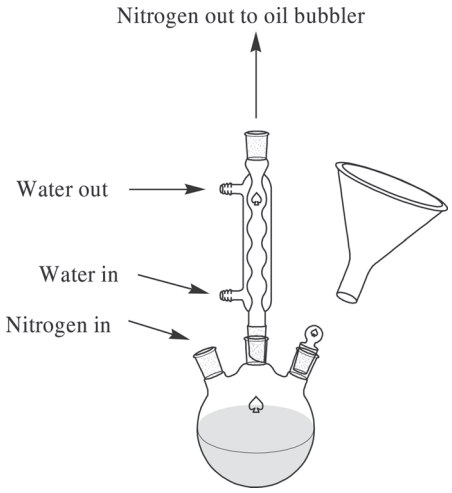

Figure 12.5. Apparatus for experiment.

EXPERIMENTAL PROCEDURE

Place 20 mL of dry N,N-dimethylaminoethanol and 500 mg (2.7 mmol) of 4-*tert*-butyl-phthalonitrile into a 50-mL three-neck round-bottom flask equipped with a magnetic stirring bar. Attach a water condenser, inlet gas adaptor, outlet gas adaptor, and oil bubbler as shown in Figure 12.5. Set the apparatus in a sand bath on a top of magnetic stirring hot plate. Flush the apparatus with nitrogen gas. Maintain a steady flow of nitrogen (~1 bubble/s). Using the side neck, add 100 mg (14 mmol) of elemental lithium. Stir for 5 min at room temperature, and then slowly heat the reaction mixture to the boiling point. Reflux the reaction mixture for additional 30 min. Transfer the reaction mixture into a 50-mL one-neck round bottom flask and evaporate the solvent in vacuo using a rotary evaporator.

Dissolve the precipitate in 20 mL of N,N-dimethylformamide, add a magnetic stirring bar and 220 mg (1 mmol) of zinc(II)acetate dihydrate. Attach a water condenser and heat the reaction mixture for 4h at 80°C. Cool down the reaction mixture and precipitate the product with 50 mL of water using a 100 mL beaker. Filter deeply colored product using fine paper filter, wash it three times with 50 mL of water and let it dry in air at room temperature.

Pack a short column with silica gel. Purify the dye with diethyl ether as the eluent. Collect the bright blue fraction and evaporate the solvent. The obtained phthalocyanine dye is pure enough for UV-Vis and MCD spectroscopy. If necessary, further purification can be achieved by precipitation of the dye dissolved in the chloroform (20 mL) by methanol (50 mL). Typical yields are 50–60%. The chemical transformations during experiment are presented in Scheme 12.1.

Note to instructor: In general, the solubility of the unsubstituted transition-metal phthalocyanines in common organic solvents is very low.[1] Introduction of the bulky tert-butyl groups on the periphery of phthalocyanine macrocycle dramatically improves the solubility of the target complex in common organic solvents.[1] Note however, that the experimental procedure leads to the formation of four statistically distributed positional isomers presented in Figure 12.6. Since the influence of tert-butyl substituents on the phthalocyanine π-system is negligible small,[1] the effective symmetry of π-system in substituted zinc phthalocyanine remains D_{4h}.

Recording of UV-Vis and MCD spectra of 2(3),9(10),17(18),23(24)-tetra-tert-butylphthalocyanine-zinc(II)

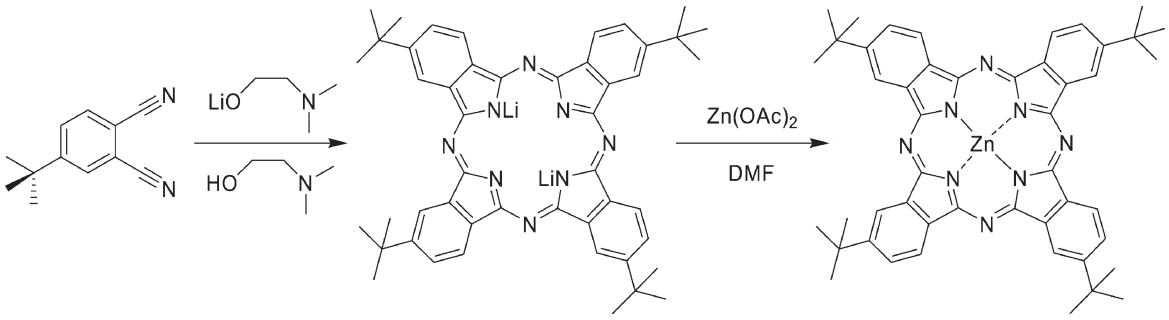

Scheme 12.1. Preparation of zinc phthalocyanine.

www.ebook3000.com

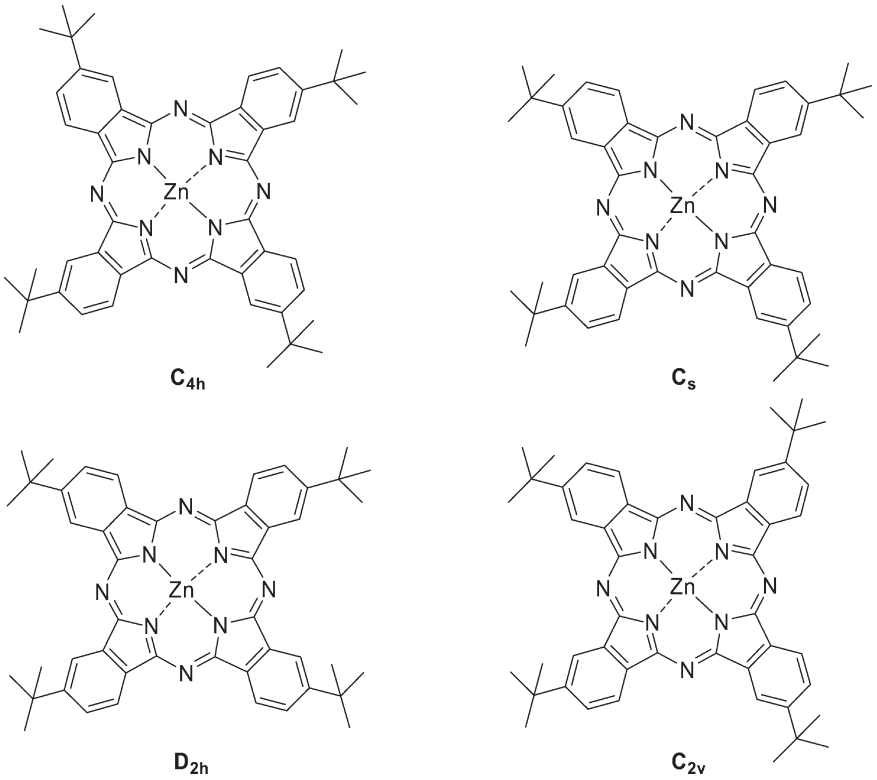

Figure 12.6. Positional isomers of Pc^{t}Zn with symmetry notation, note that the effective symmetry about the metal is D_{4h}.

SAFETY RECOMMENDATIONS

2(3),9(10),17(18),23(24)-tetra-tert-butylphthalocyanine-zinc(II) (CAS No. 39001-65-5): *Skin Contact:* May cause skin irritation. *Eye Contact:* May cause eye irritation. *Multiple Routes:* May be harmful by inhalation, ingestion, or skin absorption.

Chloroform (CAS No. 67-66-3): This product is or contains a component that has been reported to be probably carcinogenic based on its IARC, OSHA, ACGIH, NTP, or EPA classification. The National Cancer Institute (NCI) has found clear evidence for carcinogenicity. Laboratory experiments have shown mutagenic effects. ORL-RAT LD50: 695 mg/kg.

REQUIRED EQUIPMENT

1 cm glass or quartz cuvette. UV-Vis spectrometer. MCD spectropolarimeter. 100 mL and 10 mL volumetric flasks. Calibrated Pasteur pipette. Time required for experiment: 2h.

EXPERIMENTAL PROCEDURE

Preparation of 10^{-5} mol/L stock solution of 2(3),9(10),17(18),23(24)-tetra-tert-butylphthalocyanine-zinc(II). Dissolve 8.0 mg of 2(3),9(10),17(18),23(24)-tetra-*tert*-butylphthalocyanine-zinc(II) complex in 100 mL of chloroform using 100-mL volumetric flask.

Table 12.2. Chemical Data.

Compound	FW	Amount	mmol	mp, °C
2(3),9(10),17(18),23(24)-tetra-*tert*-butylphthalocyanine-zinc(II)	802.34	8 mg	0.01	>300

Using a calibrated Pasteur pipette transfer 1 mL of solution into 10-mL volumetric flask. Add 9 mL of chloroform. This is a stock solution for UV-Vis and MCD experiments.

Recording of UV-Vis spectrum of 2(3),9(10),17(18),23(24)-tetra-tert-butylphthalocyanine-zinc(II). Record the UV-Vis spectrum of 2(3),9(10),17(18),23(24)-tetra-*tert*-butylphthalocyanine-zinc(II) complex in the range of 280–900 nm using a stock solution. The spectrum should look similar to that presented in Figure 12.2. Calculate the molar extinction coefficient of the Q-band using the formula derived from Beer's law:

$$\varepsilon = Abs/(\,cl)$$

where *Abs* is absorption of the Q-band, *c* is the concentration in moles per liter, and *l* is the cell length in cm. For a pure sample of 2(3),9(10),17(18),23(24)-tetra-tert-butylphthalocyanine-zinc(II) complex, the calculated extinction coefficient should be around 200,000 L mol^{-1} cm^{-1}.

Recording of MCD spectrum of 2(3),9(10),17(18),23(24)-tetra-tert-butylphthalocyanine-zinc(II). Caution: The experiment presented below is designed for OLIS CD 17 – 20 spectropolarimeter equipped with a constant field DeSa magnet. When the electromagnet is the choice of the experimental setup, a "south" direction of the DeSa magnet corresponds to a parallel magnetic field, while a "north" direction of DeSa magnet corresponds to an anti-parallel magnetic field in the electromagnet. Other software/hardware parameters specific for a given spectropolarimeter (i.e. JASCO) may apply.

Insert a quartz cuvette with the pure solvent into the magnetic cuvette holder so that the DeSa magnet is oriented with its south pole toward the photoelastic modulator (PEM) and its north pole is toward the detectors (this orientation will be referenced below as "south"). Select a spectral range of 250 to 800 nm, bandwidth of 2 nm, number of increments of 550, integration time of 0.1 s, and number of scans of 2. Record the "south" baseline. Re-orient the magnet so that its north pole is oriented toward the PEM and the south pole is oriented toward the detectors (this orientation will be referred to as "north"). Record the "north" baseline. From the spectra menu, select "south" as a current baseline, select actual line, and assign it as a baseline. Replace a pure solvent in the cuvette with stock solution of zinc phthalocyanine, re-orient the DeSa magnet in the "south" direction and record the MCD + CD spectrum of the complex. From the spectra menu, select the "north" baseline from the spectra menu and assign it as a current baseline. Re-orient the magnet in the "north" direction and record the –MCD + CD spectrum of the complex. Select the "south" spectrum and then the "north" spectrum. Select multiple data processing from the right-click pop-up menu and choose subtract data sets command. De-select all spectra and then select the subtraction spectrum. From the right-click pop-up menu select process single data set and then apply constant command. Divide the current spectrum by a factor of 2. This is the true MCD spectrum of zinc phthalocyanine. It should be similar to that shown in Figure 12.2. In the event an in house MCD spectrometer is not available, the data presented here can be used for interpretation purposes.

Data Interpretation

The magnetic circular dichroism (MCD) method is complementary to the UV-Vis technique. Indeed, the UV-Vis and MCD spectra of a specific compound contain the same number of spectral bands. Both methods are based on the light absorption phenomenon. The band shapes and their intensities, however, are different because the MCD method detects the differential absorption of circularly polarized light in a magnetic field as a function of wavelength. For fully allowed electronic transitions, shape and intensity of MCD signal can be described as:[14]

$$\frac{\Delta A_{l-r}}{E} = 152.5Bcl\left[A_1\left(-\frac{df}{dE}\right)+\left(B_0\,\frac{C_0}{kT}\right)f\right]$$

where ΔA_{l-r} is the differential absorbance of left and right circularly polarized light, *E* is the energy coordinate in cm^{-1}, *B* is the magnetic field strength, *c* is the concentration of the sample, *l* is the path length in cm, *k* is the Boltzmann constant, *T* is the temperature in

www.ebook3000.com

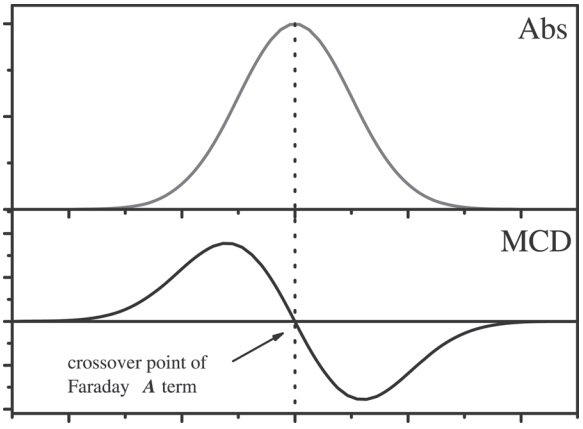

Figure 12.7.

K, and *f* is the normalized band shape function (typically Gaussian function). The intensity and shape of the MCD curve depends on the magnitudes of so-called Faraday A_1, B_0, and C_0 terms.

In the case of the diamagnetic PcZn complex with effective D_{4h} symmetry, only Faraday A_1 and B_0 terms are expected in MCD spectra because C_0 terms are dominate only in open-shell systems with degenerate ground states. The Faraday A_1 term appears if the excited state is degenerate (i.e. ^1E_u states in the case of PcZn). The crossover point of MCD Faraday *A* term corresponds to the band maximum in UV-Vis spectrum. For instance, the Q band in the UV-Vis spectrum of PcZn predominantly originates from a $2a_{1u} \rightarrow 7e_g$ symmetry allowed transition and results in the MCD Faraday *A* term, Figure 12.7.

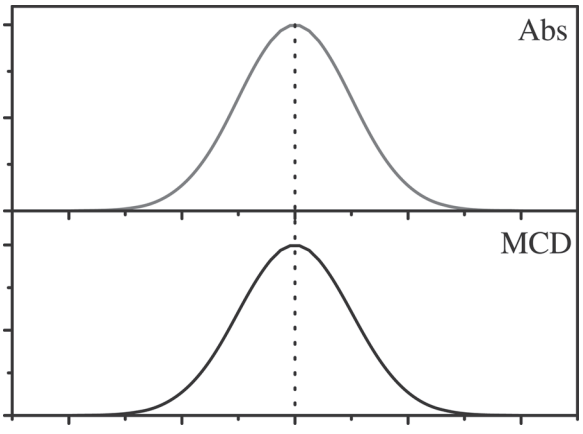

Figure 12.8.

Mixing of an excited state with the nearby transitions by the magnetic field results in MCD Faraday B_0 terms, which can be observed as negative or positive amplitude Gaussian-shaped bands. The maximum (positive or negative) amplitude in MCD Faraday B_0 term corresponds to the maximum amplitude in the respective UV-Vis band. In the case of PcZn (if selection rules allow), all excitations from non-degenerate to non-degenerate MOs will result in MCD Faraday *B* terms, Figure 12.8.

In order to find whether or not the first excited state in the PcZn complex is indeed degenerate, we need to explore the MCD and UV-Vis spectra of this complex recorded previously. Specifically, we should find a Faraday A_1 term in the MCD spectrum, which crossover point corresponds to the maximum magnitude in the Q-band in UV-Vis spectrum of the same compound. If present, the Faraday A_1 term will be indicative of the degeneracy of the first excited state in the PcZn complex.

THEORETICAL MODELING OF EXCITED STATES IN ZINC PHTHALOCYANINE

Note to instructor: For this part of the laboratory we used HyperChem software, but it also can be easily done with Gaussian/GaussView, GAMESS, Spartan, and other computational software packages. In these cases, specific adjustments to the software used should be made. The molecular geometry of PcZn can be optimized at molecular mechanics, semi-empirical, or DFT levels, while excitation energies can be predicted at semi-empirical (ZINDO/S, AM1, or PM3) or TDDFT levels of theory. Combination of ZINDO/1 and ZINDO/S methods allows one to obtain a reliable D_{4h} molecular geometry of the PcZn complex and compute energy of the first ^1E_u excited state within 2h.

In this section, we will confirm the degeneracy of the first excited state in the PcZn complex using a computational chemistry approach. Specifically, semi-empirical ZINDO/1 and ZINDO/S methods[15] will be used for geometry optimization and the calculation of the excitation energies, respectively. First, draw the PcZn molecule using HyperChem software:

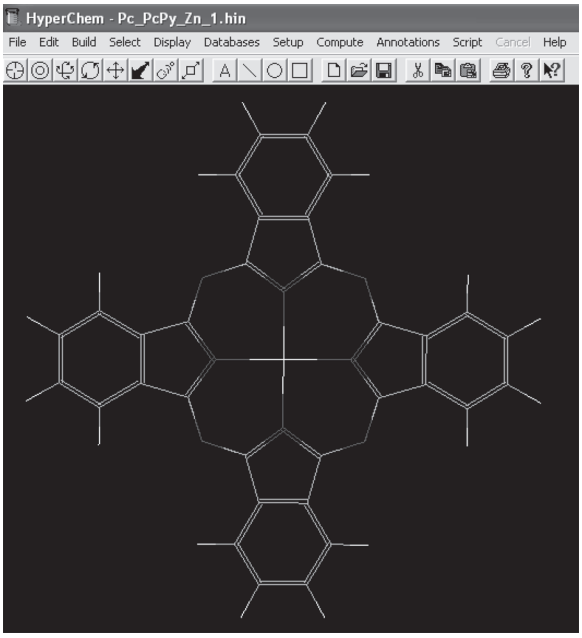

From the pop-up menu under the "Setup" command choose "semi-empirical" and then ZINDO/1 method. Set the options presented below:

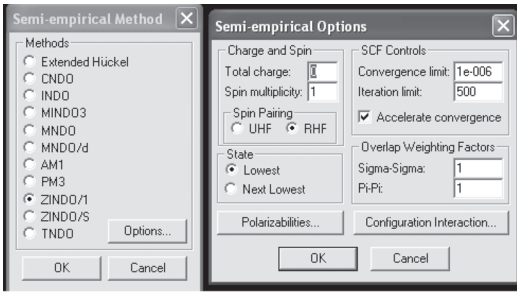

Click OK. From the "Compute" popup menu choose geometry optimization and then one of the conjugate gradient optimization methods available with convergence criterion of 0.01 kcal/(Å mol):

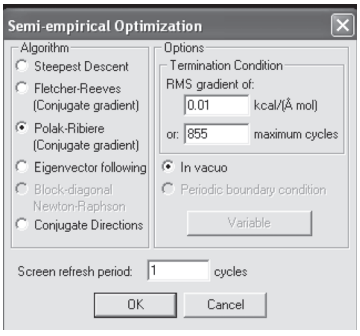

Click OK. Wait until structure will be optimized. Save the optimized structure. From the "Compute" popup menu run a single point calculation to make sure that the optimized structure of PcZn belongs to D_{4h} point group:

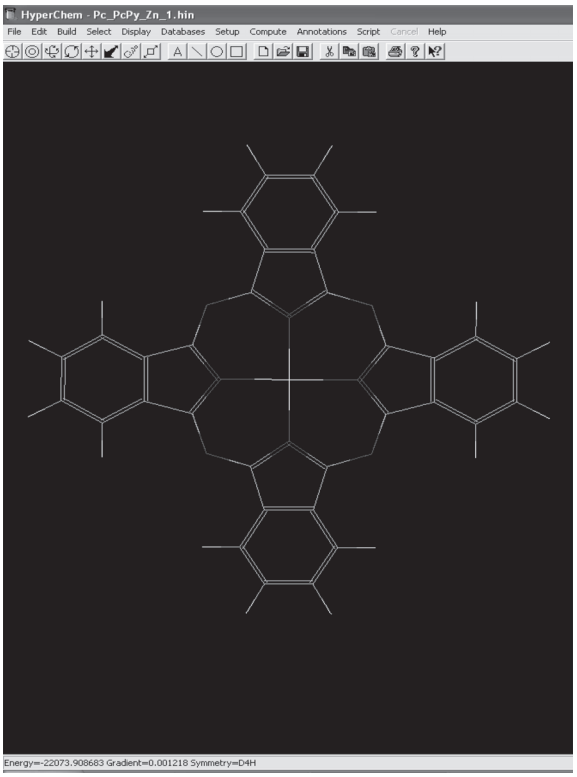

If this is not the case, follow the "note to instructor" procedure presented below.

Note to instructor: Unlike many other commercial and freeware computational chemistry programs (i.e. Gaussian, GAMESS etc.) HyperChem software does not take advantage of the molecular symmetry in calculations. As a result, quite often instead of a final D_{4h} symmetry of PcZn, geometry optimization can lead to the PcZn structure with C_1, C_2, C_{2v} and other symmetries. If this is the case, the following approaches can be suggested. In the first approach, the initial molecular geometry of PcZn should be constructed within the D_{4h} point group followed by optimization of the target compound at ZINDO/1 level of theory. If this approach fails, please use the listed below coordinates of PcZn (save it as *.hin):

www.ebook3000.com

forcefield mm+
sys 0 0 1
view 40 0.096799 62.5 22.5 0.1532973 -0.5495418 -0.8212818 0.3725489 0.8019191 -0.4670472 0.9152635 -0.2343706 0.3276632 -4.4541e-007 -1.7236e-007 -62.5
seed 0
mol 1
*atom 1 - Zn ** - -0.01087332 9.658437e-010 -1.148085e-008 2.367923e-008 4 2 s 3 s 4 s 5 s*
*atom 2 - N ** - -0.1836057 5.793099e-009 1.980295 6.050277e-008 3 1 s 6 a 7 a*
*atom 3 - N ** - -0.1836057 4.543098e-009 -6.123919e-008 -1.980295 3 1 s 8 a 9 a*
*atom 4 - N ** - -0.1836071 -4.077926e-009 -6.944906e-008 1.980295 3 1 s 10 a 11 a*
*atom 5 - N ** - -0.1836081 -1.360145e-009 -1.980295 4.968414e-008 3 1 s 12 a 13 a*
*atom 6 - C ** - 0.2299848 4.515698e-009 2.801831 -1.11015 3 2 a 14 a 15 s*
*atom 7 - C ** - 0.2299848 -1.243169e-009 2.801831 1.11015 3 2 a 16 s 20 a*
*atom 8 - C ** - 0.2299852 1.356679e-009 1.11015 -2.801831 3 3 a 14 a 17 s*
*atom 9 - C ** - 0.229986 7.910984e-010 -1.11015 -2.801831 3 3 a 18 a 19 s*
*atom 10 - C ** - 0.2299843 -1.742389e-009 1.11015 2.801831 3 4 a 20 a 21 s*
*atom 11 - C ** - 0.2299843 -5.987071e-010 -1.11015 2.801831 3 4 a 22 s 24 a*
*atom 12 - C ** - 0.229985 7.917786e-010 -2.801831 -1.11015 3 5 a 18 a 23 s*
*atom 13 - C ** - 0.2299843 -6.749918e-010 -2.801831 1.11015 3 5 a 24 a 25 s*
*atom 14 - N ** - -0.2608399 1.99142e-009 2.392244 -2.392244 2 6 a 8 a*
*atom 15 - C ** - -0.02513123 3.244185e-009 4.198385 -0.71199 3 6 s 16 a 26 a*
*atom 16 - C ** - -0.02513123 -5.271903e-009 4.198385 0.7119899 3 7 s 15 a 27 a*
*atom 17 - C ** - -0.02513075 -1.404575e-009 0.71199 -4.198385 3 8 s 19 a 28 a*
*atom 18 - N ** - -0.2608399 -9.539124e-011 -2.392244 -2.392244 2 9 a 12 a*
*atom 19 - C ** - -0.02513123 -1.829189e-009 -0.71199 -4.198385 3 9 s 17 a 29 a*
*atom 20 - N ** - -0.2608395 -2.153896e-009 2.392244 2.392244 2 7 a 10 a*
*atom 21 - C ** - -0.02513123 -4.686729e-011 0.7119901 4.198385 3 10 s 22 a 30 a*
*atom 22 - C ** - -0.0251317 3.088464e-010 -0.7119901 4.198385 3 11 s 21 a 31 a*
*atom 23 - C ** - -0.02513123 1.19408e-009 -4.198385 -0.7119901 3 12 s 25 a 32 a*
*atom 24 - N ** - -0.2608414 -5.302269e-010 -2.392244 2.392244 2 11 a 13 a*
*atom 25 - C ** - -0.02513123 -3.475552e-010 -4.198385 0.7119901 3 13 s 23 a 33 a*
*atom 26 - C ** - -0.02625465 6.796945e-009 5.407044 -1.421629 3 15 a 34 a 42 s*
*atom 27 - C ** - -0.02625513 -8.904222e-009 5.407044 1.421629 3 16 a 35 a 43 s*
*atom 28 - C ** - -0.02625513 -1.681077e-009 1.421629 -5.407044 3 17 a 36 a 44 s*
*atom 29 - C ** - -0.02625465 -7.262431e-010 -1.421629 -5.407044 3 19 a 37 a 45 s*
*atom 30 - C ** - -0.02625465 3.004166e-010 1.421629 5.407044 3 21 a 38 a 46 s*
*atom 31 - C ** - -0.02625465 1.465518e-009 -1.421629 5.407044 3 22 a 39 a 47 s*
*atom 32 - C ** - -0.02625513 2.103157e-009 -5.407044 -1.421629 3 23 a 40 a 48 s*
*atom 33 - C ** - -0.0262537 -9.288652e-010 -5.407044 1.421629 3 25 a 41 a 49 s*
*atom 34 - C ** - -0.0323329 2.480627e-009 6.595299 -0.7012091 3 26 a 35 a 50 s*
*atom 35 - C ** - -0.0323329 -4.965208e-009 6.595299 0.7012091 3 27 a 34 a 51 s*
*atom 36 - C ** - -0.0323329 -1.888297e-009 0.7012091 -6.595299 3 28 a 37 a 52 s*
*atom 37 - C ** - -0.0323329 -3.387433e-010 -0.7012091 -6.595299 3 29 a 36 a 53 s*
*atom 38 - C ** - -0.03233242 2.156566e-010 0.7012091 6.595299 3 30 a 39 a 54 s*
*atom 39 - C ** - -0.0323329 8.435137e-010 -0.7012091 6.595299 3 31 a 38 a 55 s*
*atom 40 - C ** - -0.03233337 1.564338e-010 -6.595299 -0.7012092 3 32 a 41 a 56 s*
*atom 41 - C ** - -0.03233242 1.460499e-010 -6.595299 0.7012091 3 33 a 40 a 57 s*
*atom 42 - H ** - 0.04154247 1.258546e-008 5.413798 -2.517094 1 26 s*
*atom 43 - H ** - 0.04154247 -1.159978e-008 5.413798 2.517094 1 27 s*
*atom 44 - H ** - 0.04154253 -1.444871e-009 2.517094 -5.413798 1 28 s*
*atom 45 - H ** - 0.04154247 2.404619e-009 -2.517094 -5.413798 1 29 s*
*atom 46 - H ** - 0.04154253 2.706645e-010 2.517094 5.413798 1 30 s*
*atom 47 - H ** - 0.04154253 2.02408e-009 -2.517094 5.413798 1 31 s*
*atom 48 - H ** - 0.04154271 2.674626e-009 -5.413798 -2.517094 1 32 s*
*atom 49 - H ** - 0.04154241 -7.2195e-010 -5.413798 2.517094 1 33 s*
*atom 50 - H ** - 0.03577399 5.956298e-009 7.553578 -1.233363 1 34 s*
*atom 51 - H ** - 0.03577399 -9.743057e-009 7.553578 1.233363 1 35 s*
*atom 52 - H ** - 0.03577405 -3.234849e-009 1.233363 -7.553578 1 36 s*
*atom 53 - H ** - 0.03577405 -1.873805e-010 -1.233363 -7.553578 1 37 s*
*atom 54 - H ** - 0.03577405 -5.021591e-011 1.233363 7.553578 1 38 s*
*atom 55 - H ** - 0.03577405 9.724215e-010 -1.233363 7.553578 1 39 s*
*atom 56 - H ** - 0.03577423 2.209861e-009 -7.553578 -1.233363 1 40 s*
*atom 57 - H ** - 0.03577399 -1.310499e-009 -7.553578 1.233363 1 41 s*
endmol 1

Once optimization is done within the D_{4h} point group, we must confirm that the optimized structure represents the local or global minimum on potential energy surface. To do so, click on "Vibrations" from the "Calculate" popup menu. Once the calculations are done, click on the "Vibration spectrum" command from "Calculate" popup menu. This will bring a new window with calculated vibration spectrum of PcZn:

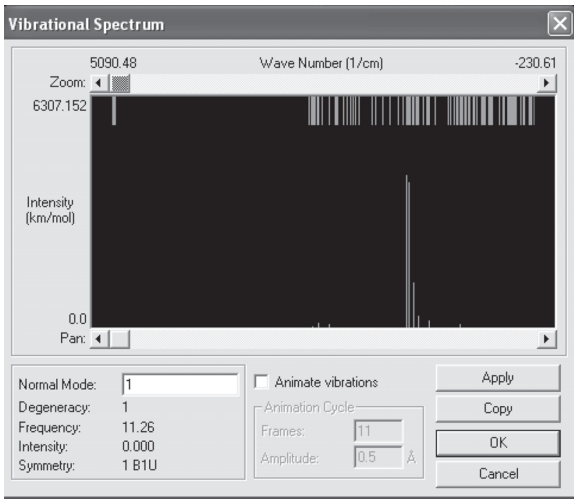

If during optimization the molecule falls into local or global minimum on the potential energy surface, all calculated frequencies must be positive (i.e. in our case, the lowest energy frequency of B_{1u} symmetry was calculated at 11.26 cm^{-1}). Next, we need to calculate the vertical excitation energies of PcZn. To do so, from the setup menu choose the semi-empirical ZINDO/S method and set the following options:

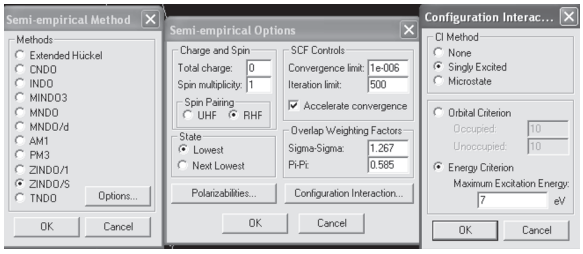

Click OK and then from the "Calculate" menu choose single point. Once the calculation is done, choose the electronic spectrum from the "Calculate" menu:

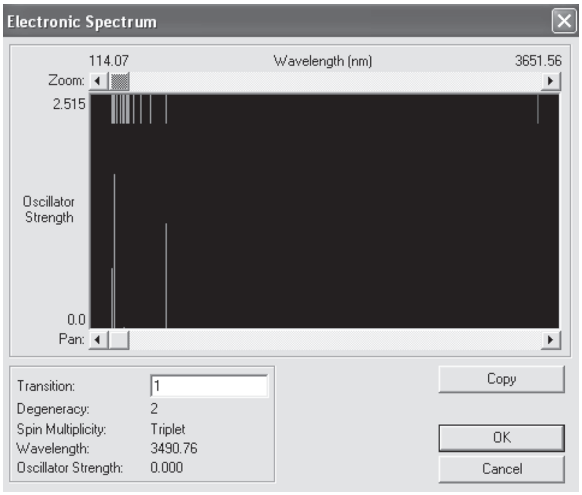

Find first transition with singlet spin multiplicity:

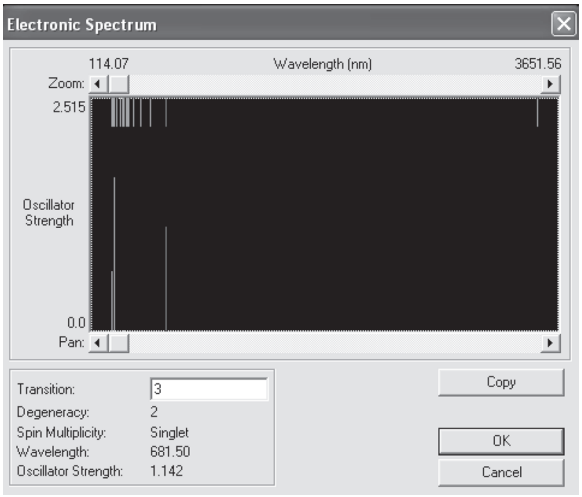

The first doubly degenerate $1E_u$ excited state in UV-Vis spectrum of PcZn was calculated at 681.5 nm in excellent agreement with experimental MCD data (Figure 12.2).

QUESTIONS

1. Search current and historical literature and suggest a mechanism for the formation of lithium phthalocyanine in the reaction between phthalonitrile (or substituted phthalonitrile) and lithium alkoxide.

www.ebook3000.com

2. Explain what MLCT and LMCT transitions are and how they can be avoided.
3. Give an explanaion for the Jahn-Teller effect in $[Ti(H_2O)_6]^{3+}$ and how it can lift a degeneracy through lowering of symmetry.
4. What Mulliken symbols would you expect if an electronic state is degenerate?
5. Using a MO diagram of benzene, indicate which $\pi - \pi^*$ transitions are possible and point out which would be degenerate.
6. Give other than $\pi - \pi^*$ examples of electronic transitions in inorganic chemistry where transition metals are involved and compare their extinction coefficients to PcZn.
7. Research current literature and give an overview of a class of compounds for the photodynamic therapy of cancer.
8. Give examples for macrocyclic complexes that are important in biochemistry (enzymes etc.).

REFERENCES

1. Leznoff, C. C.; Lever, A. B. P., Eds. *Phthalocyanines: Properties and Applications;* VCH Publishers: New York, 1990-1996; Vol. 1–4.
2. McKeown, N. B.; Budd, P. M. *Chem. Soc. Rev.* **2006,** 35, 675-683. Kaliya, O. L.; Lukyanets, E. A.; Vorozhtsov, G. N. J. *Porph. Phthalocyan.* **1999**, **3**, 592–610.
3. Juzenas, P. *Trends in Cancer Research* **2005**, *1*, 93–110. O'Riordan, K.; Akilov, O. E.; Hasan, T. *Photodiag. Photodynamic Ther.* **2005**, 2, 247–262.
4. Elemans, J. A. A. W.; van Hameren, R.; Nolte, R. J. M.; Rowan, A. E. *Adv. Mater.* **2006**, *18*, 1251-1266. Rao, C. N. R.; Govindaraj, A. *Acc. Chem. Res.* **2002**, *35*, 998–1007.
5. de la Torre, G.; Vazquez, P.; Agullo-Lopez, F.; Torres, T. *J. Mat. Chem.* **1998**, *8*, 1671-1683. Chen, Y.; Hanack, M.; Blau, W. J.; Dini, D.; Liu, Y.; Lin, Y.; Bai, J. *J. Mat. Sci.* **2006**, 41, 2169–2185. Wrobel, D.; Dudkowiak, A. *Mol. Cryst. Liq. Cryst.* **2006**, *448*, 617–640.
6. Stillman, M. J. In *Phthalocyanines: Properties and Applications;* Leznoff, C. C., Lever, A. B. P., Eds.; VCH Publishers: New York, 1993; Vol. III, Chapter 5; pp 227–296.
7. Anderson, J. S.; Bradbrook, E. F.; Cook, A. H.; Linstead, R. P. *J. Chem. Soc.* **1938**, 1151–1156.
8. Edwards, L.; Gouterman, M. *J. Mol. Spectrosc.* **1970**, *33*, 292.
9. Edwards, L.; Dolphin, D. H.; Gouterman, M. *J. Mol. Spectrosc.* 1970, 35, 90.
10. Nyokong, T. N.; Gasyna, Z.; Stillman, M. J. Inorg. Chem. **1987**, *26*, 1087.
11. Mack, J.; Stillman, M. J. *J. Phys. Chem.* **1995**, *99*, 7935.
12. VanCott, T. C.; Rose, J. L.; Misener, G. C.; Williamson, B. E.; Schrimpf, A. E.; Boyle, M. E.; Schatz, P. N. *J. Phys. Chem.* **1989**, *93*, 2999.
13. Fitch, P. S. H.; Wharton, L.; Levy, D. H. *J. Chem. Phys.* **1978**, *69*, 3424–3426.
14. Piepho, S. B.; Schatz, P. N. *Group Theory in Spectroscopy with Applications to Magnetic Circular Dichroism,* Wiley, New York, 1983.
15. Ridley, J.; Zerner, M. C. *Theor. Chim. Acta* **1973**, *32*, 111–134. Anderson, W. P.; Edwards, E. D.; Zerner, M. C. *Inorg. Chem.* **1986**, *25*, 2728–2732.

www.ebook3000.com

Index

www.ebook3000.com